INFORMATION TO USERS

This manuscript has been reproduced from the microfilm master. UMI films the text directly from the original or copy submitted. Thus, some thesis and dissertation copies are in typewriter face, while others may be from any type of computer printer.

The quality of this reproduction is dependent upon the quality of the copy submitted. Broken or indistinct print, colored or poor quality illustrations and photographs, print bleedthrough, substandard margins, and improper alignment can adversely affect reproduction.

In the unlikely event that the author did not send UMI a complete manuscript and there are missing pages, these will be noted. Also, if unauthorized copyright material had to be removed, a note will indicate the deletion.

Oversize materials (e.g., maps, drawings, charts) are reproduced by sectioning the original, beginning at the upper left-hand corner and continuing from left to right in equal sections with small overlaps. Each original is also photographed in one exposure and is included in reduced form at the back of the book.

Photographs included in the original manuscript have been reproduced xerographically in this copy. Higher quality 6" x 9" black and white photographic prints are available for any photographs or illustrations appearing in this copy for an additional charge. Contact UMI directly to order.

University of Alberta

CATALYTIC WET AIR OXIDATION OF ETHYLENE GLYCOL IN A

TRICKLE-BED REACTOR

by

Alison Fiona Miller

©

A thesis submitted to the Faculty of Graduate Studies and Research in partial fulfillment of

the requirements for the degree of **Doctor of Philosophy**

in

Chemical Engineering

Department of Chemical and Materials Engineering

Edmonton, Alberta

Spring 1998

Canada

University of Alberta

Faculty of Graduate Studies and Research
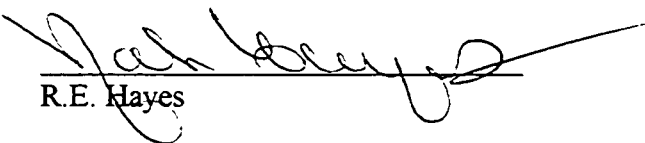
The undersigned certify that they have read, and recommend to the Faculty of Graduate Studies and Research for acceptance, a thesis entitled *Catalytic Wet Air Oxidation of Ethylene Glycol in a Trickle-Bed Reactor* submitted by *Alison Fiona Miller* in partial fulfillment of the requirements for the degree of *Doctor of Philosophy* in *Chemical Engineering*.

K.T. Chuang (supervisor)

F.T.T. Ng (external examiner)

S. Stanley

S.E. Wanke

R.E. Hayes

Date: 1997 December 15

To Dan,

for all his love and support

Abstract

Wastewater from many sources must be treated to remove contaminants before it can be discharged to the environment. Biological treatment is the primary method used for the removal of organic compounds, although it is not specifically designed for this purpose. As concern increases regarding the discharge of organic compounds, more effective methods such as catalytic wet air oxidation are being explored. In this study, the oxidation of ethylene glycol, (a major component in deicing fluid for aircraft) was studied, both as a model compound and in its own right.

In this research, a trickle-bed reactor was designed and constructed to study catalytic wet air oxidation. Platinum supported on a hydrophobic material was selected for the catalyst. At 110°C, ethylene glycol was oxidized completely to carbon dioxide and water. At slightly lower temperatures, the oxidation products were glycolic acid and carbon dioxide as well as a number of other byproducts. A major challenge of the work was minimizing mass transfer effects and catalyst deactivation. A gradual drop in ethylene glycol conversion was attributed to irreversible poisoning of the catalyst by trace metals, and competitive adsorption of byproducts with ethylene glycol. The rate of reaction was found to have a half order dependence on ethylene glycol concentration. Competitive adsorption between ethylene glycol and glycolic acid was also accounted for in the rate of reaction model. Sodium hydroxide was found to increase the conversion to glycolic acid and decrease the conversion to carbon dioxide.

Acknowledgements

There are many people that helped me at various points throughout my thesis. It is not possible to acknowledge everyone here, but I do thank them.

Specifically, I would like to thank the following people. My supervisor, Dr. Karl Chuang provided guidance throughout my thesis. Discussions with Dr. Sieg Wanke, Dr. Bing Zhou, and Dr. Shimin Tong were very helpful at various points throughout my thesis. I would like to thank Keith Faulder, Ron van den Heuvel, and Bob Scott in the machine shop, and Walter Boddez and Richard Cooper in the instrument shop for building and later modifying my equipment. Andrée Koenig's assistance with the chromatography and with resources was greatly appreciated.

I give heartfelt thanks for the emotional support provided to me by my husband, Dan Rasmussen, my parents, Margaret and Alistair Miller, and my dear friend, Linda Martin Traykovski.

Finally I would like to acknowledge the financial support from NSERC, the University of Alberta, the Department of Chemical and Materials Engineering, and my supervisor, Dr. Karl Chuang.

Table of Contents

List of Tables

List of Figures

Nomenclature

a	external catalyst surface per unit bed volume
A_A	surface area of platinum atom ($8.4 \, \text{Å}^2$)
A_P	surface area of platinum particle
B	breadth of the diffraction peak at half its maximum intensity (radians)
C_{EG}	final concentration of ethylene glycol (mol/L)
C_{GA}	final concentration of glycolic acid (mol/L)
c_s	oxygen concentration at the catalyst surface (mol·cm^{-3})
$c^{\bullet}$	saturation concentration of oxygen in water (mol·cm^{-3})
D	dispersion of platinum
D_{AB}	diffusion coefficient of solute A in solvent B
d_p	particle diameter
d_t	tube or reactor diameter
f	fugacity (bar)
F_{AO}	inlet flow rate of A (mol/h)
h	Henry's law constant
H_o	external liquid holdup
ΔH_r	heat of reaction
k	reaction rate constant
k'	reaction rate constant, including any dependence on oxygen pressure and glycolic acid concentration
k''	reaction rate constant, including any dependence on glycolic acid concentration as well as the known dependence on ethylene glycol concentration
k_{ls}	overall liquid mass transfer coefficient
K_1	reaction rate constant
K_2	reaction rate constant
K_{crit}	dimensionless value calculated to determine if flow is uniformly distributed
M_B	molecular weight of solvent
N_S	number of surface atoms
N_T	total number of atoms

P_{O2} partial pressure of oxygen (kPa)

r rate of reaction (mol·s·cm^{-3})

$-r_A$ rate of reaction of A (mol·h^{-1}·g^{-1})

$-r_{EG}$ rate of reaction ethylene glycol (mol·h^{-1}·g^{-1})

t diameter of the crystal particle

T temperature

ΔT change in temperature

V_A volume of platinum atom (15.1 Å^3)

V_P volume of platinum particle

W weight of catalyst (g)

x mole fraction of oxygen in solution

x_A conversion of A

y radial distance

z axial distance

α order of reaction in terms of ethylene glycol concentration

β order of reaction in terms of oxgyen pressure

ε void volume of the bed

ϕ solvent association factor; 2.26 for water

λ wave length of th ex-ray emissions (1.54178Å)

μ solution viscosity (kg·m^{-1}·s^{-1})

ν solute molal volume at normal boiling point (m^3/kmol)

θ_B angle at which the maximum intensity occurs (Bragg angle)

1. Introduction

Biological treatment is the primary method for treating wastewater before discharging it to the environment. It is designed to remove biological oxygen demand, total suspended solids and toxicity. While it does not specifically target organic compounds, it does remove a significant portion of them. With increasing awareness of the environmental impact of organic compounds, new methods, specifically targeting these compounds, are being developed.

A wide range of organic compounds are found in process water streams. Volatile organic compounds are those compounds which can be stripped from water with air. Considerable research has been done on the treatment of these compounds. Semi-volatile organic compounds cannot be removed from water by air stripping. They can be extracted using a solvent or adsorbed onto a solid. When the concentration of semi-volatile organic compounds is low, such that their recovery is not economically viable, the preferred method for treating the water is to oxidize these compounds in the liquid phase. Ethylene glycol, a semi-volatile organic compound, was selected for study, both as a model compound and in its own right; it is a major component of aircraft deicing fluid and as such is present in the water runoff at airports.

Catalytic wet air oxidation is a promising method for treating a wide range of organic compounds in water. The objective of this study was to gain an understanding of the oxidation of ethylene glycol, a model compound for other semi-volatile organic

compounds, over a hydrophobic catalyst, in a trickle-bed reactor. A supported platinum catalyst was used to accelerate the oxidation of ethylene glycol. A hydrophobic catalyst support concentrated the ethylene glycol from the water. The experiments were carried out in a trickle-bed reactor, so that results could more easily be scaled up for industrial use.

To develop a process for industrial use, it is necessary to understand the parameters affecting the system. To this end, mass transport effects were studied and minimum gas and liquid flow rates to eliminate such effects were determined. Temperature plays a role both in the rate of reaction and in the rate of mass transport of reactants and products. The identity of reaction intermediates is helpful in understanding the results. The effects of ethylene glycol concentration and oxygen pressure on conversion were studied at one temperature. Deactivation of the catalyst was studied and attributed to trace metal poisoning and competitive adsorption by one or more reaction byproducts. A model was developed to describe all of the characteristics of the observed deactivation.

2. Background

2.1 Biological Treatment of Wastewater

The biological degradation of organic compounds, in terms of the end result, is the same as their chemical oxidation. Both processes add oxygen to the compounds, forming partial oxidation products and deep oxidation products, (which will generally include carbon dioxide and water). With biological oxidation, micro-organisms incorporate the oxygen into the structure of the organic compound during the metabolic process. If the biological oxidation of waste compounds is allowed to occur in the environment, it depletes oxygen from the waterways that are essential to other organisms, most notably fish. Another limitation of biological oxidation is the selectivity of the micro-organisms. Not all organic compounds are readily or completely metabolized. Some compounds accumulate in the food chain where harmful effects can occur. The most well known instance of this occurring is with PCB's. Therefore, it is preferable to oxidize any organic compounds in wastewater before it is released to the environment.

Biological treatment is the most widely used approach for the removal of organic compounds from wastewater. Aeration lagoons, a common form of biological treatment, are designed to remove biological oxygen demand, total suspended solids and toxicity. Generally several days are required for the biological reactions to occur. This method is obviously not suitable for streams containing materials toxic to micro-organisms. Nor is it designed to target the removal of organic compounds. For example, on average one third

3

to half of the organically bound chlorine in the effluent of pulp mills is removed. This includes the volatile portion which is air stripped. It does not reflect the variability of biodegradation of compounds. The compounds that do not degrade significantly in the lagoon, will also be the slowest to degrade in the environment. While these compounds may not be particularly toxic, some of the degradation products are more toxic. With increasing awareness of environmental impact of organic compounds, additional treatment methods targeting organic compound are being explored and developed.

2.2 Selection of Ethylene Glycol for this Study

Many compounds in wastewater are in sufficiently low concentrations that it is not economical to attempt to reclaim them. Depending on the volatility of the compounds, different treatment methods are possible. Considerable research has gone into developing methods to treat volatile organic compounds (VOCs). VOCs are normally referred to as the purgeable fraction of organic compounds and defined as those compounds that are less than two percent soluble in water, boil at or below 150°C and are amenable to analysis by gas chromatography (PACE report 85-6). Because they are readily stripped by air from water, the treatment of VOCs is simplified because it does not have to take place in the liquid phase; rather it is carried out in the gas phase. However, many compounds in wastewater are not readily removed from the liquid phase by air stripping. Semi-volatile organic compounds are non-purgeable, but are solvent extractable and amenable to analysis by gas chromatography (PACE report 85-6). If there are sufficient quantities to warrant it, the compounds can be recovered. Otherwise, the compounds must be

4

destroyed either in the liquid, or first concentrated on a solid and then destroyed. If possible, it is preferable to destroy the organic compound in situ, since this reduces the number of steps in the process. This research focuses on semi-volatile compounds, specifically ethylene glycol.

Numerous compounds found in wastewater from many different sources fit into this category. One of the most well known class of compounds is chlorophenols from the pulp and paper industry. Another source of semi-volatile organic compounds in wastewater is deicing fluid. A combination of one or more of ethylene glycol, propylene glycol and diethylene glycol are the primary components of deicing fluids. Deicing fluid is used routinely in the winter to control ice formation on aircraft (Klecka et al., 1993). A major portion of the fluid spills onto the apron and is eventually collected by the airport sewer system.

Biodegradation in the environment of the major components of deicing fluid has been studied and found to be successful (Jank et al., 1974; Sabeh and Narasiah, 1992; Klecka et al., 1993). Testing of biological treatment was found to be fairly effective as a treatment method for ethylene glycol and propylene glycol and somewhat variable for diethylene glycol. The time required for degradation was found to be a strong function of temperature. In the case of ethylene glycol at 20°C, three days were required; when the temperature dropped to 8°C, this time increased to 14 days. In a study by Kilroy and Gray (1992), when ethylene glycol was added to an existing activated sludge treatment, concentrations of ethylene glycol higher than 0.1% caused a deterioration in the floc structure and increased the scum formation on the surface of the aeration basin.

These results give an indication of the residence time and hence the size of treatment lagoon that would be required, if the wastewater were to be treated completely. Biological treatment is an important first step in water treatment. However, it is not always practical to have the large treatment lagoons required to oxidize organic compounds completely. A faster treatment method for oxidizing the organic compounds in the water would require less space. Therefore, ethylene glycol was selected for study in a chemical oxidation process. Ethylene glycol also serves as a model compound. The system developed for its treatment should be fairly readily adaptable for the treatment of other semi-volatile organic compounds, particularly other alcohols and their partial oxidation products (aldehydes and carboxylic acids).

2.3 Chemical Oxidation Processes

Various new technologies are being developed as possible methods for targeting the removal of organic compounds. The reaction equilibrium for the oxidation of organic compounds lies far to the right for all but the most extreme conditions. However, the activation energy is such that at ambient conditions, in the absence of micro-organisms or some extra energy, oxygen does not react at a significant rate with many organic compounds, certainly not those that are present in wastewater. Those compounds that oxygen does react with are rapidly oxidized to more stable partial oxidation products. There are several options available to facilitate the oxidation reaction.

The most obvious solution is to increase the temperature. This approach is used in wet air oxidation. Mishra et al. (1995) did a comprehensive review of this topic, including

6

catalytic wet air oxidation in the topic. Wet air oxidation technology requires sufficiently high temperatures, with correspondingly elevated pressures to ensure non-volatilization of water, for the self-sustained, complete oxidation of various organic materials. Temperatures in the range of 300°C and pressures of 10 MPa are often required (Sanger et al., 1992). Wet air oxidation processes have potential in advanced waste treatment facilities, although the severe reaction conditions affect the economics of the process considerably.

Other options that are being explored involve more moderate conditions than wet air oxidation. Energy can be added to the system in the form of light. Ultraviolet light on its own is not very effective in the destruction of organic compounds. It has been used successfully in combination with the stronger oxidizing agents, hydrogen peroxide and ozone, to completely oxidize a range of compounds (Yue, 1993). Similarly, visible light has been used with dye sensitizers, where the dye adsorbs light and transfers the energy to oxygen (Li et al., 1992). A major drawback of both these processes is the necessary clarity of the process water. Furthermore, hydrogen peroxide and ozone add considerably to the cost of the process. Any dye that is added to the water must be removed prior to discharging the water.

Similarly electrochemical oxidation has been successfully demonstrated (Comninellis, 1992). An electric current is applied across the water using an anode and a cathode. The major drawback of this method is the expense of the large quantity of electricity required.

The other main area of research in the chemical oxidation of organic compounds is the use of a catalyst in the system. By using a catalyst to lower the activation energy of the oxidation reaction, lower operating temperatures and pressures can be used. The key issue in a catalytic oxidation process is the catalyst. Small amounts of organic compounds dissolved in large amounts of water require excellent physical and chemical properties in the catalyst. Hot acidic aqueous solutions often occur during processing of wastewater; these solution can promote the solubility of some metal oxides in their higher oxidation states and consequently, deactivate an otherwise favourable catalyst. Metals present in wastewater may also deactivate a catalyst (Pintar and Levec, 1992a). A highly active, nonselective catalyst is required for economic removal of trace contaminants such that the reaction can be carried out at lower temperatures. Another consideration in the removal of trace contaminants is that, if oxidation is incomplete, compounds more toxic than the trace contaminant may be formed (Spivey, 1987).

2.4 Catalytic Wet Air Oxidation – A Brief Survey of the Literature

Relatively few investigations have been published for the oxidation of organic compounds in aqueous solutions that do not involve biological treatment. Very few quantitative rate data are found. Rate equations for the liquid phase catalytic oxidation have been published for model pollutants such as formic acid, acetic acid and phenol (Pintar and Levec, 1992a).

Among the earliest kinetic work for catalytic wet air oxidation is that of Sadana and Katzer (1974). The reaction studied was catalytic oxidation of phenol in a semi-batch

8

reactor with copper oxide (CuO) supported on γ-alumina as the catalyst. A first order

dependence of initial rate on phenol concentration and one-half order with respect to

oxygen was reported.

Imamura et al. (1988) have studied the activity of a series of different catalysts in

wet air oxidation. The reaction conditions were 200°C and 1.0 MPa oxygen pressure and

2.0 MPa nitrogen pressure with 2000 ppm of total organic carbon. Rhodium and platinum

supported on cerium (IV) oxide were found to have lower catalyst activity than

ruthenium, although these noble metals all exhibited higher activity than that of

homogeneous copper catalyst. The ruthenium catalyst was highly active towards

poly(ethylene glycol) and some low molecular weight compounds with a high content of

oxygen, such as formaldehyde, ethylene glycol and formic acid. It had moderate activity

for oxidation of less highly oxygenated compounds, such as n-propyl alcohol, phenol and

acetic acid.

Ito et al. (1989) studied catalytic wet air oxidation using a cobalt oxide (Co_2O_3)

catalyst in a batch process at 200°C and 368 kPa oxygen pressure. Their work included

both mono and disubstituted alkanes: C_1–C_4 alcohols, amines and carboxylic acids. When

Ito et al. studied disubstituted alkanes, generally they found that compounds substituted

on both sides of the alkyl chain were much more readily decomposed than the

corresponding monosubstituted ones. The rate decreased with increasing number of

carbon atoms and increasing distance between the two groups, which suggests that two

closely located groups cooperate with each other to enhance reactivity. A simplified

reaction scheme was proposed for each functional group studied. In all cases the reaction

paths were assumed to be first order with respect to the reactant and independent of all other compounds. In the case of alcohols, the proposed mechanism had formic acid as a reaction intermediate. For alcohols with two or more carbons in the chain, a radical reaction is proposed with ethenal as an intermediate.

Work done by Pintar and Levec (1992ab) looked at three different catalysts ((1) copper oxide, zinc oxide and alumina oxide catalyst; (2) copper oxide supported on alumina; (3) copper, manganese, and lanthanum supported on zinc aluminate spinel) for the oxidation of organic compounds frequently found in industrial wastewater (phenols, nitrophenols, chlorophenol, tertiary butyl alcohol, methyl vinyl ketone, naphthalene sulfonate). In a typical experimental run, fresh catalyst was added into a continuous stirred tank reactor containing distilled water and a small amount of the organic compound being studied. The temperature was in the range of 105 to 130°C and the pressure was 0.46 to 1.3 MPa. Only about 50 % of the initial carbon content of the model pollutant was converted to carbon dioxide. The remainder of the carbon was found in a polymeric product strongly adsorbed onto the catalyst surface. A heterogeneous-homogeneous reaction mechanism was proposed, where radicals generated on the catalyst surface were an intermediate step in the proposed reaction mechanism. The formation of carbon dioxide was proposed to follow a heterogeneous pathway. The polymerization reaction was believed to follow a homogeneous free radical mechanism. Switching to a trickle-bed reactor in place of the CSTR was found to eliminate the formation of polymeric products. In the case of phenol, the reaction rate was accelerated appreciably when a small amount

10

(0.1 wt%) of hydrogen peroxide was added to the phenol solution before starting the kinetic run.

Sanger et al. (1992) studied wet air oxidation of chlorophenols at a range of temperatures, with and without added hydrogen peroxide and with and without a series of catalysts containing oxides of manganese, copper or iron, alone and supported on silica (SiO_2) or alumina (Al_2O_3). In the absence of a catalyst and hydrogen peroxide, no reaction occurred. In the presence of hydrogen peroxide, the catalysts each containing one of manganese, iron or copper effectively destroyed 3-chlorophenol at 200°C. Only the manganese catalyst was effective in the absence of hydrogen peroxide. The iron containing catalysts were effective at temperatures as low as 60°C; in a batch reactor, complete destruction of the chlorophenol within one hour was reported with the Fe/SiO_2 catalyst. The copper oxide catalyst was successfully reused without any treatment between runs. The iron catalyst supported on silica lost activity if removed from the system and dried; however, this activity was restored by recalcining the catalyst. In this study, a continuous reactor achieved complete destruction of the chlorophenol over the iron catalyst at temperatures greater than 60°C in less than one minute. This faster rate of reaction was attributed to the hydrogen peroxide being added immediately prior to the reaction, and not (as was the case in the batch reactor) being heated with the test solution. Hydrogen peroxide degrades quite rapidly with increasing temperature.

3. The Trickle-Bed Reactor

3.1 Selection of a Trickle-Bed Reactor

To understand why a trickle-bed reactor was selected for this study, the original objectives of the project must be recalled. The original objective for this thesis was to develop a method for the treatment of fairly low concentrations of semi-volatile compounds in wastewater, using ethylene glycol as the model compound. Then, a model for the reactor was to be developed. Ideally, this method was to readily scale-up for industrial use.

The treatment method of the aqueous solution, that is to say how the organic compounds would be removed from the wastewater, was a key criterion in selecting the reactor. In choosing a reactor with ease of scale-up as a selection criterion, other potentially important design elements were more difficult to study. The choice of a trickle-bed reactor meant that it was more difficult to study the kinetics of the reaction. However, the reactor choice meant it was possible to study the behaviour of a hydrophobic catalyst in such a reactor. The hydrophobic catalyst was not readily wetted by an aqueous solution, even though the solution contained a small amount of organic material. A procedure was developed so that good liquid distribution and liquid contact with the catalyst could be achieved.

Several factors were considered in the choice of reactor: (1) number of phases required; (2) batch versus continuous operation; (3) degree of catalyst handling. The type

of data required and the reaction being carried out were also important parameters. In addition, provisions should have been made in the event of transient catalyst behaviour and catalyst decay.

The need for a three-phase reactor came about in the following manner:

A liquid phase was established when it was decided to study a semi-volatile organic compound. Ethylene glycol is a semi-volatile compound, and as such, it is not readily stripped from water.

The gas phase resulted from the selection of air or oxygen as the oxidant. The driving factor behind this choice was the low cost and ease of use of either air or oxygen. The primary alternatives to oxygen were chlorine based oxidants, ozone, and hydrogen peroxide. Chlorine based oxidants were discarded as an option based on the low acceptability of chlorine-containing wastes; the objective of this project was to improve water quality and as such the chlorinated compounds would still have to be recovered from the water, adding to the complexity. Ozone must be produced on site which involves a large capital investment and was beyond the scope of this project. Hydrogen peroxide is expensive relative to air or oxygen and would be difficult to introduce effectively into a system, because it rapidly degrades at operating temperatures.

Both hydrogen peroxide and air/oxygen oxidant require some sort of a catalyst if the reaction is to proceed at an acceptable rate under moderate conditions. As well as traditional catalysts, ultraviolet irradiation or electric current could be used to introduce the extra energy to increase the rate of reaction. UV irradiation can only be used on very shallow depths of water, making the processing of large volumes of water unattractive.

For the quantities required, electricity is prohibitively expensive for treating wastewater. The third phase for the system resulted from the choice of a solid catalyst. Given that the project was aimed at the cleanup of wastewater, it was not acceptable that the treatment process add contaminants to the water. The catalyst for the system had to be easily recovered. For this reason, a heterogeneous catalyst was selected over a homogeneous catalyst introducing a third, solid phase.

When the reactor design was selected, ease of scale-up for industrial use was considered an important attribute of the reactor. Therefore, continuous operation was preferable to batch operation and, within that constraint, a tubular reactor was preferable to a CSTR. Within these constraints, there are two main choices of reactor: a fixed bed reactor or a slurry reactor (CSTR).

The reactor design chosen for studying the oxidation of ethylene glycol was a trickle-bed reactor. A trickle-bed reactor is defined as a fixed bed reactor in which the gas and liquid phases flow cocurrently downward (Satterfield, 1970). This is the definition that will be used exclusively throughout this work. This reactor has the advantage over other fixed bed reactors that cocurrent downflow gives better liquid distribution over the catalyst and higher liquid flow rates are possible without flooding (Satterfield, 1970). There is no advantage in having countercurrent flow from a reaction standpoint since oxidation reactions are essentially irreversible.

Both slurry reactors and trickle-bed reactors have advantages and disadvantages from an operational standpoint. The advantages of one tend to be the disadvantages of the other.

Briefly, the key features of a trickle-bed reactor are as follows:

(1) The conversion in a trickle-bed reactor can be predicted with reasonable accuracy using a plug flow reactor design equation. Under isothermal conditions, with kinetics that are faster at higher concentrations (as is the case in this study), higher conversions are achieved in plug flow reactors than CSTRs. (2) An additional step is not required to separate the catalyst from the liquid phase. (3) The low ratio of liquid to solid minimizes polymerization side reactions. (4) Poor temperature control occurs when the reactions are highly exothermic or endothermic. (5) Internal mass transfer limitations are more difficult to overcome than in a CSTR, since larger catalyst particles are required in a fixed bed reactor.

Slurry reactors have good temperature control and easy heat recovery. The catalyst is readily removed and replaced if its working life is short. The catalyst effectiveness factor approaches unity because very small catalyst particles are used(Satterfield, 1975). The disadvantages of the slurry reactor include the residence time distribution being close to that of a CSTR. Catalyst removal by filtration may be difficult. A high ratio of liquid to solid allows homogeneous free-radical side reactions to become important if they are possible (Pintar and Levec, 1992ab).

15

A trickle-bed reactor was selected for this study for the following reasons:

(1) With this system, temperature control was not expected to present much trouble since the organic compounds were in dilute solution representing no more than a few percent of the total volume.

(2) One of the objectives of this research was to find a catalyst with an acceptable deactivation rate; therefore, the catalyst had to be used from one run to the next, in order to observe any deactivation. Minimal catalyst handling, without an additional step to separate the catalyst from the process water, makes for an easier system.

(3) A caution concerning the use of a slurry reactor comes from the work of Pintar and Levec. About 50% of the initial carbon content of their model pollutant was converted to a polymeric product strongly adsorbed onto the catalyst surface when a CSTR was used. The formation of polymeric product was eliminated by employing a trickle-bed oxidation reactor, where the high solid to liquid ratio favours the heterogeneous reaction, i.e. the formation of carbon dioxide (Pintar and Levec, 1992b).

(4) A trickle-bed reactor is relatively easy to construct and scale-up.

3.2 Equipment

A schematic diagram of the equipment is given in Figure 3.1. The gas flow rates were controlled by two mass flow controllers, one from Matheson, the other from Unit Instruments. Oxygen, nitrogen, air or a combination of two of them were sparged into the bottom of a saturator filled with liquid water, using a sparger from the Mott Metallurgical Corporation, micron grade 2 with an area of 85 cm^2.
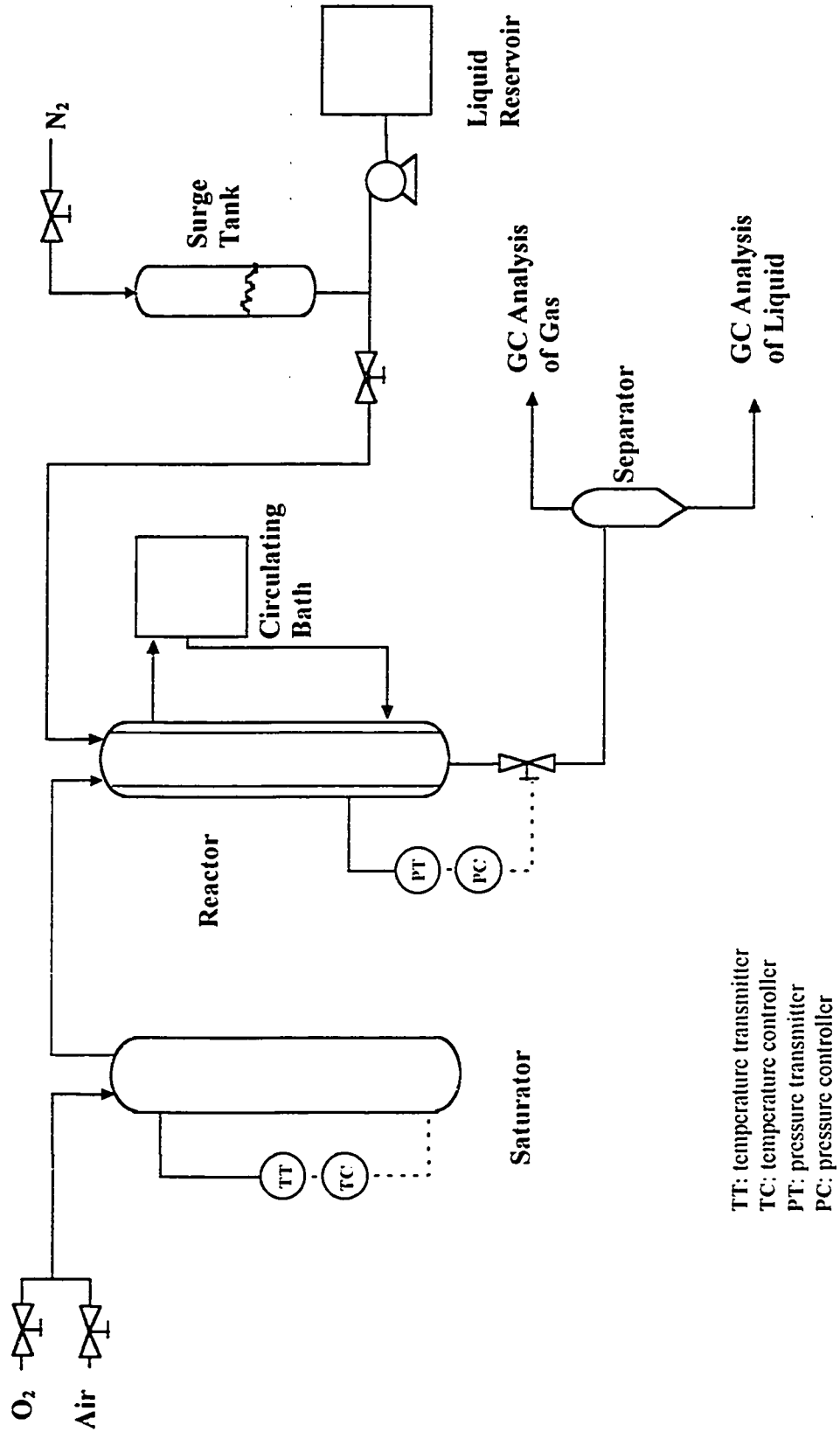
Figure 3.1: Schematic Diagram of Equipment

N₂

Surge
Tank

Liquid
Reservoir

GC Analysis
of Gas

Separator

GC Analysis
of Liquid

Circulating
Bath

Reactor

PT PC

Saturator

TT TC

O₂

Air

TT: temperature transmitter
TC: temperature controller
PT: pressure transmitter
PC: pressure controller

A temperature control loop controlled the rate of heating of the saturator. The temperature of the control loop was measured by a type J thermocouple at the top of the saturator. A second, type J thermocouple measured the temperature of the gas stream leaving the reactor. This temperature was considered to be the gas feed temperature, and was assumed to be saturated with water vapour. No drop in temperature was detected at the entrance of the reactor which would indicate vapourization was occurring in the reactor, supporting this assumption. It was not possible to control the gas feed temperature directly because too great a time delay existed between the heater output and the gas feed temperature. Following the thermocouple measuring the gas feed temperature, heating tape was wrapped around the feed line to prevent condensation in the line. The setpoint of the temperature control loop (and therefore of the saturator) was manually adjusted to ensure the gas feed temperature was maintained at the desired level. On average, after the initial startup, one temperature adjustment per day was required to the setpoint of the control loop to maintain the desired gas feed temperature. In general, the saturator was operated about 40°C hotter than the in-line temperature, and therefore, it was reasonable to assume saturation.

Liquid was pumped from a reservoir with an LMF Milton Roy, electronic diaphragm pump, with a flow rate of 0.38 to 38 mL/min. A surge tank was used to smooth the pulse delivery of the pump. During startup, the pressure in the surge tank was increased with an air feed. A needle valve was used to control the liquid flow rate during startup, when the pressures of the system were not yet at steady state. A rotameter monitored the liquid flow rate. The liquid was preheated by passing it through the liquid of

the heating bath. A heating tape wrapped around the liquid feed line was used to complete the heating. A rheostat was used to manually control the voltage to the heating tape, and hence the temperature of the liquid feed. The temperature of the liquid feed was monitored at the entrance to the reactor with a type J thermocouple. This heating tape was also used to maintain the line temperature of the gas feed.

The gas and liquid streams were fed cocurrently into the trickle-bed reactor. The reactor consisted of a 2.7 cm inside diameter, stainless steel tube 102 cm in length. The flanges at the top and the bottom of the reactor were removable to allow for changing the reactor bed. The reactor tube was jacketed by a second 5 cm outside diameter tube. A Polystat constant temperature circulating bath containing ethylene glycol maintained the bed temperature. Four type J thermocouples measured the temperature profile along the bed length.

A pressure sensor measured the pressure at the top of the reactor. At the exit to the reactor, a Badger control valve, K trim, controlled the pressure, using the information from the pressure sensor via a transducer.

The effluent from the reactor was fed to a separator. Gas samples were measured on-line. The gas stream passed through a bed of desiccant (silica gel) to remove the water vapour. No difference in the amount of carbon dioxide in the gas stream was detected when the silica gel was not in place. Gas analysis was done with a Hewlett Packard 5730 Gas Chromatograph using a 10' x 1/8" column packed with 80-100 mesh HayeSep D. Liquid samples were collected periodically. The amount of acidity was determined by titrating a sample with a Mettler DL21 titrator. The amount of ethylene glycol remaining

in the liquid was determined with a Hewlett Packard 5890 Gas Chromatograph using a HP-17 capillary column (50% phenyl and 50% methylsiloxane copolymer; 10 m × 0.53 mm × 2.0μm film thickness). An internal standard of 1,3-propanediol was added to the liquid samples to improve the accuracy of the results.

3.3 Results and Discussion

3.3.1 Reactor Bed Loading

At this stage, steps were taken to ensure consistent flow distribution and minimal wall flow. It should be pointed out that the standard rule of thumb of eight or ten to one, column to packing diameter, used for fixed bed flow with one phase, does not apply when there is two phase flow. Satterfield (1975) states that narrow diameter TBRs such as those found in laboratory work have liquid migrating to the wall, up to a steady state fraction corresponding to as much as 30 to 60 percent of the total at ratios of reactor diameter to particle diameter of as much as ten to one. This fraction drops with increasing ratio of column diameter to packing diameter and is a function of flow rate.

Herskowitz and Smith (1978) studied liquid distribution of an air/water system over various typical catalyst supports. They concluded that the equilibrium flow distribution was uniform (across the column) for a tube to particle diameter ratio greater than approximately 18. The catalyst and inert support used in this study were of particle diameter, d_p, 0.30 mm to 0.85 mm (20 to 50 mesh) and the tube diameter, d_t, of 2.70 cm for a d_t/d_p between 32 and 90. Assuming that the bed was packed uniformly, the flow would be uniform, once an equilibrium flow was established. In the interest of minimizing

the pressure drop, it would have been preferable to work with a support with a narrower range in diameter, perhaps 20 to 30 mesh. However, for the purposes of this work, this range was acceptable since the supply of the larger spheres was limited.

To ensure uniform flow distribution, a glass tube of 2.5 cm diameter was packed with catalyst and inert support as if packing the reactor for a run. The glass tube allowed observation of the catalyst bed. Alumina was used as the inert material because a material that would adsorb dye from an aqueous solution was required. A dilute aqueous solution of ethylene glycol with a few drops of red food colouring was then fed into the top of the column and allowed to trickle through the catalyst bed via gravity. The flow distribution was checked by way of the evenness of the colour distribution.

Using these results, the following procedure was developed for packing the reactor. A point source was used to feed the water. When the liquid was fed directly onto the 20 to 50 mesh particles, the initial liquid distribution was poor. The distribution was greatly improved by making the first section of the bed $^1/_4$ inch ceramic rings (Norton Company). Essentially, this had the effect of a multipoint distribution. It can be further understood in the framework of an equation developed by Koros (1986):

$$K_{crit} = \frac{y^2}{\sqrt{d_p}\ z} \leq 4 \qquad \textit{for uniform flow} \qquad (3.1)$$

where y in the radial distance and z is the axial distance down the bed. With the initial section being $^1/_4$ inch ceramic rings, 2 cm were required to achieve uniform flow. Therefore, in all runs, at least 4 cm of ceramic rings were packed at the top of the reactor bed.

This section was followed by approximately 10 cm of crushed ceramic rings (20 to 50 mesh), a low surface area, inert material to ensure that a steady flow was established. It was not sufficient to just add the dry support into the reactor, since this did not lead to a uniform distribution. Adding the support into a layer of water gave a sufficiently uniform bed and led to a uniform flow pattern. The catalyst mixed with the crushed inert was carefully added to the column in small portions to ensure even packing. Each addition was washed down with water, remixed with a wire, and gently pressed down. Below this section, a calming zone of crushed inert was placed in the same manner as the other inert material. Finally, a section of tightly rolled mesh screen was used to support the reactor bed. This avoided a sharp transition and correspondingly a distinct pressure change at the bed exit. See Figure 3.2 for an example of the reactor bed packing.

gas inlet

liquid inlet

3 cm

>4cm;
6 to 15 cm

1/4" ceramic rings

≅10 cm

20-50 mesh crushed ceramic rings

Type J thermocouples

≅50 cm for
most runs

Pt catalyst + 20-50 mesh crushed
ceramic rings

5-7 cm

20-50 mesh crushed ceramic rings

8 cm

York mesh
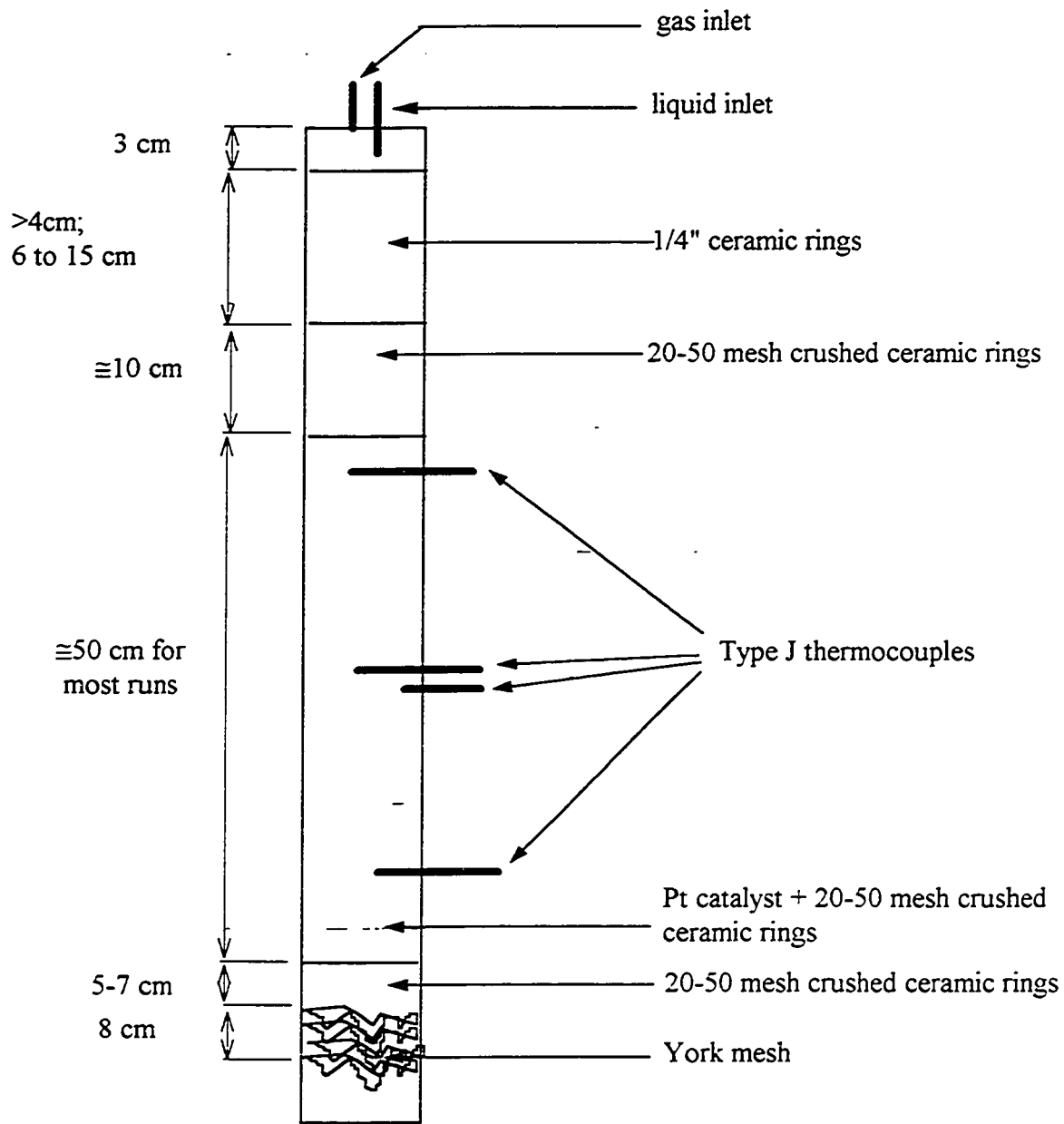
Figure 3.2: Schematic of reactor bed packing, showing typical lengths of the various sections of the bed.

3.3.2 Reproducibility and Temperature Control

In preliminary experiments studying the overall catalyst performance, a catalyst consisting of 1.0 (wt)% platinum on a styrene divinyl benzene copolymer support was loaded into the reactor in an undiluted form. During this early stage of experiments, the liquid flow rates were considerably lower than later experiments. Furthermore, the equipment was not set up for continuous running, so frequent shut downs occurred.

A number of interesting phenomena were observed. (1) Complete conversion of ethylene glycol to carbon dioxide was achieved at temperatures of 100°C, with a liquid flow rate of 4.6 mL/min and an ethylene glycol concentration in water of 0.18 mol/L. Because the flow rates determine the residence time of the reactants, the conversion is a function of liquid flow rate as well as temperature. (2) Temperature control was poor in these experiments with a 20°C temperature range observed over the length of the reactor bed at an nominal operating temperature of 90°C (88 to 108°C). (3) Results were not very reproducible from one run to the next (see Table 3.1). (4) At lower temperatures and/or higher liquid flow rates, where complete conversion was not achieved, the conversion improved with time, in particular when the reactor was not in operation for extended periods of time (see Table 3.1). In these early experiments, glycolic acid had yet to be identified as one of the reaction products. Hence only conversion to carbon dioxide is reported in this table.

Table 3.1: Increase in catalyst activity with the number of days of operation.

Sample Date	Temperature °C	% ethylene glycol converted to CO_2
95-07-28	90	10.0
reactor off for 3 days		
95-08-02	90	18.1
same reactor configuration, new batch of catalyst		
95-08-10	90	13.6
95-08-11	90	14.3
reactor off for 2 days		
95-08-14	90	16.0
attempt to regenerate catalyst in situ with O_2 gas, 90°C and atmospheric conditions		
95-08-21	90	4.6
95-08-22	90	7.6
95-08-23	90	4.3
95-08-31	90	20.8
95-08-24	110	26.6
reactor off for three days		
95-08-28	110	54.1
95-08-30	110	57.0

Reactor shut down overnight. The operating conditions were as follows: oxygen pressure 300 kPa; oxygen flow rate 550-590 mL/min (ambient conditions); liquid flow 6.6-6.7 mL/min; ethylene glycol concentration 0.18 mol/L.

3.3.2.1 Temperature Control

The temperature was measured with four type J thermocouples, three along the length of the reactor and the fourth at the bottom of the catalyst bed to obtain the temperature rise across the reactor. The location of the thermocouples is shown in Figure 3.3. The temperature variation along the length of the catalyst bed was worse than anticipated. The heat of reaction in converting ethylene glycol to glycolic acid is -492 kJ/mol (calculated from data in International Critical Tables) and in converting ethylene glycol to carbon dioxide is -1189 kJ/mol (calculated from data in TRC Thermodynamic Table; Non-hydrocarbons). The temperature rise in the reactor indicated that minimal heat exchange was occurring between the reactor bed and the jacketing liquid (See Appendix A). On reflection, it became apparent that the catalyst support is a very good insulator, with stationary air/liquid pockets trapped inside the pores of the material.

The solution to the large temperature rise was two-fold. Increasing the liquid flow rate resulted in lower conversion per unit volume of water, (although the rate of reaction increased because it was mass transfer limited at low flow rates), and hence a smaller temperature increase. The second part of the solution was to decrease the rate of reaction, by reducing the amount of platinum, either through lower platinum loadings or dilution of the catalyst bed. Both of these approaches were taken.

Following these changes, the temperature difference across the bed was less than 2 K for all operating conditions at 80°C. Typically, a 1 K difference across the bed was observed and depending on the operating conditions (and hence the rate of reaction), 1.0 to 1.5 K difference was observed along the length of the bed.

gas inlet

liquid inlet

1/4" ceramic rings

34.4 cm

20-50 mesh crushed ceramic rings

21.6 cm

Type J thermocouples

2.5 cm

21.6 cm

Pt catalyst + 20-50 mesh crushed ceramic rings

20-50 mesh crushed ceramic rings

York mesh
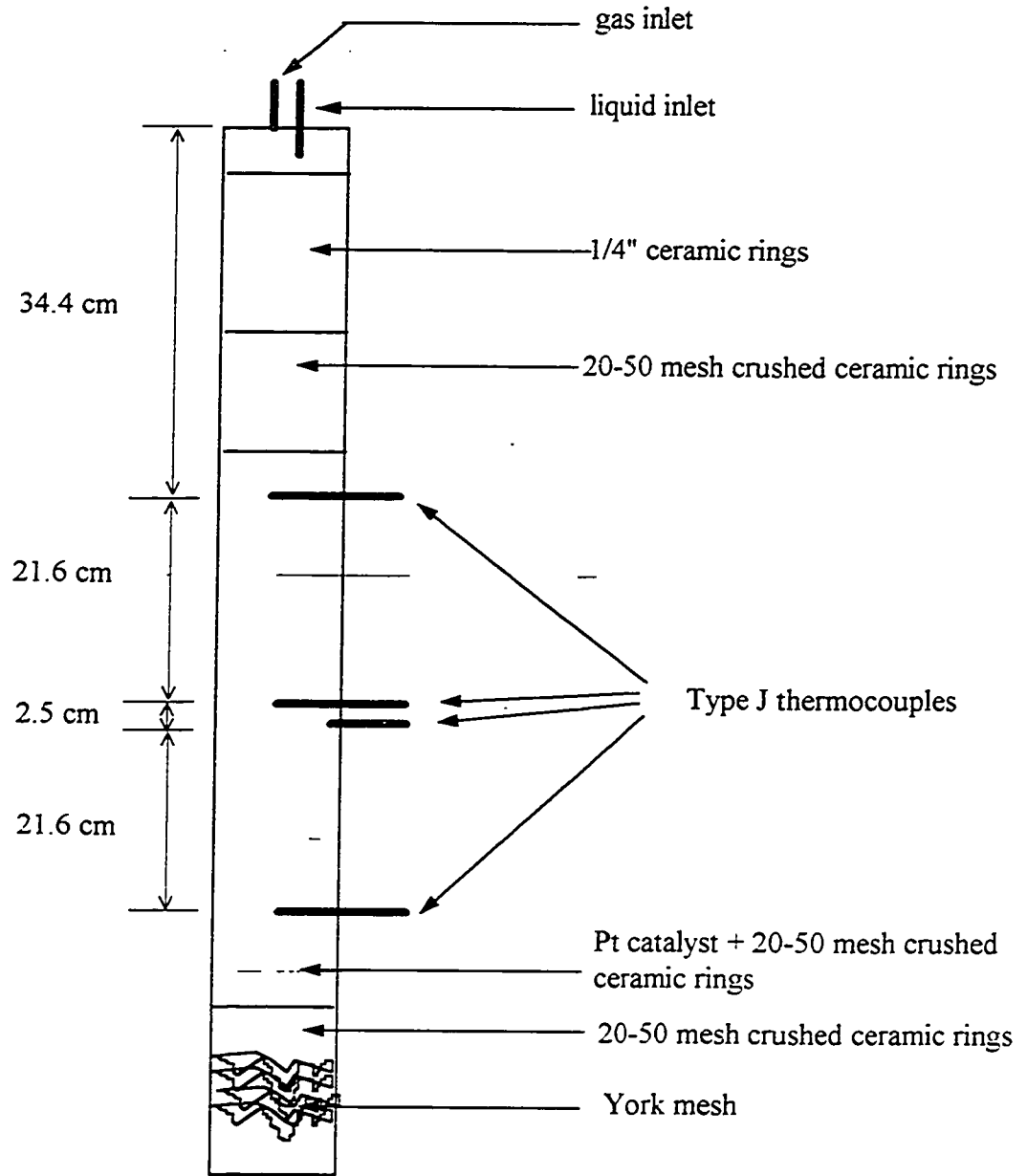
Figure 3.3: Schematic of reactor bed packing, showing the placement of the thermocouples

3.3.2.2 Improving the Reproducibility

Before addressing the problems encountered with reproducibility of results, it is useful to understand the different flow regimes that occur in a trickle-bed reactor. The classic paper of Charpentier and Favier (1975) divides all results into foaming and non-foaming liquid. For non-foaming liquid systems, such as was encountered in this work, there are three well defined regimes as well as the transition regimes. Trickling flow is the low interaction (or gas-continuous) regime, where little interaction occurs between the gas and liquid. All of the experiments in this research were conducted in this regime. The pulse regime is characterized by considerable gas-liquid interaction. Transition from trickling flow to pulsing flow occurs when the gas and/or liquid flow is increased sufficiently. The third regime, the spray regime, occurs at very high gas and low liquid flow rates.

Clues to the reproducibility problems can be found in the literature. In a trickle-bed reactor, the liquid phase flows downward in rivulets and may cover only a fraction of the external surface of the particles especially at low superficial velocities. The rate of reaction for partially wetted catalyst particles may be higher or lower than that obtained with completely wetted particles, depending on whether the limiting reactant is present only in the liquid or in both flowing phases. When the limiting reactant has a low vapour pressure at the operating conditions, decreasing the wetting efficiency decreases the liquid-solid mass transfer area and the active surface of the catalyst, respectively, causing the rate of reaction to drop (Herskowitz and Smith, 1983).

The method of reactor start-up often plays a role in reactor performance, particularly in the gas continuous regime, where the liquid trickles over the packing. Two

separate groups (Kan and Greenfield, 1978, 1979; Christensen et al., 1986) studied the hydrodynamics of trickle-bed reactors (cocurrent downflow of gas and liquid) and observed that the pressure drop and liquid holdup for specified gas and liquid flow rates were dependent on the manner in which the flows were established. The multiplicity was intimately connected with the liquid distribution in the bed.

Both Kan and Greenfield (1978, 1979) and Christensen et al. (1986) agreed that the multiplicity of steady states was the result of both rivulet and film flows occurring. Christensen et al. (1986) were able to observe the flow in the column. Starting from no liquid flow, as the liquid flow began, the liquid was seen to move down the column in a few large rivulets. Subsequently, liquid traveled down these rivulets and did not appear to spread any more. The rivulets were apparently very stable. On increasing the liquid flow, the rivulets would grow in size, but seldom in number. When pulsing was reached, the liquid was spread evenly over the packing (film flow). On reducing the liquid flow rate, this evenly spread distribution was apparently maintained and no coalescence of these films into rivulets could be observed.

The presence of multiple hydrodynamic states in trickle flow is significant in the start-up and operation of trickle-bed reactors in the trickle regime. Two common start-up practices are:

1. Establish the liquid flow rate and then introduce the gas.

2. Establish the desired gas flow rate and then introduce the liquid.

The first strategy is better than the second one. For the best distribution of liquid in the reactor, the liquid flow should be increased to its highest possible value or until pulsing

inception, whichever is lower, and subsequently reduced to the desired operating point (Christensen et al., 1986).

Once one is aware of this phenomenon, other references concerning the start-up procedures can be found in the literature. Herskowitz and Smith (1978) reported better reproducibility of data when the column was initially filled with liquid and the liquid flow was increased, rather than decreased; the position of the rivulets was more stable with increasing flow. Enright and Chuang (1978) found that catalyst bed flooding was required before maximum performance was achieved.

However, in this study, more than consistent start-up procedures were required to achieve reproducible results. Part of the answer lies in the results of Enright and Chuang (1978) who studied deuterium exchange between hydrogen and water over a hydrophobic catalyst in a fixed-bed reactor. They found that flooding the catalyst bed prior to start-up led to the maximum performance. In addition, they diluted the catalyst bed with hydrophilic support of the same shape and size as the catalyst, such that they compared a 100% catalyst bed with ones that were 50% and 25% catalyst, with the balance being hydrophilic support. The performance of the diluted bed was as good as or better than that of the undiluted bed. On its own, the hydrophobic support led to poor liquid distribution.

At this point in this study, a careful inspection of the catalyst bed following a run revealed that parts of the bed were dry, and gave no indication of having been wetted at any point during the run. Different start-up procedures were tried. As shown in Table 3.2, the procedure used had a substantial impact on the conversion achieved. The lowest conversion was observed when the oxygen flow was turned on first and the liquid flow

was not turned on until the operating pressure was reached. The highest conversions

resulted when the maximum amount of liquid was used to start-up the reactor.

Table 3.2: Effect of different startup procedures.

Run Number	Start-up procedure	% conversion of EG to CO_2	% conversion of EG
951030	Switched on both liquid and gas at startup	11.54	25.5
951031	Switched on gas; on reaching operating pressure, switched on liquid	7.32	18.7
951102	Started with liquid at high flow, with small amount of gas; gradually brought to operating conditions	16.90	31.4
951108	Same as 951102, only maintained high liquid/low gas flow rates for a period once operating pressure was reached	22.06	54.6

All runs are with the same catalyst bed (~80 g, 1% Pt on styrene divinyl benzene

copolymer). Operating conditions were as follows: temperature 80°C; O_2 pressure

300 kPa; O_2 flow rate 580 and 590 mL/min; liquid flow rate between 6.4 and 6.6 mL/min;

ethylene glycol concentration 0.18 M.

Separately, a run was carried out where the catalyst bed was flooded with liquid and allowed to drain. The liquid flow rate was higher than the previous runs (10 mL/min as compared with 6.5 mL/min) so the results cannot be directly compared. At 80°C, 42% conversion of ethylene glycol was achieved with 20% being converted to carbon dioxide. Although the operating conditions were not the same and hence there was a lower liquid residence time, it appears that flooding the catalyst bed prior to startup did improve performance. It is possible that not draining the reactor prior to startup would have resulted in higher conversion. This conclusion is based on the result of Enright and Chuang (1978) who found that even a brief interruption of the liquid flow caused the reaction rate to drop. However, both high liquid flow rates during startup and flooding the bed prior to startup were not entirely successful because the catalyst floats in water. Therefore, another method was required to improve liquid distribution. Crushed ceramic rings of the same size as the catalyst were added to the catalyst bed to improve the liquid distribution and help maintain the integrity of the bed.

Poor liquid distribution does not explain why the reactor performance improved with time. One would expect that liquid distribution would vary from one startup to the next, but not that it would consistently improve with running time (see Table 3.1). Figure 3.4 shows one run where the reactor was not shut down at any time. The rate of conversion of ethylene glycol increased over the duration from 24 % at the first sample point to 36 % at the end of the run.

In the past, hydrophobic catalysts have been used for isotopic exchange of deuterium between water and hydrogen (Enright and Chuang, 1978, Kawakami et al.,

32
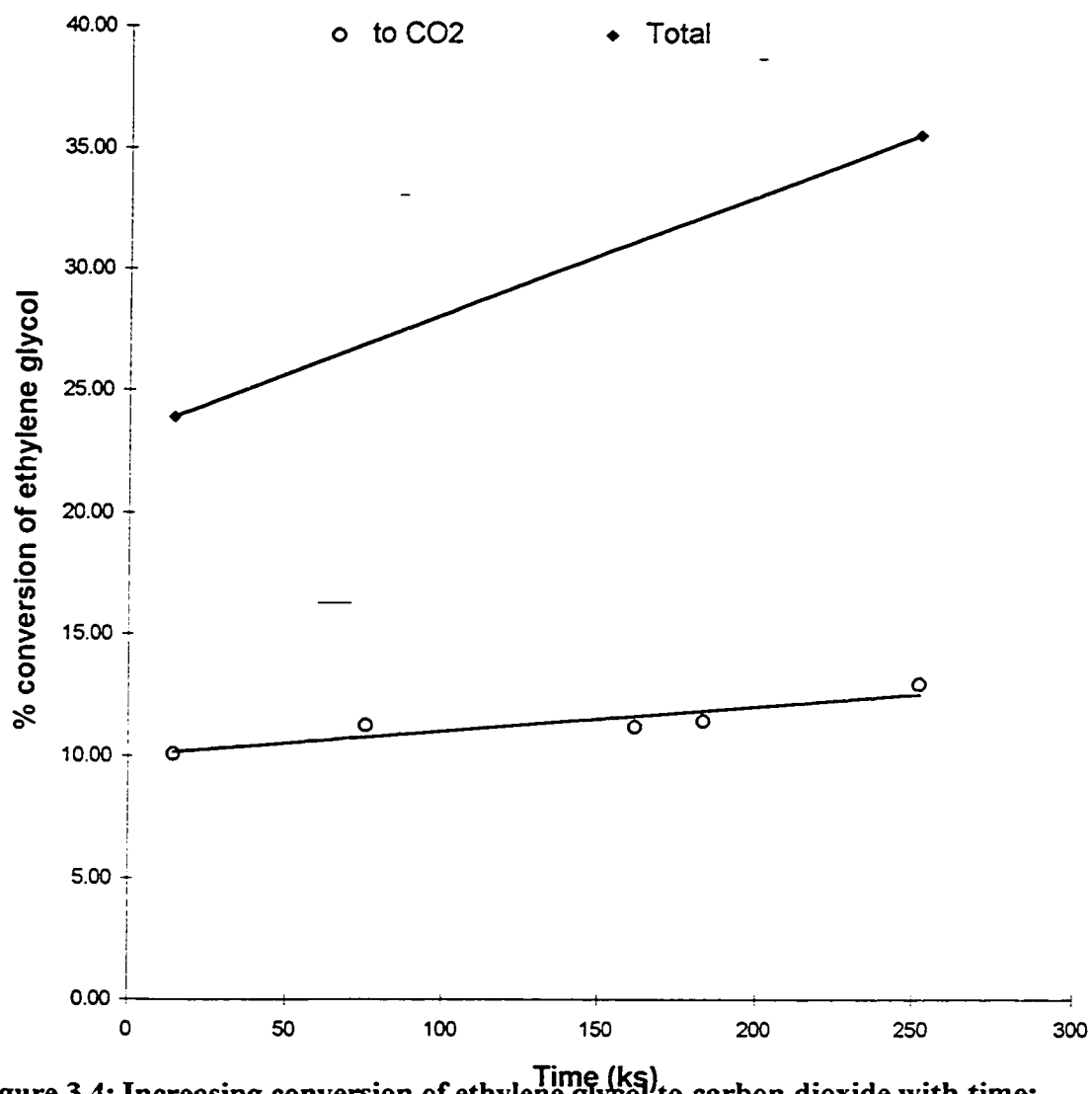
Figure 3.4: Increasing conversion of ethylene glycol to carbon dioxide with time; Run 950905.

Operating conditions: temperature 80°C; O_2 pressure 300 kPa; O_2 flowrate 580 mL/min; liquid flow 4.65 mL/min; 0.18 M ethylene glycol in aqueous solution.

Note: 1 hour = 3.6 ks; 1 day = 86.4 ks

1988), the oxidation of methanol in a water stream (Cheng and Chuang, 1992) and the partial oxidation of propylene (Liang et al., 1997). In all cases, the volatility of the reactant in the liquid phase ensures that a sufficiently high vapour pressure at the operating conditions, such that the reaction proceeds rapidly in the gas phase. The hydrophobic nature of the catalyst served to limit adsorption of water into the pores of the catalyst and thereby increases the accessibility of the hydrogen and oxygen to the catalyst surface. Both these gases have low solubilities in water, and hence limit the reaction rate when a traditional hydrophilic support is used.

However, in this work, one of the reactants studied was ethylene glycol, a semi-volatile organic compound. Its vapour pressure is plotted versus temperature in Figure 3.5. All of the experiments in this research were at temperatures of 120°C or less. The vapour pressure of ethylene glycol under these conditions is not sufficient for a reasonable rate of reaction in the vapour phase. Therefore, unlike previous work with volatile compounds, it was not enough to ensure uniform flow distribution of the liquid. It was also necessary to ensure complete wetting of the catalyst. In this study, the primary purpose of the hydrophobic catalyst was to concentrate the ethylene glycol onto the catalyst sites. However, before this could happen, the ethylene glycol, either in the water or the gas phase, had to contact the catalyst. One of the methods to improve the contact was to presoak the catalyst in ethylene glycol; the conversion improved dramatically (see Figure 3.6). Following this treatment, the catalyst behaves essentially like a hydrophilic catalyst, in that the liquid solution wets the surface. It would be instructive to compare the liquid film thickness on this hydrophobic catalyst support to that found on a hydrophilic

34
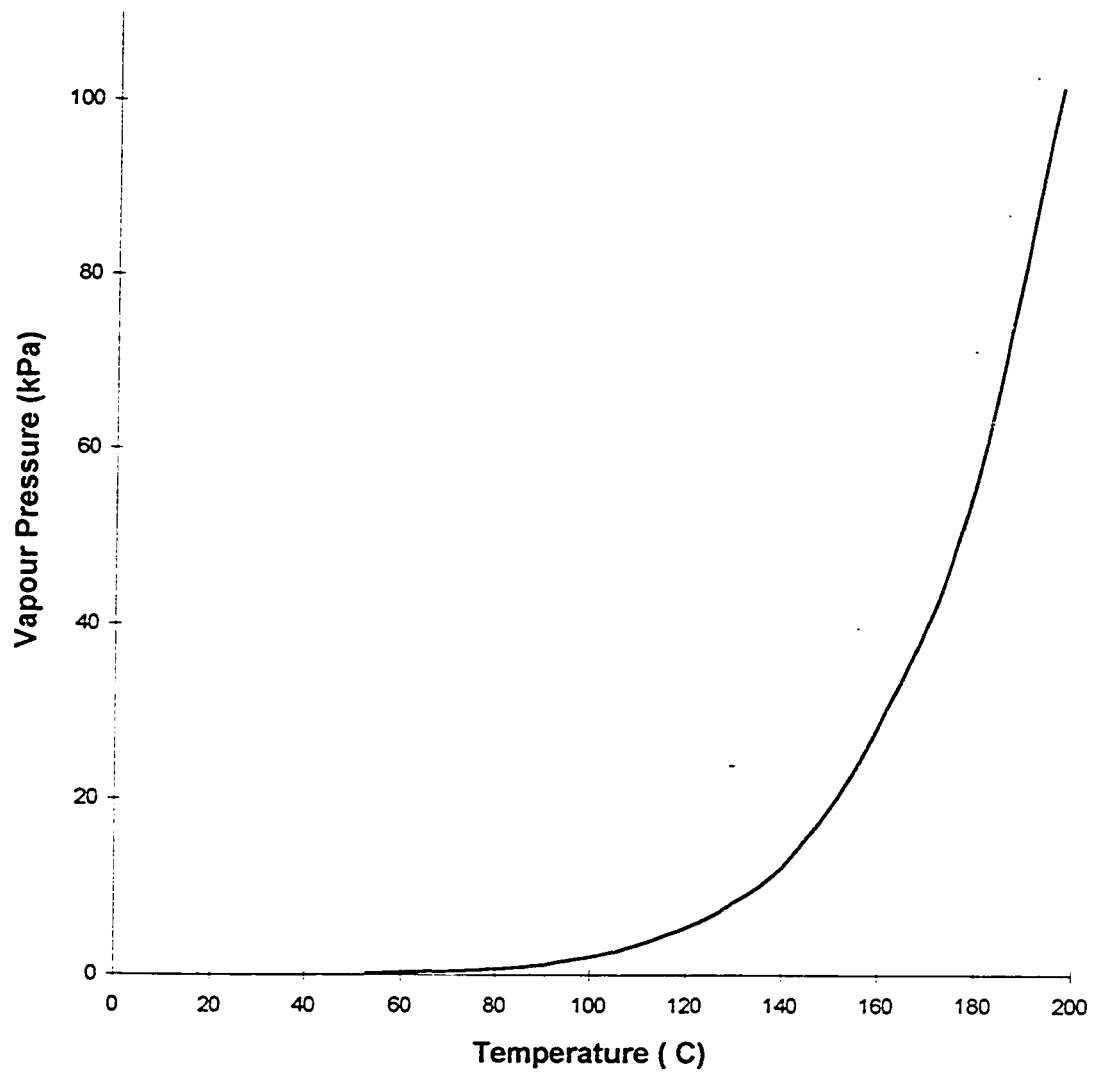
Figure 3.5: Vapour pressure of ethylene glycol as a function of temperature.

Data from Perry's Handbook of Chemical Engineering (Perry and Green, 1984)
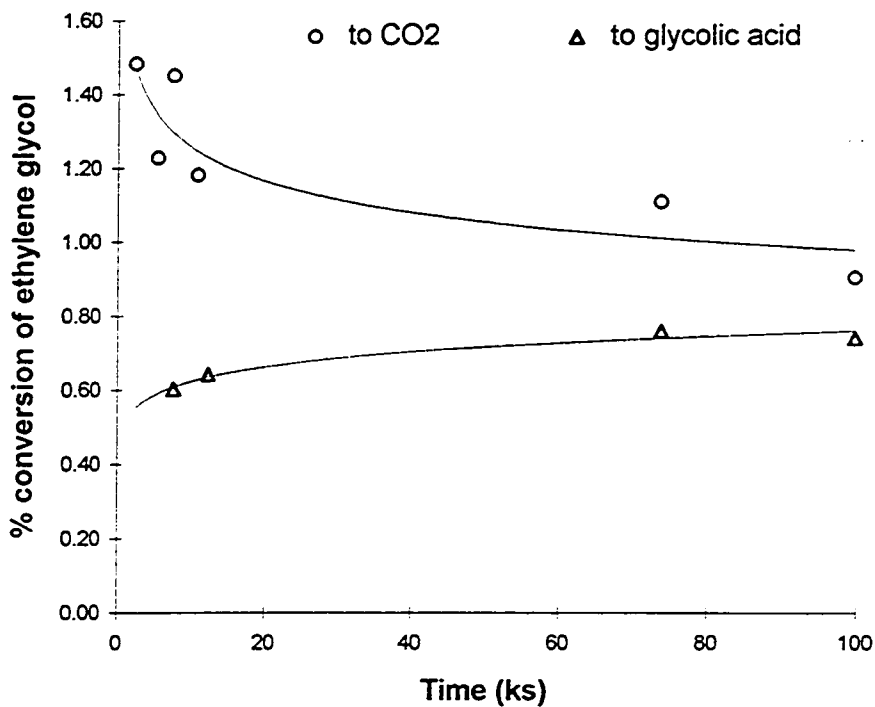
Figure 3.6a: No presoaking of catalyst; just mixed with crushed ceramic rings; Run 970307
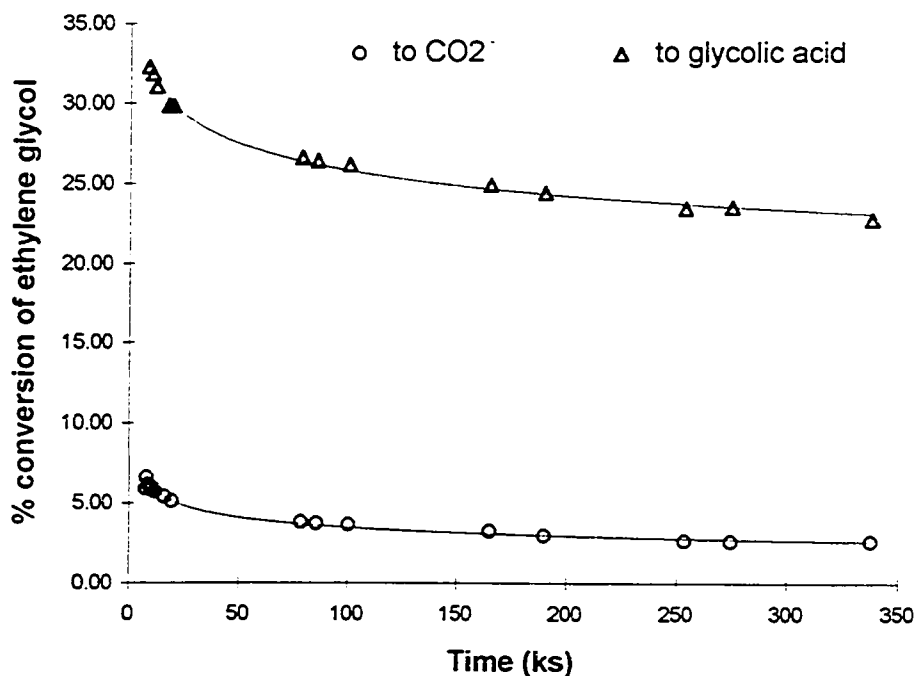
Figure 3.6b: Catalyst presoaked in ethylene glycol and mixed with crushed ceramic rings; Run 961202.

Both runs were at 80°C, 300 kPa O_2 pressure, 450 mL/min O_2 flow rate, 20 mL/min liquid flow rate; ethylene glycol concentration 0.090 M

support. No comparable hydrophilic catalyst support was tested in the reactor so this comparison was not possible. A thinner liquid film would be an advantage, since it would decrease the distance oxygen would have to diffuse through the liquid to the catalyst surface.

3.3.3 Mass Transfer

In a trickle-bed reactor (cocurrent downflow of gas and liquid), at sufficiently low liquid and gas flow rates, the liquid trickles over the packing in essentially a laminar film or in rivulets, and the gas flows continuously through the voids in the bed. Sometimes termed the gas-continuous region, this type of flow is usually encountered in laboratory and pilot-scale operations, as was the case in this study. As gas and/or liquid flow rates increase the behaviour observed is described, successively, as rippling, slugging or pulsing flow. At high liquid rates and sufficiently low gas rates, the liquid phase becomes continuous and the gas passes in the form of bubbles; this is sometimes termed dispersed bubble flow (Satterfield, 1975).

The gas continuous regime often suffers from mass transfer limitations, due to the low interaction between the gas and liquid. Therefore, at this point, experiments were undertaken to measure mass transfer resistances. If the catalyst was completely surrounded by liquid, dissolved gas must be transported from the gas-liquid interface to the bulk liquid and then the liquid-solid interface. Satterfield (1975) provides a useful starting point in these experiments. Satterfield states that most commonly the mass transfer limiting reactant is the gaseous species; the gaseous reactant is usually present in

substantial stoichiometric excess and in relatively high fractional concentration in the vapour phase as well as being relatively insoluble in the liquid. If this is the case, it is valid to assume no significant mass transfer resistance in the gas phase.

In these experiments, Satterfield's criteria were met at higher oxygen pressures. The catalyst was presoaked in ethylene glycol. This treatment ensured complete catalyst wetting. Oxygen was the gas phase reactant. Oxygen has a low solubility in water. The majority of these experiments were carried out with a total pressure of 347 kPa where 47 kPa represents the vapour pressure of water at 80°C. The remainder of the vapour phase was oxygen and nitrogen. When the oxygen pressure was 300 kPa, no gas phase resistance occurred. The gas phase consists only of oxygen and water vapour under these conditions. At oxygen pressures of 150 kPa, this represented a large fraction of the vapour phase and a stoichiometric excess of oxygen. However, at oxygen pressures of 25 and 50 kPa, mass transfer limitations were observed and were thought to originate from the gas phase limitations (see Chapter 6, Figure 6.8). Additional experiments would be required to determine the point at which oxygen levels are such that mass transfer limitations occurred.

Checking for mass transfer limitations is a two step process. First external mass transfer limitations must be eliminated. Then internal mass transfer or pore-diffusion limitations are examined. Satterfield (1970, 1975) recommends an additional step in checking for external mass transfer limitations. He cautions that even with substantial mass transfer limitations throughout the liquid film, the observed rate of reaction may change relatively little with a large change in flow rate. Therefore, having assumed no mass

transfer within the gas phase, a mass balance can be done on the oxygen diffusing through the liquid film around a single spherical pellet (diameter d_p). Essentially, the rate of reaction of oxygen must be equal to the rate of mass transfer of oxygen:

(rate of reaction)(volume of sphere) = (rate of mass transfer through liquid)

or

$$r \frac{\pi d_p^3}{6} = k_{ls} \pi d_p^2 \left(c^* - c_s\right) \tag{3.1}$$

where r is the rate of reaction in $(mol \cdot s \cdot cm^{-3})$, k_{ls} is the overall liquid mass transfer coefficient $(cm \cdot s^{-1})$, c^* is saturation concentration of oxygen in water, and c_s is the oxygen concentration at the surface of the catalyst. For significant mass transfer limitations. $c_s < 0.95c^*$ and:

$$\frac{10 \, r \, d_p}{3c^*} > k_{ls} \tag{3.2}$$

The value of k_{ls} can be estimated from D_{AB}, the diffusion coefficient, divided by the average film thickness, Δ, where Δ can be approximated as the external liquid holdup, H_o, divided by the external catalyst surface per unit bed volume, a:

$$k_{ls} = \frac{D_{AB} \, a}{H_c} \tag{3.3}$$

Experimental checks for external mass transfer were carried out at 80 and 90°C. The bed length and gas and liquid flow rates were increased proportionately. For example, the flow rates were doubled when the bed length was doubled. Two different gas flow rates were used for each catalyst bed loading. No difference was found between the two gas flow rates. When the conversion stopped changing with increasing flow rates, external

mass transfer effects were no longer rate limiting (see Figures 3.7 and 3.8). A liquid flow rate of 20 mL/min was selected for the standard operating conditions. With some of these data, a mass balance as per equation 3.1 was carried out as an additional check (see Appendix B.1).

At this point, one further check was carried out to ensure that internal diffusion was not introducing any mass transfer limitations. Two different catalyst sizes were prepared (20 to 50 mesh and > 50 mesh) and tested at the same conditions. The results are shown in Figure 3.9. No significant differences were observed between the two catalyst particle sizes at 80°C; therefore the reaction rate was not limited by internal diffusion. At 90°C, the reaction rate appears to be slightly faster with the smaller particles (>50 mesh), indicating that internal diffusion was limiting the reaction rate. Further experiments should be carried out at this temperature before kinetic work is attempted.

Based on these results, the reaction kinetics should not be influenced by mass transfer effects up to temperatures of 80°C as long as the oxygen pressure is high enough that mass transfer limitations in the gas phase are not rate limiting.
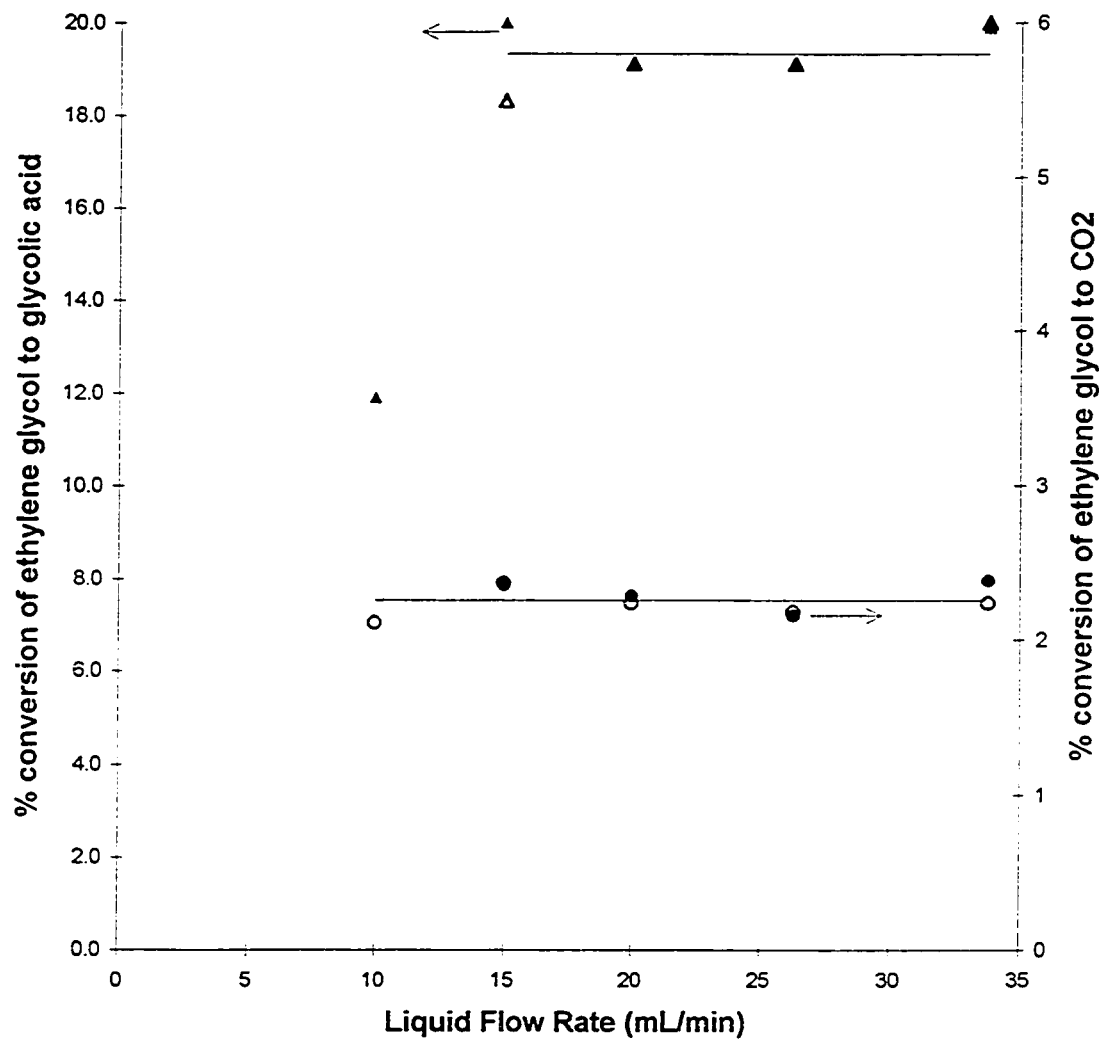
Figure 3.7: Checking for external mass transfer limitations at 80°C and 300 kPa O_2 pressure.

Open and closed symbols represent two different ratios of the gas flow rate to the catalyst volume for each liquid flow rate. Data for figure in Table B.1.
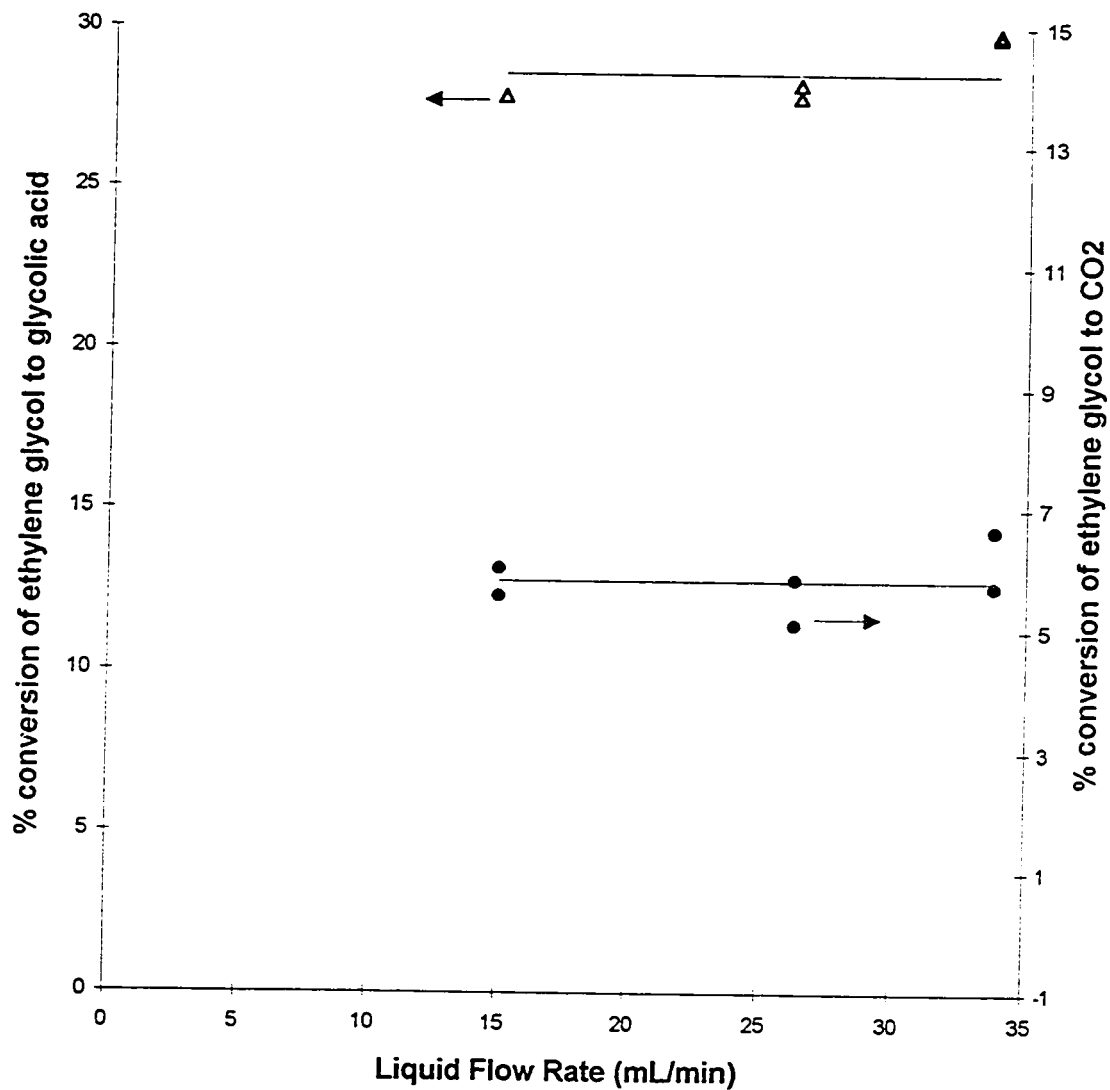
Figure 3.8: Checking for external mass transfer limitations at 90°C and 300 kPa O_2 pressure.

Open and closed symbols represent two different ratios of the gas flow rate to the catalyst volume for each liquid flow rate. Data for figure in Table B.2.
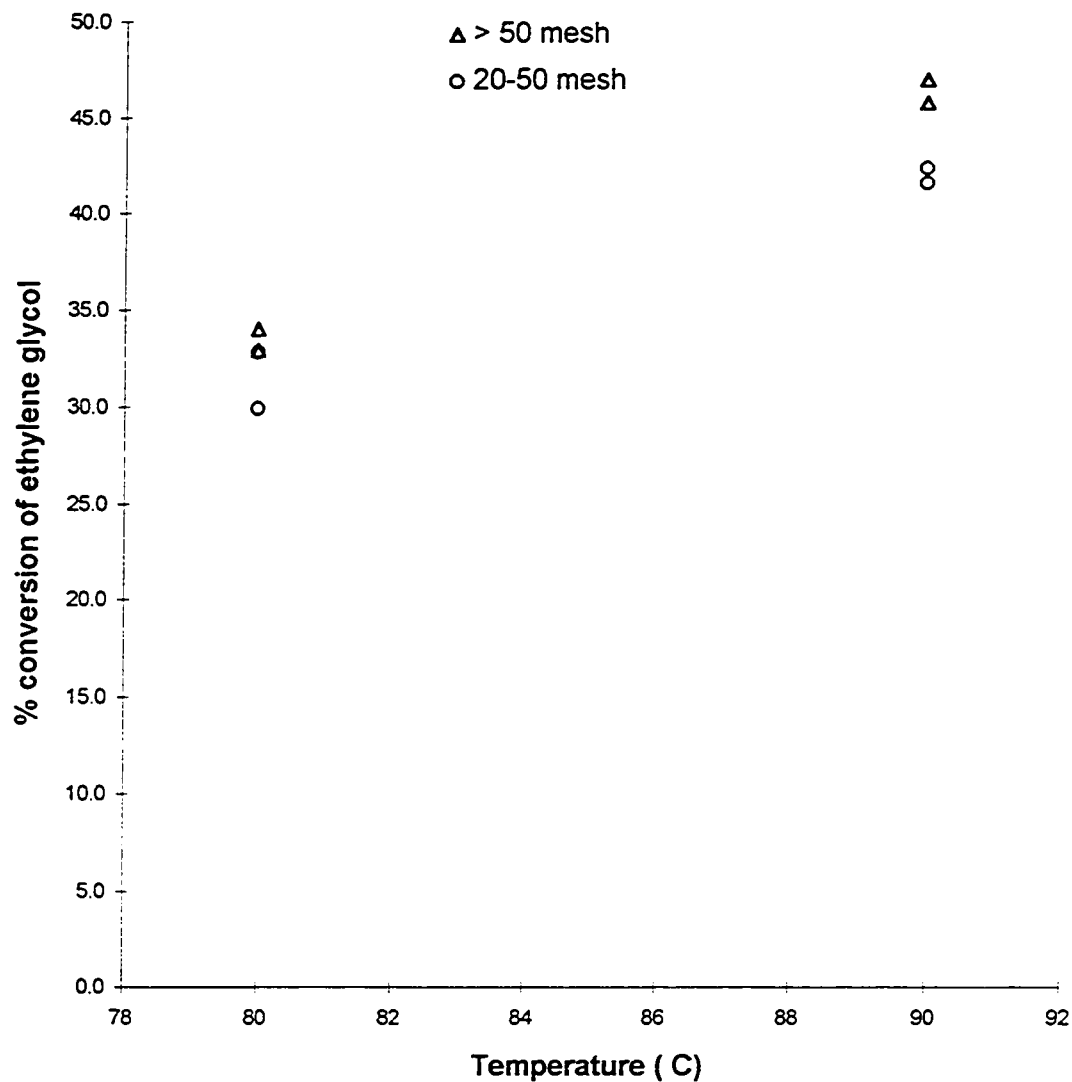
Figure 3.9: **Checking for internal diffusion effects: a comparison between two different sizes of catalyst.**

Oxygen pressure 300 kPa; liquid flow rate 15 mL/min; ethylene glycol concentration 0.18 M; two different gas flow rates were used for each catalyst size. Data for figure in Table B.3.

3.3.4. Mass Balance

An essential aspect of understanding the chemistry and kinetics of the reaction is a closed mass balance with respect to carbon. All of the carbon entering the reactor as ethylene glycol must be accounted for in the exit streams; otherwise possible accumulation in the reactor cannot be ruled out.

Before carrying out any reactions, a blank run was done using all of the materials normally used to pack the reactor with heat treated SDB in place of the platinum catalyst. No reaction products were observed in either the gas or liquid effluent streams. The pH of the liquid effluent was essentially neutral at 6.5. In the effluent water, 0.6 % more ethylene glycol was detected than was fed into the system. This is not significant and could arise from error in the measurements or could possibly arise from a small amount of the ethylene glycol used to presoak the SDB being washed off. From this result, two conclusions can be drawn: (1) None of the packing materials apart from the platinum on the catalyst influenced the reaction rate. (2) During the reaction, the SDB did not adsorb ethylene glycol in amounts exceeding the initial presoak.

Because not all of the reaction products could be positively identified (see Chapter 5, The Chemistry), it was not possible to quantify individually each product in the effluent. The first approach taken was to react all of the ethylene glycol to form carbon dioxide and water. It was essential in these experiments that all of the ethylene glycol be converted to carbon dioxide. Any products remaining in the liquid phase risked being overlooked. In both of the experiments reported here, the mass balance on carbon did not close (see Table 3.3). In the first experiment, five percent extra carbon was converted to

carbon dioxide. This experiment was conducted near the beginning of the research; it is probable that the results were due to fluctuations in the system. In the second experiment, eight percent of the carbon was unaccounted for. This may in part be error. However, the results should not be discounted. Any products in the effluent stream other than glycolic acid and carbon dioxide were not measured. Also, it may indicate that some of the carbon remained in the reactor.

Table 3.3: **Mass balance on carbon with complete conversion of ethylene glycol.**

| RUN | % conversion of ethylene glycol | | | Mass Balance |
	to CO_2	to GA	overall	% EG unaccounted for
95.06.27	105	---	100	-5
96.02.02	89	3	100	8

Conditions for Run 95.06.27: Oxygen pressure 300 kPa; oxygen flow rate 560 mL/min; liquid flow rate 4.6 mL/min; ethylene glycol concentration 0.18 M; no presoak of catalyst.

Conditions for Run 96.02.02: Oxygen pressure 300 kPa; oxygen flow rate 530 mL/min; liquid flow rate 10 mL/min; ethylene glycol concentration 0.18 M; catalyst presoaked in methanol.

The carbon mass balance was checked further in an experiment with only partial conversion of ethylene glycol. Total organic carbon (TOC) analysis was done on the liquid effluent to ensure that all of the products in the liquid phase were accounted for in the mass balance. This combined with the carbon dioxide in the gas phase was compared with the amount of carbon in the feed stream. These results indicated that initially as much as five percent of the organic material remained in the reactor (Table 3.4). With increasing time-on-stream, this imbalance declined appreciably. After approximately two days (167 ks) of running, only 0.6 mg/min or 1.5 % of the carbon remained unaccounted for. The results from the blank run indicated that additional ethylene glycol was not adsorbed by the SDB. A likely explanation for the missing carbon is that a small degree of oligimerization occurred in the reactor. These partial oxidation products accumulated faster than the ethylene glycol was removed from the catalyst and support; as the catalyst deactivated, less of the partial oxidation products were produced, and as a result less remained in the reactor. Once sufficient time elapsed (dependent on the operating conditions), a balance between accumulation and removal (either via reaction, or desorption) would be reached, a steady state would be reached, and the mass balance closed.

Table 3.4: Mass balance on carbon over time for Run 970422.

	← IN →	← OUT →		
Time	**Carbon**	**CO₂**	**TOC in effluent***	**Mass Balance IN-OUT**
ks	mg/min	mg/min	mg/min	mg/min
1.8	43.1	4.5	36.3	2.3
20	43.1	2.6	39.5	1.0
167	43.1	2.0	40.5	0.6

Operating conditions for Run 970422: 80°C; O_2 pressure 300 kPa; O_2 flow rate 450 mL/min; liquid flow rate 20 mL/min; 0.090 M ethylene glycol.

*TOC analysis by Norwest Labs, Edmonton using the auto persulphate/UV digestion colorimetric method.

4. The Catalyst

4.1 Choice of Catalyst

A supported platinum metal catalyst was selected for the experiments. Platinum group metals are known to have catalytic activity in a wide range of oxidation reactions including alcohols (Butt and Petersen; 1988). Golodets (1983) states that the resistance of metals to the formation of bulk oxides is of primary importance. At temperatures of less the 100°C, minimal formation of platinum oxide is expected. Furthermore, in similar systems, platinum tends to favour deep oxidation whereas palladium generally leads to partial oxidation products. Sawyer and Abraham (1994), from a survey of the literature, report that in all cases, intermediates when a platinum catalyst was used were equal to or less than the intermediates found with non-platinum catalysts. Both the variety and the amount of intermediates were reduced by the addition of platinum.

A hydrophobic support, as opposed to a more conventional hydrophilic support such as alumina, was used for the platinum. The concept behind this choice was that, in an aqueous solution, organic compounds would be preferentially adsorbed onto a hydrophobic support. In this manner, relative to a hydrophilic support, the organic compounds would have increased concentrations on the catalyst support. Previously, hydrophobic catalysts have been used to reduce or eliminate deactivation by water vapour owing to capillary condensation and slow desorption of the water vapour. In the work by Cheng and Chuang (1992), methanol was successfully stripped and oxidized in one

column using a hydrophobic catalyst (platinum supported on ceramic rings coated with a small quantity of fluorinated carbon and Teflon), without any observed deactivation. Chuang et al. (1994) attributed the high activity and selectivity observed in the catalytic oxidation of formaldehyde to the hydrophobicity of the catalyst. Liang et al. (1997) attributed the high rate of reaction obtained in the partial oxidation of propylene to acrylic acid to the direct contact of the gas phase reactants with the catalyst. Since the catalyst surface was not wetted by water, the gas phase reactants did not first have to dissolve in the water present to reach the catalyst.

4.2 Catalyst Preparation

Platinum was impregnated onto spheres (20 to 50 mesh) of styrene divinyl benzene copolymer (SDB), which was purchased from HayeSeparations. Either a 4.0 (wt)% Pt solution from Johnson Matthey, or a 5.5 (wt)% Pt solution from Colonial Metals, Inc. was used as the platinum source. Both solutions were tetraamine platinum (II) nitrate ($[Pt(NH_3)_4](NO_3)_2$) in water. To wet the catalyst, isopropanol was mixed with water in the ratio of 1.0 to 3.6. For every 100 g of catalyst being prepared, 225 mL of isopropanol in water solution was used. The catalyst support was added to this solution and allowed to stand with periodic, gentle swirling, for about 20 minutes, until bubbling stopped. The cessation of bubbling indicated that the pores of the catalyst were filled with liquid. At this point, the appropriate amount of the platinum solution for the desired final platinum loading was added to this mixture. This procedure was not completely standardized until the batch of catalyst made in January 1996.

For the standardized procedure, the beaker containing the catalyst solution was then placed on an inclined, rotary evaporator under an infrared lamp. The lamp was not turned on for the first 15 minutes to ensure that a uniform distribution of platinum was achieved. Once the infrared lamp was switched on, the beaker containing the catalyst was rotated until a buildup of static charge on the SDB indicated that it was dry; generally 20 to 24 hours were allowed. Care was required in drying the catalyst to ensure that it did not char. The lamp was placed 3 to 5 cm from the mouth of the beaker. Any closer than this and the risk of charring was high.

The impregnated SDB was placed in a 3.5 cm diameter U-tube. Hydrogen flowed at a rate of 100 mL/min over the SDB at 180°C for 18 hours to reduce the platinum salt to platinum metal. The U-tube with the SDB was allowed to cool and then purged with nitrogen, prior to heating it in air with a flow rate of 100 mL/min (ambient conditions). The SDB was heated to 90°C for one hour, and then heated at a rate of 1 K/min to 180°C. The temperature was kept at 180°C for 6 hours to calcine the catalyst.

4.3 Preparation of the SDB

Before using any blank SDB support in the reactor, it was pretreated so that it would as closely as possible resemble the support with platinum metal deposited on it. The same process as that used to make catalyst was attempted to prepare blank catalyst support. This method was unsuccessful. Some time during the final calcination step, the heating of the SDB in air at 180°C, the SDB charred. The charring was worst at the entrance to the U-tube and at the radial centre of the SDB bed. In addition a strong

smelling liquid had soaked the glass wool at the exit to the reactor. This liquid was a result of partial decomposition of the SDB. It is concluded that there is a residue of organic material on the SDB which is harmlessly oxidized at lower temperatures in the presence of activated platinum. The presence of a residue on the SDB is supported by the observation of a strong smell on some of the lots of untreated SDB. In the absence of platinum, the residue reacts with oxygen at higher temperatures. The reaction is sufficiently exothermic that the SDB is charred. This mechanism also explains why it is important not to dry the slurry of SDB too quickly during the impregnation step. At this stage, the platinum is in the form of an inactive salt. If too much heat is added to the beaker, the residue on the SDB reacted exothermically with the oxygen in the air.

By lowering the temperature to 165°C, some degree of success in preparing the support was achieved. It was not possible to determine the exact temperature that was required, because it varied with the batch of SDB support. Since the charring was worst at the entrance to the U-tube, it is believed that reducing either the air flow or the percentage of oxygen in the feed would help ameliorate this problem.

As further evidence to explain the behaviour of the catalyst support, the untreated SDB and the platinum catalyst were extracted with methanol. Then, the methanol from each extraction was injected into a gas chromatograph. No peaks apart from that of methanol were observed in the case of the catalyst. However, several peaks were observed in the extract of the untreated SDB. This result is consistent with the theory that a residue on the SDB was responsible for the charring observed.

The nature of the residue was not determined. The supplier of the SDB triply washed the SDB in acetone as the final preparation step. The normal boiling point of acetone is 56°C, so it is highly unlikely that this is responsible for the charring although it may be in part or wholly responsible for the strong smell found on some lots of SDB. When the styrene divinyl benzene copolymer is manufactured, styrene is used as the starting material. Styrene is soluble in acetone; however, depending on the effectiveness of the acetone wash, styrene may be the residue on the SDB.

4.4 Catalyst Characterization

To understand the behaviour of a catalyst better, it is helpful to characterize its key properties. In this study the following properties were determined: the surface area and pore size distribution of the catalyst support, both with and without platinum; the average metal crystallite size was measured and used to calculate the metal dispersion of the platinum.

4.4.1 Data from BET Measurements

The surface area and the pore size distribution of the SDB were measured on an Omnisorp 360 analyzer, an instrument which uses nitrogen to measure the BET surface area. One of the main reasons for supporting a noble metal catalyst is to increase the amount of metal surface area available for reaction. Generally, the larger the surface area available for supporting of the metal, the greater the dispersion of metal that can be achieved. There is an obvious upper limit on this; if the high surface area is at the expense

of pore sizes, the pores may become too small for the metal atoms to access the pores. This surface area will not affect the metal dispersion. Furthermore, the small pores in particular are susceptible to pore blockage both when the catalyst is being made and during operation. Table 4.1 shows the results from the BET measurements for both untreated catalyst support and freshly prepared catalyst.

All of the samples measured had very high surface areas. This is the nature of the SDB support. There were only slight differences observed between the catalyst support and the prepared catalyst with the exception of lot 395 and the catalyst prepared using it. The slight differences can be explained as the result of the platinum crystallites either blocking pores or creating new surface, or variability within the lot. In the case of lot 395, it is possible that the batch of SDB had a higher degree of variability than was typical. Some difference in total surface area measured occurred between lots, and in the case of lot 150, it is suspected of affecting the platinum dispersion. The pore size distribution varied significantly between different lots of the SDB. Some of the variability of platinum dispersion and hence catalyst activity and deactivation is likely a result of the different distribution of pore sizes.

Table 4.1: Pore size distribution and surface area from BET measurements for various batches of catalyst support and catalyst.

Sample	lot 91	lot 91 +1.0% Pt	lot 150 +1.0% Pt	lot 395	lot 395 +0.34%Pt	lot 511 +0.34%Pt	lot 511 +0.34%Pt	lot 535	lot 535 +0.34% Pt
				←	Pore Volume (mL/g)	→			
Catalyst batch (if applicable)	NA	95.12.12	96.02.23/27	NA	97.06.27	97.01.20	97.03.07	NA	97.04.21
Pore Radius (nm)									
> 30	0.0	.00148	0.0	0.0	0.0	0.0	0.0	0.0	0.0
30-20	.00432	.00515	.00236	.00257	0.0	0.0	0.0	.00519	.00351
20-10	.00767	.00808	.01193	.03046	.05449	.0103	.00401	.04124	.03061
10-5	.02675	.02624	.05125	.1569	.2119	.09737	.07603	.1687	.1481
5-4	.1577	.1625	.1804	.07711	.07769	.1254	.1015	.07916	.08173
4-3	.2437	.2359	.1715	.1001	.09507	.1464	.1211	.09588	.1025
3-2	.1367	.142	.1374	.1271	.1103	.1494	.1529	.117	.1242
2-1	.09865	.1061	.1076	.1046	.09494	.119	.1324	.1123	.1011
Total pore volume above 1 nm	.6755	.6874	.6624	.5991	.6445	.6479	.5881	.6194	.5918
% of pore volume >5 nm	5.7	6.0	9.9	31.7	41.3	16.6	13.6	34.7	30.8
BET surface area (m²/g)	808	814	609	742	674	841	845	759	755

In addition to these samples, a reference sample 8571 of alumina with a published area of 158.0 m^2/g was measured. The measured area was 157.6 m^2/g.

4.4.2 Data from X-ray Diffraction

The mean crystallite size of the platinum was determined via the x-ray diffraction technique on a Philips x-ray diffractometer. The x-ray diffractometer measures the diffraction intensity as a function of diffraction angle, 2θ. The peak broadening is inversely proportional to the mean crystallite size. The Scherrer formula (Klug and Alexander, 1954; Cullity, 1956) relates the two:

$$t = \frac{0.9\lambda}{B \cos \theta_B}$$

where t = the diameter of the crystal line particle

λ = the wave length of the x-ray emissions (1.54178Å)

B = the breadth of the diffraction peak at half its maximum intensity, in radians

θ_B = the angle at which the maximum intensity occurs (Bragg angle).

See Appendix C for the values of B and θ_B used in the calculations. The diameter of the crystal particles is of value in comparing results from different catalysts, since the size of the crystallite sometimes affects the rate of reaction; more importantly, it can be used to calculate the metal dispersion.

Most reactions catalyzed by supported metals take place on the metal surface and often, as is the case here, the support is inert. It is useful when dealing with more than one catalyst (and hence different metal dispersions) to compare catalytic reaction rate per unit area of exposed metal (Gates, 1992). The dispersion, which is defined as the number of metal surface atoms divided by the total number of metal atoms impregnated on the catalyst, was calculated from the crystallite size by assuming the particles of platinum on the surface of the support were hemispheres (see Appendix C). Table 4.2 shows the

average crystallite size and the platinum dispersion for some of the catalyst samples

prepared.

Table 4.2: Mean crystallite size and platinum dispersion calculated from x-ray diffraction data.

Catalyst Batch	Description	Mean Crystallite size (nm)	Platinum Dispersion
95.12.12	1.0%Pt; lots 51 & 150	3.89	0.28
96.02.23/27	1.0%Pt; lot 150	4.62	0.23
96.09.05	0.34%Pt; lot 150	2.82	0.38
97.01.20	0.34%Pt; lot 511	2.85	0.38
97.03.07	0.34%Pt; lot 511	2.66	0.41
97.04.21	0.34%Pt; lot 535	4.04	0.27
97.06.27	0.34%Pt; lot 395	3.08	0.35

In this study the mean size of the crystallites was between 2.7 and 4.6 nm. For the

smallest particles, it was more difficult to estimate the crystallite size, because the peak

was broad and not very distinct. Figure 4.1 shows the results from the x-ray diffraction.

The peaks in the cases of catalyst samples 97.01.20 and 97.03.07 were quite broad and

difficult to analyze accurately. For this reason the dispersion calculated from these two

batches and that of 96.09.05 were considered indistinguishable. However, for
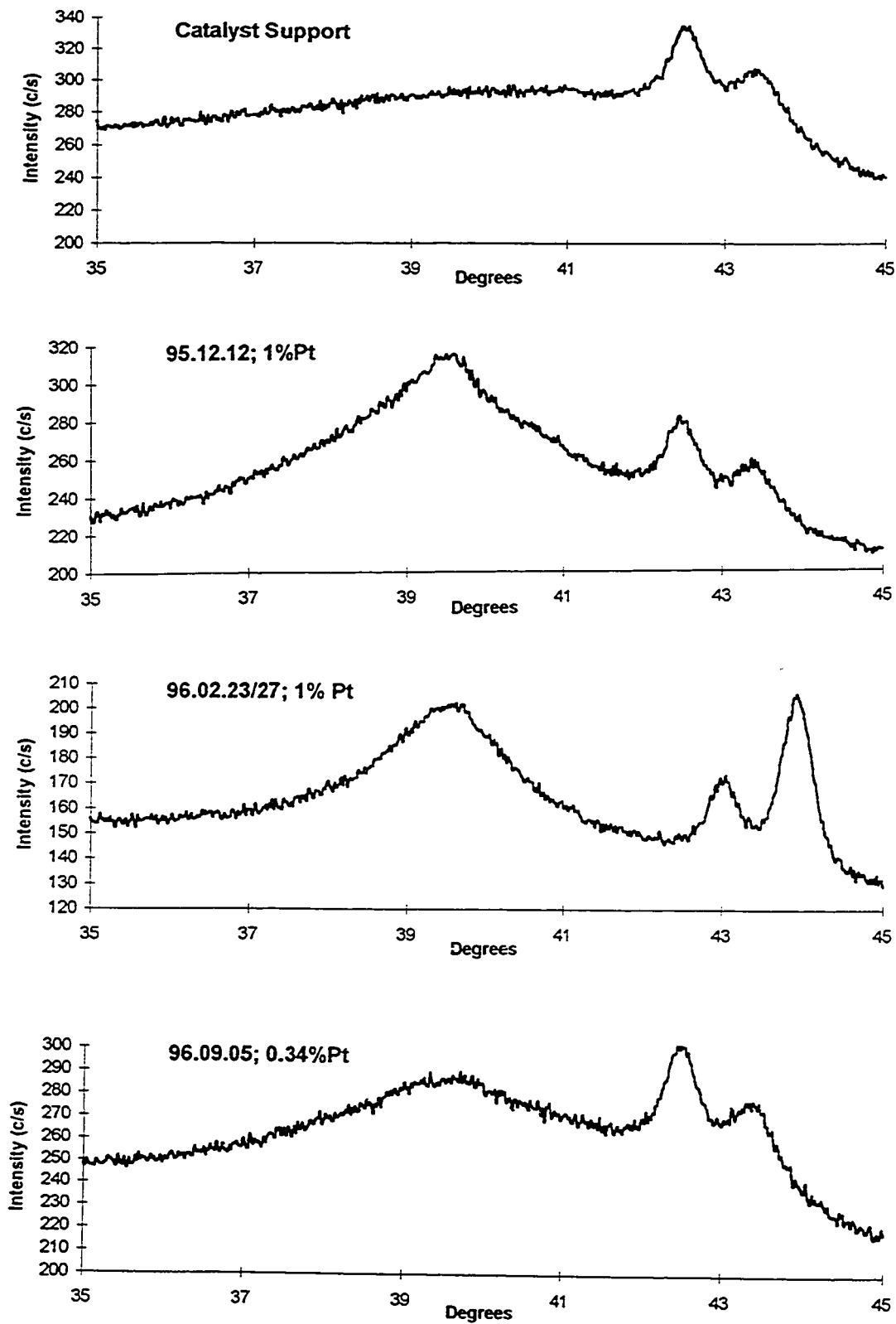
Figure 4.1: Results from x-ray diffraction measurements.
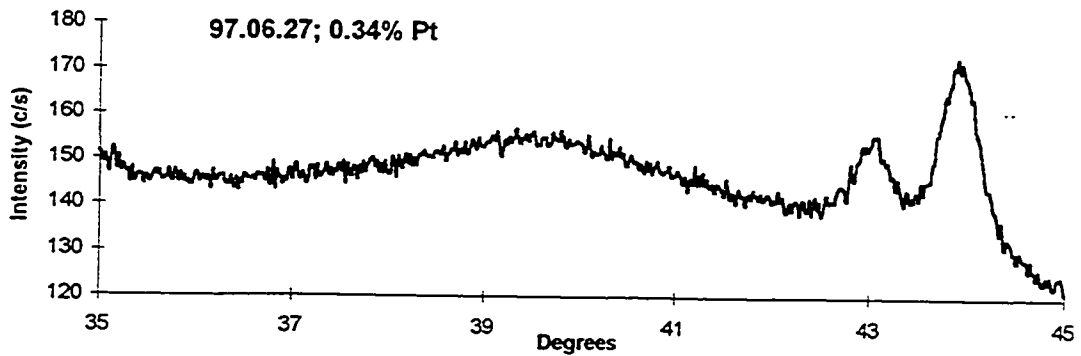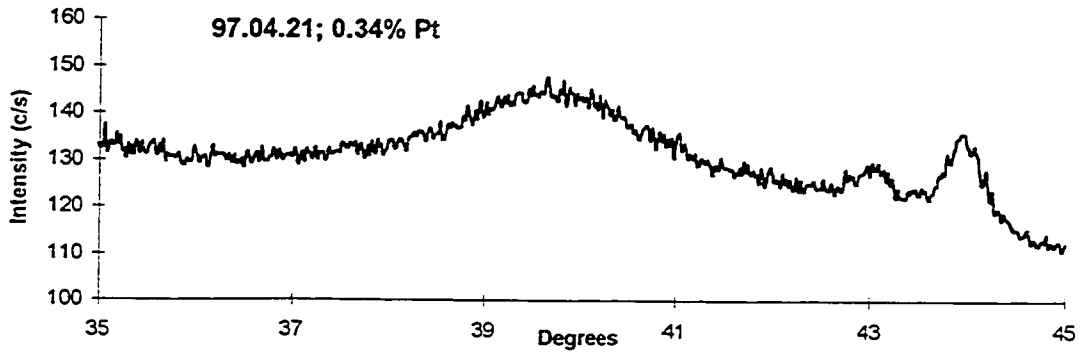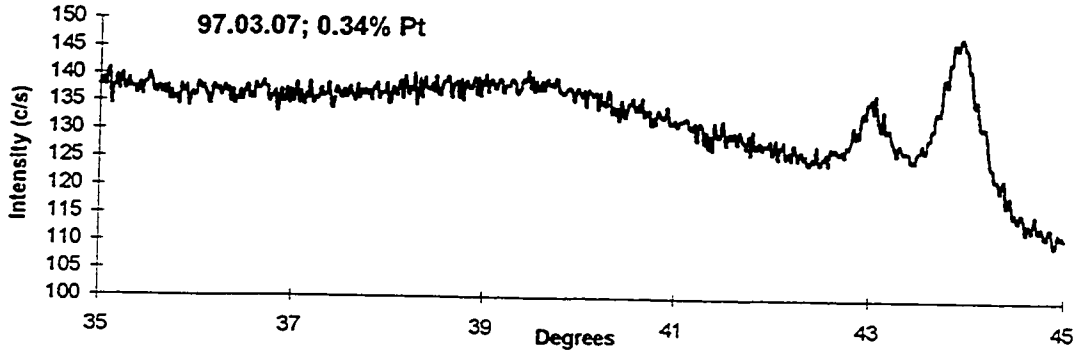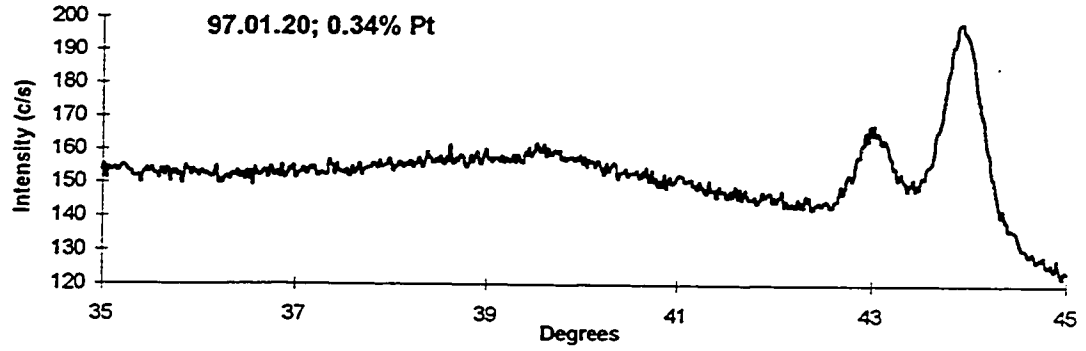
Figure 4.1 con't: Results from diffraction measurements.

the purposes of this study, approximate values were still useful. A comparison between samples was made recognizing the limitations and imprecise nature of the measurements.

Valid comparisons can be made from the results where the catalyst had lower platinum dispersions. From these results, one observes that the higher platinum loadings resulted in lower dispersions, as one would expect. However, within each platinum loading significant variability occurred between catalyst batches. The two catalyst samples with one percent platinum loadings had different metal dispersions. If the results from the x-ray diffraction are examined carefully, it is apparent that the curve for the first of these two samples (95.12.12) does not look like a normal distribution; rather it has a slight bump on the right hand side of the main peak. This is likely a second, smaller peak corresponding to a different crystal line, specifically platinum oxide. The formation of platinum oxide particles occurs during the calcination period. The small particles are particularly prone to oxidation because of the larger percentage of exposed platinum surface. It is likely that the higher dispersion of the platinum metal is an artifact of this small secondary peak. The reason for this peak in the first sample but not the second can be partially attributed to the difference in method of catalyst preparation which was not completely standardized until after catalyst batch 95.12.12. The large difference in surface area of the two SDB lots may also be a contributing factor. Everything else being the same, higher metal dispersions occur on higher surface area supports.

The platinum dispersion results from the 0.34 % platinum loadings were also variable. The platinum dispersion results from catalyst batches 96.09.05, 97.01.20 and 97.03.07 were considered to be indistinguishable. It is reassuring that the two batches of

catalyst made from the same lot of SDB support had essentially the same properties (see Tables 4.1 and 4.2). Both 97.06.27 and 97.04.21 had noticeably lower dispersions. In particular, catalyst batch 97.04.21 had a markedly lower platinum dispersion than all of the other batches. It is probable that the large variation in the properties of the SDB between lots is the cause of much of the variability observed in the different catalyst batches. Various trends exist in the pore size distribution that may help explain the reasons for this variability; both of these samples had a larger percentage of pore volume greater than 5 nm than the others. However, this does not completely explain the variability; if this was the case, the dispersion of catalyst batch 97.06.27 would be higher than that of 97.04.21 instead of the reverse.

Perhaps the most useful piece of information in these results is the degree of variability present, from one batch of SDB to another, and one batch of catalyst to another. The impact of this variability should be considered when analyzing and interpreting the results from reactor runs studying the deactivation and the kinetics.

4.5 Properties of the Styrene Divinyl Benzene Copolymer

Prior to using catalyst presoaked with ethylene glycol in the reactor, the change in diameter of SDB spheres when soaked in ethylene glycol was measured using a micrometer. Eight spheres were measured and then soaked in ethylene glycol for five hours. The spheres were again measured. The average diameter of the spheres increased by 2.8%. This was considered to be a relatively small amount and not enough to significantly affect the hydrodynamics of the reactor.

The fresh support and catalyst were very hydrophobic and were not easily wetted by dilute solutions of ethylene glycol. This presented a problem in the trickle-bed reactor. An attempt was made to measure how much ethylene glycol would be adsorbed from a 0.18 mol/L ethylene glycol solution (an intermediate concentration used in liquid feed for the reactor) by a given amount of SDB support. Into one small glass vial, 40 g of 0.18 mol/L ethylene glycol solution was added, which represented a total of 0.45 g of ethylene glycol. This was the control vial. To a second vial containing 40 g of 0.18 mol/L ethylene glycol solution was added 0.40 g SDB support. Both vials were then placed on a shaker, such that the samples were shaken back and forth. Unfortunately, the sample platform, complete with samples, periodically fell off the shaker. It was estimated that of the one week for which the samples were to have been shaken, that the actual time on the shaker was closer two or three days.

Nonetheless, useful information was gained. On analysis of the two vials via GC, the ethylene glycol concentration of the control sample remained unchanged at 0.18 mol/L. In the vial containing the SDB, the ethylene glycol concentration dropped to 0.16 mol/L, equivalent to an adsorption by the SDB of 0.05 g of ethylene glycol, or 11 % of the available ethylene glycol. From this test, it was concluded that the SDB does indeed successfully concentrate ethylene glycol from a dilute liquid solution. This result is consistent with the findings of Gustafson et al. (1968). These researchers studied the adsorption of various organic compounds by styrene divinyl benzene copolymers.

Work of Stevens and Kerner (1975) suggests that a different choice of hydrophobic support would improve the adsorption of some organic compounds. Stevens

and Kerner reported that aromatic-based adsorbents (such as the SDB used here) are particularly effective for adsorbing nonpolar organic compounds from aqueous solution, whereas acrylic-based adsorbents show good attraction for more polar solutes. For materials of intermediate polarity, they suggest adsorbents based on acrylic esters, such that there is an attraction for both the hydrophobic and the hydrophilic end of a molecule. Before an acrylic-based or acrylic ester-based adsorbent can be tested in place of the SDB that was used as the catalyst support, high surface area materials would be required.

In another experiment, the structural properties of the SDB were studied. In a beaker, a dilute solution of ethylene glycol was stirred with a magnetic stirrer, at sufficient rate to create a vortex in the liquid. Without a vortex, the SDB floated on the surface of the solution. Within a few hours, the solution started to turn cloudy. After 24 hours, none of the original SDB spheres remained, and the solution was opaque. The SDB spheres had completely disintegrated into a fine powder. In this study, because a lab scale trickle-bed reactor was used, this phenomenon did not present any difficulties. However, in a slurry reactor or a fluidized bed and possibly an industrial scale trickle-bed reactor, the poor structural integrity of the SDB could be a serious problem.

5. The Chemistry

Before any sort of kinetic analysis could be attempted, as many of the reaction products as possible were identified.

The gas and liquid streams were analyzed separately for oxidation products. In the gas phase, water and oxygen and possibly nitrogen (depending on the run) were present before any reaction occurred. Prior to analysis, water was removed from the gas using a tube filled with indicating silica gel. The silica gel was changed regularly based on its colour which changed from blue (dry) to pink (saturated). A gas sample was then taken using an on-line sampling valve to inject it into the gas chromatograph.

5.1 Gas Phase Product Identification

Given the nature of ethylene glycol, a semi-volatile organic compound, there were not many volatile reaction products that could be expected. The possible oxidation products in the gas stream were the partial oxidation products, either volatile organic carbon compounds (VOCs) or carbon monoxide, and the complete oxidation product, carbon dioxide.

An Ecolyzer CO Analyzer was used to check for the presence of any carbon monoxide in the gas effluent stream. A 200 ppm standard of CO in N_2 was used to calibrate the instrument. No carbon monoxide was detected in the sample stream (sensitivity <1 ppm). These results are consistent with the literature. Mallat and Baiker

(1994) reported that carbon monoxide is strongly adsorbed on platinum surfaces. Abbas and Madix (1981), found that carbon monoxide adsorbs on Pt (111) and oxidizes rapidly to carbon dioxide in the presence of surface oxygen.

The presence of carbon dioxide was established by comparing the gas chromatogram of a carbon dioxide standard in nitrogen with that of the effluent gas stream. The retention time of the carbon dioxide in the standard matched that of the sample. Confirmation that carbon dioxide was being formed came from the mass balance when complete conversion occurred. Approximately all of the carbon measured in the ethylene glycol feed was accounted for by the carbon dioxide measured in the effluent stream (see Chapter 3 on the trickle-bed reactor).

No other compounds were detected in the gas stream by the gas chromatograph indicating that VOCs were not present. This result is supported by the mass balance calculations in Chapter 3 and the liquid phase analysis. The absence of VOCs is logical when the products detected in the liquid phase are considered. There are not many VOCs that are possible oxidation products of ethylene glycol. The only VOCs that can reasonably be expected in the gas phase are aldehydes resulting from the oxidation of ethylene glycol. However, the aldehyde precursor of glycolic acid, hydroxyacetaldehyde, is not a VOC and neither formic acid nor acetic acid was detected in the liquid phase (see section 5.2.2) making the presence of the corresponding aldehydes unlikely.

5.2 Liquid Phase Product Identification

5.2.1 Mass Spectra Analysis

Several techniques were used to identify the products formed in the liquid phase. The initial approach taken was to have samples analyzed by gas chromatography with a mass spectrophotometer (GC-MS). These results were then compared with those in the computer library (see Appendix D).

This approach was not entirely satisfactory for several reasons. The library used was the standard one, not one generated on the instrument used; this results in discrepancies between the spectra observed and those in the library. Appendix D shows the actual mass spectrum of ethylene glycol compared to the one in the library. While the computer program correctly identified the ethylene glycol peak, it is easy to understand how more complicated molecules would present problems. In addition, the nature of mass spectrometry is a hindrance. When a compound enters the spectrophotometer, cations are formed; the instrument detects these cations, rather than the starting molecule. The fragmentation observed depends on structure of the molecule, hence the importance of a spectra library. Highly oxygenated compounds tend to form such stable fragments associated with the oxygen that the parent cation is often very difficult to observe. As well, rearrangement of the atoms is possible. Finally, in using GC-MS, it was assumed that the compounds of interest were compatible with gas chromatography. Carboxylic acids are difficult to detect, because they are very polar and do not elute as sharp peaks from the chromographic column. Di-acids are particularly difficult because they do not vapourize significantly at the injection temperatures.

However, that said, some useful information was gained via GC-MS. A suggestion made by the library for two of the peaks observed (scan 213 and 238; Appendix D) was 1,3-dioxolane. A sample of this compound was then injected into the GC used for the liquid analysis to compare the retention times. The retention time of the 1,3-dioxolane was very much less than that of the peak in question. Therefore, 1,3-dioxolane was not one of the partial oxidation products.

However, on examination of the chemistry of ethylene glycol, the formation of compounds containing the 1,3-dioxolane structure would appear likely. In the presence of an acid, ethylene glycol will react with a carbonyl compound in a condensation reaction (Rebsdat and Mayer, 1987):

$$\text{(structure: ethylene glycol with two OH)} + \text{O=C}\genfrac{}{}{0pt}{}{R}{R'} \xrightarrow{H+} \text{(1,3-dioxolane with R, R')} + H_2O \tag{5.1}$$
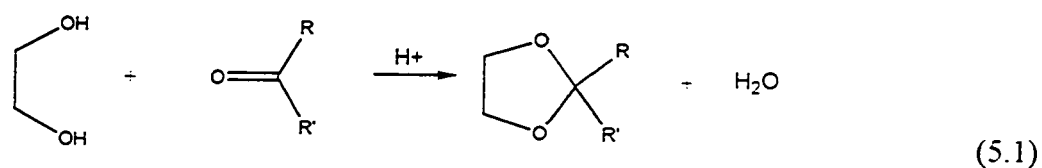
It is reasonable to expect that a carboxylic acid would react in a similar manner, resulting in a 1,3-dioxolane compound. Shown in equation 5.2 is ethylene glycol reacting with glycolic acid to form 2-hydroxy-2-hydroxymethyl-1,3-dioxolane. Glycolic acid was later confirmed as one of the reaction products.

$$\text{(ethylene glycol, OH OH)} + \text{O=C}\genfrac{}{}{0pt}{}{OH}{CH_2OH} \xrightarrow{H+} \text{(2-hydroxy-2-hydroxymethyl-1,3-dioxolane)} + H_2O \tag{5.2}$$
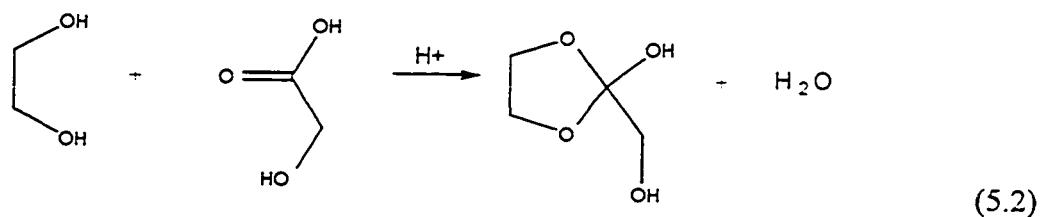
Furthermore, the GC-MS peak associated with the 1,3-dioxolane compound was not smooth, suggesting that it was actually a number of similar compounds. This is readily

explained in the framework of this chemistry. A different R group in equation 5.1 would result in a slightly different compound.

For two of the other peaks detected, the spectra library included esters in the list of suggested compounds. None of the compounds suggested were available commercially and therefore the retention times could not be measured in the GC. However, the compounds suggested were unlikely to be the reaction products, because methyl groups were involved; it is improbable that the carbon-carbon bond would have been broken without the molecule reacting further. Esterification, another condensation reaction, is a probable reaction for ethylene glycol in the presence of an acid (Rebsdat, Mayer, 1987). The classic reaction to make polyester is via this mechanism using dimethyl terephthalic acid (Seymour and Carraher, 1988). The same mechanism with ethylene glycol reacting with glycolic acid would be as follows:

$$(5.3)$$
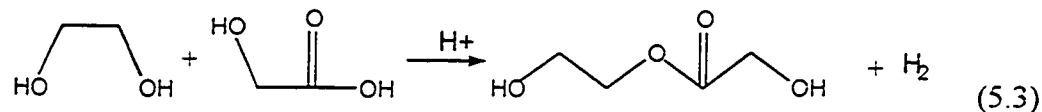
or similarly, two glycolic acid molecules could react with each other.

The GC-MS also detected small peaks with higher molecular weights, suggesting that some dimerization/polymerization occurred in the reactor. This supports the above reaction mechanism. With the exception of carbon dioxide and water, none of the molecules detected were smaller than ethylene glycol.

5.2.2 Derivatization of Compounds

It was attempted to derivatize any carboxylic acids via silylation. The principle behind this technique was to create a more stable compound from the standpoint of mass spectrometry. In the case of carboxylic acids, the derivatized compounds are more volatile and gas chromatography can be used successfully. In this way, it was hoped that the structure of the unknown compounds could be determined. The basis procedure was to evaporate the water from a reacted sample. The sample was added to the solvent, methylene chloride and the silylation agent, BSTFA (Bis(trimethylsilyl)trifluoro-acetamide)) plus one percent TMCS (chlorotrimethylsilane), was added to the solution. Alcohols react most readily, but carboxylic acids are still expected to react quickly at room temperature (Blau and King, 1978).

These experiments were unsuccessful. No silylated compounds were detected in the GC-MS analysis. This result was not fully understood. However, the ethylene glycol, the predominant compound in the evaporated sample, would be expected to react most readily with the derivatizing agent. Before any further attempts at silylation, it was decided that a sample largely free of ethylene glycol would be required. This avenue was abandoned, because of the problems encountered and lack of expertise in the area.

Glycolic acid was successfully identified in the liquid following derivatization with methanol in a dilute solution of hydrochloric acid (see Appendix D). The procedure is similar to that given by Gottstein et al. (1989). The approach involved replacing the

hydrogen of the hydroxyl group of the carboxylic acid with a methyl group in the presence of an acid catalyst. In the case of glycolic acid, the reaction of interest was:

$$HOCH_2COOH + CH_3OH \rightarrow HOCH_2COOCH_3 + H_2O \qquad (5.4)$$
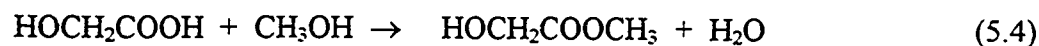
As with silylated compounds, these derivatized compounds were easily analyzed using gas chromatography.

Briefly, the procedure was as follows:

1. A solution of 7% hydrochloric acid (from 38% solution in water) in methanol was prepared.

2. Derivatized standards of acetic acid, ethylene glycol, formic acid, glycolic acid and oxalic acid were prepared by adding the 0.1 mmol of each standard to 5 mL of HCl solution to give a 0.02 M solution. A reactor sample was prepared in the same fashion. All the standards and samples were heated at 60°C for 30 minutes to carry out the derivatization.

3. The standards and samples were then injected into a GC using FID to find their retention times. The presence of all but glycolic acid was ruled out. By spiking a dilute sample with glycolic acid, the presence of glycolic acid was tentatively confirmed.

One further set of analysis was done for carboxylic acids (see Appendix D). Two liquid samples from the reactor, one collected at 80°C and the other at 90°C, were analyzed by ion chromatography. No formic or acetic acid was detected. This result combined with absence of any small molecular weight molecules in the GC-MS analysis, is

69

strong support for the absence of VOCs in the gas phase. A large amount of glycolic acid was detected. Oxalic acid was found at levels less than one percent of that of the glycolic acid. Trace amounts of two other carboxylic acids were also detected. Based on their retention times, citric and tartaric acid were their suggested identities. The chemistry does not support this conclusion. It is more likely that an oxygen molecule links the pairs of carbons as a result of an esterification reaction, similar to the one shown in equation 5.3.

6. Catalyst Deactivation

In this study of the oxidation of ethylene glycol, it was observed that the catalyst deactivated very rapidly initially, and then more gradually. The rate of deactivation was found to be a function of several factors, but most dramatically, a function of oxygen pressure with less deactivation being observed at lower pressure. This chapter explores the cause(s) of deactivation, and proposes a mechanism for the deactivation.

6.1 Background

Catalyst deactivation in the most general of terms is the loss of catalytic activity. With time the catalyst activity decreases under otherwise steady state conditions. This decrease in activity can be the result of either physical or chemical processes. Normally these processes occur simultaneously with the main reaction.

The major catalyst deactivation mechanisms are generally divided into the following categories: fouling (which includes coking), sintering, and poisoning. In addition there are several other mechanisms that are sometimes important: pore blockage via coke or metal deposition on the internal pore structure of the catalyst; destruction of active surface via detachment from the support (including leaching); and incorporation of the active component into the support structure in an inactive form (Butt and Petersen, 1988).

Fouling can also be caused by any material in the system that blocks access to catalyst sites. Fines can block the entrance to catalyst pores. Coke can block both the

entrances to catalyst pores and the active sites. Coking is the process of formation of hydrogen-deficient carbonaceous residues on the surface of the catalyst, most often in reactions involved in hydrocarbon processing. The number of active sites available is reduced by covering them with large molecules referred to as "coke". Macroscopic amounts of coke can be formed, sufficient to alter the internal pore structure of a porous catalyst or catalyst support and physically block access of reactants (Butt and Petersen, 1988).

Sintering is the loss of active surface area by the agglomeration of small metal crystallites into larger ones in the case of supported metal catalysts, or the collapse of pore structure and loss of internal surface area in the case of supports or oxide catalysts. These processes are normally physical rather than chemical in nature. Most often, it is the result of prolonged high temperature exposure.

Poisoning is the strong chemisorption of impurity materials onto a catalyst surface that blocks the access of reactants to active sites. It may be reversible or irreversible. Poisoning occurs at the level of monolayer coverage. Catalyst poisons have been grouped into three main categories by Hegedus and McCabe (1984): poison adsorption, poison-induced surface reconstruction and compound formation between the poison and the catalyst. The first category is discussed in the following paragraphs. Briefly, chemical induced surface restructuring occurs when a poison changes the morphology of the active surface. This may lead to either an increase or decrease in catalyst activity. Compound formation between a poison and a catalyst is not clearly delineated from poison

adsorption. It refers to the formation of new chemical species from the poison precursor and the catalyst, such as $Pt-O_2$ from atomic oxygen adsorbed on platinum.

One of the most common mechanisms for the adsorption of poison species is through competitive adsorption with the reactive species, either reversibly or irreversibly. A poison is considered to be reversible if the catalyst activity recovers (i) upon the removal of the poison from the feedstream under actual reaction conditions, or (ii) upon changing the feedstream or operating conditions.

The amount of poison present is not a good measure of the degree of catalyst deactivation. Both the size and nature of a poison will dictate the degree of poisoning observed. A catalyst poison works in either or both of the following ways: (1) it can block a geometrically fixed number of sites, preventing the reactants from reaching the active site; (2) the electronic properties of the catalyst can be altered via chemical interaction between the poison and the catalyst. Electronic effects may poison a greater radius of the catalyst than the geometric proportions of the poison would predict. A poison may even modify the electronic structure of the metallic crystal lattice (Hegedus and McCabe, 1984).

The effectiveness of a poison also depends on the reaction that is being catalyzed. The more active sites that a reactant requires, the more readily that it will poisoned. For example, if a reactant requires only one active site, any unpoisoned site will catalyze the reaction. However, if two or more active sites are required, they must be adjacent. Generally, molecules have the ability to move on the active surface of the catalyst. In this way the required number of active sites is found. However the presence of a poison will

inhibit this rearrangement by occupying sites. If the poison lacks mobility and the reaction involves two or more reactants, an adsorbed molecule may be isolated by the poison and unable to participate in the reaction.

6.2 Possible Causes of Deactivation

The approach taken in this study was to consider as many causes of deactivation as possible and then to eliminate them based on experimental evidence. In this system, both fouling and sintering can be discounted as the cause of deactivation. A clean system was used without any fines in the either the gas or liquid. Coking would not be expected to occur at such moderate temperatures particularly in an oxygen rich atmosphere. This is supported by the fact that no carbonaceous residue was observed on the catalyst when it was removed from the reactor, and that reactivation was achieved at low temperatures in the absence of oxygen. Sintering is an equally improbable explanation, both because the operating temperatures were low and because reactivation of the catalyst was achieved by simply replacing the oxygen in the gas feed with nitrogen. Re-dispersion of platinum is difficult to achieve and is not likely to occur at such low temperatures. Having ruled out the possibilities of sintering and coking, there are still many possible explanations for the deactivation observed.

The remaining possible causes of deactivation can all be classified as poisoning. The possible poisons for the catalyst were traces of metal impurities in the feed, impurities in the catalyst support, by-products, either identified (such as glycolic acid), or unidentified, or oxygen. In addition to catalyst poisoning as the cause of deactivation, it is

possible that a depletion of ethylene glycol in the catalyst support was responsible for the deactivation observed. Strictly speaking, this would not be deactivation, since no catalyst activity would be lost. Rather, it would be a reflection of a diminishing supply of ethylene glycol in a position most accessible to the catalyst.

6.3 Experimental

Deactivation of the catalyst for this system was studied under various conditions. In all of these experiments, the reactor was packed as described in the chapter on the trickle-bed reactor. The catalyst was presoaked in ethylene glycol unless otherwise indicated. The temperature was 80°C. At this temperature mass transfer effects and temperature gradients were minimal. The catalyst had sufficient activity to achieve some complete oxidation and considerable partial oxidation of ethylene glycol. The total pressure was either 347 kPa or 497 kPa, where 47 kPa is the vapour pressure of water at 80°C and the balance was oxygen and/or nitrogen. The oxygen/nitrogen flow rate was 450 mL/min (at room temperature and pressure) at 347 kPa; to obtain the same gas velocity inside the reactor at 497 kPa, the gas flow rate was increased proportionately to 675 mL/min. The liquid flow rate was 20 mL/min. A description of the catalyst in each run is given in Table 6.1.

Table 6.1: Description of the catalyst used in each run.

Run	Catalyst Batch	Catalyst Lot #	Pt Loading (wt)%	Amount of Catalyst (g)
960524	60223/27	150	1.0	10.7
960909	60905	150	0.34	30.0
961125	61121⁻	511	0.34	25.0
961202	61121	511	0.34	25.0
961209	61121	511	0.34	25.0
970123	70120⁺	511	0.34	25.0
970317	70307	511	0.34	25.0
970324	70307	511	0.34	25.0
970401	70325	511/535	0.34	25.0
970422	70325	511/535	0.34	25.0
970527	60223/27	150	1.0	8.25
970728	70627	395	0.34	25.0
970805	70627	395	0.34	25.0

$^-$ Catalyst not calcined.

$^+$ Extra oxygen treatment for catalyst.

6.4 Results and Discussion

6.4.1 Deactivation and Reactivation

In Run 960909, shown in Figure 6.1, the catalyst deactivation was measured under the following conditions: the total pressure was 347 kPa with an oxygen pressure of 300 kPa, the ethylene glycol concentration in the liquid was 0.090 mol/L. The catalyst deactivated more rapidly initially and then more slowly, over a number of weeks, to near steady state. At day 16, the reactor was shut down for four days. When the reactor was restarted, the reaction rate was constant for two days, before deactivation was again observed.

After 28 days of recording the deactivation of Run 960909, the oxygen pressure was lowered and the reactor was run for more than two weeks at oxygen pressures between 225 kPa and 40 kPa. Then, the oxygen pressure was returned to 300 kPa and the catalyst activity was measured. As shown in Figure 6.2, the conversion of ethylene glycol rose dramatically as a result of the operation at reduced oxygen pressure. However, the catalyst deactivated more rapidly than when it was fresh. The new activity of the catalyst, after four days of deactivation, corresponded to approximately day ten of the original 28 day deactivation curve. The rate of deactivation at this point was approximately the same as that found at that point in the original deactivation curve.

In another experiment, Run 960524, the reactor was operated at both 497 kPa and 347 kPa total pressure with a range of oxygen pressures for approximately forty days. The ethylene glycol concentration ranged between 0.022 mol/L and 0.18 mol/L during this time, although the concentration was predominately 0.090 mol/L or 0.18 mol/L. The catalyst was then reactivated either using nitrogen (partial pressure of oxygen equal to
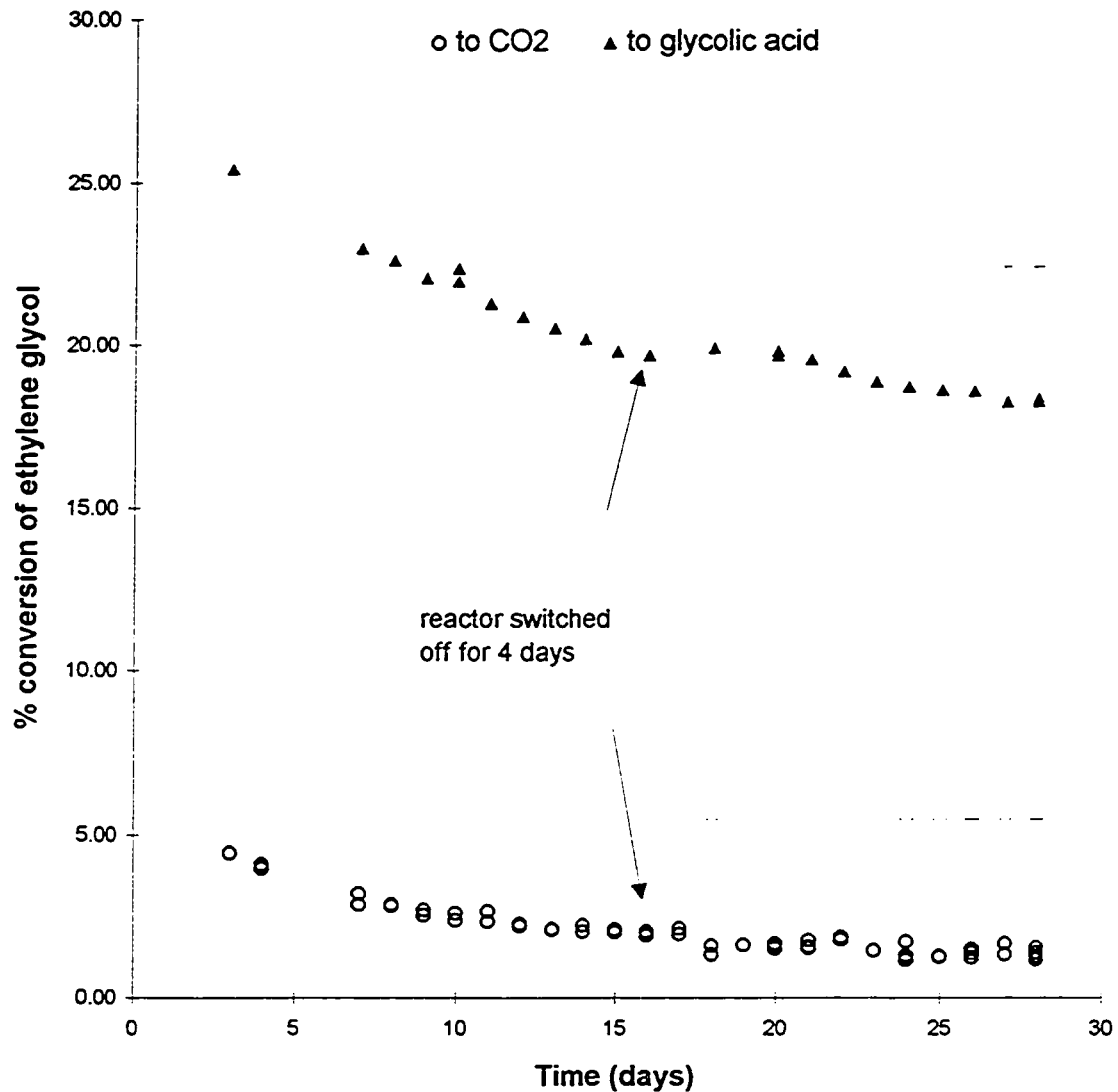
Figure 6.1: Deactivation of fresh catalyst; Run 960909.

Operating conditions: 80°C; 300 kPa O_2 pressure; O_2 flow rate 450 mL/min; liquid flow rate 20 mL/min; 0.090 M ethylene glycol concentration.
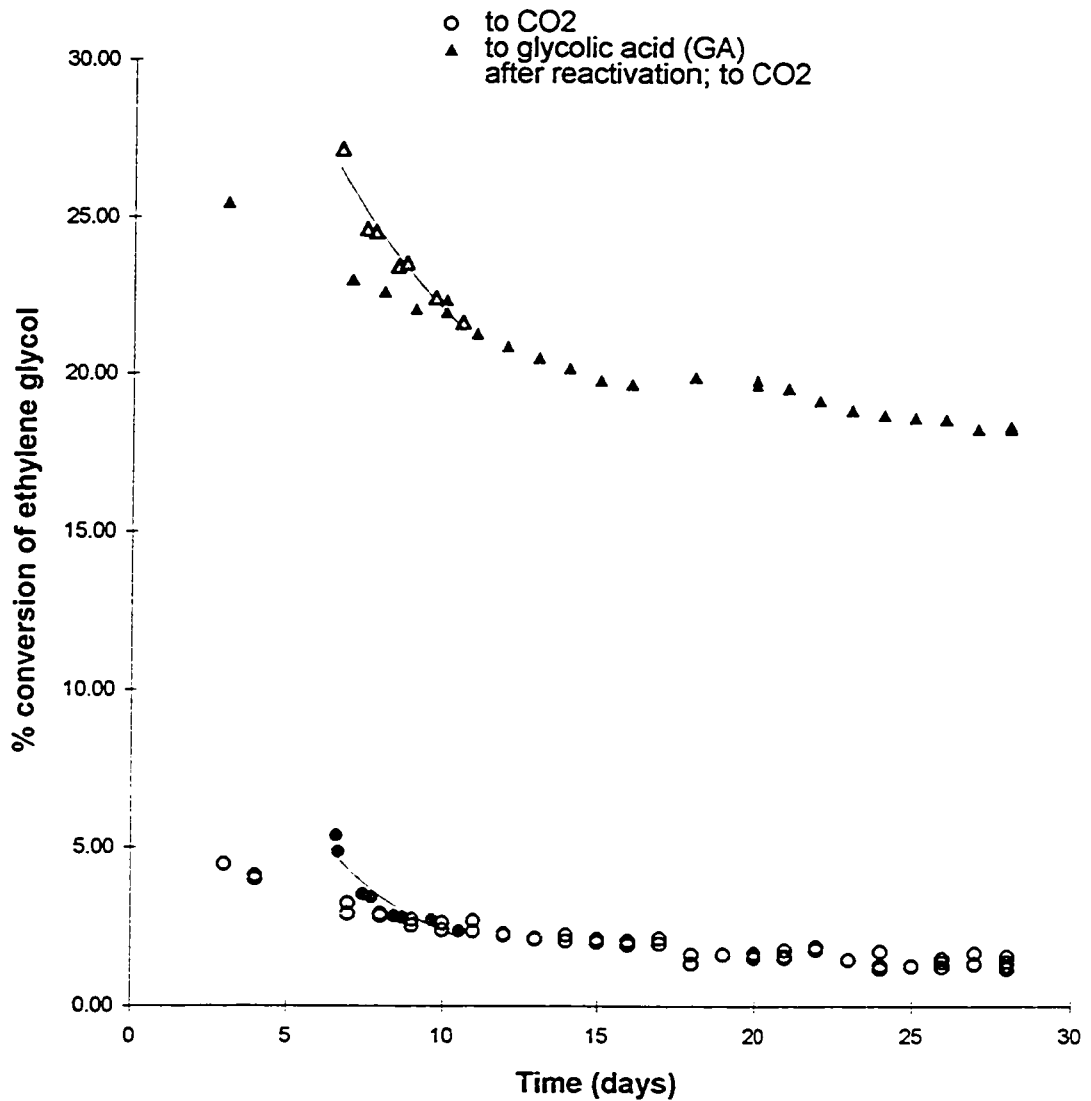
Figure 6.2: Deactivation following more than two weeks of reduced oxygen pressure; Run 960909.

Operating conditions: 80°C; 300 kPa O_2 pressure; O_2 flow rate 450 mL/min; liquid flow rate 20 mL/min; 0.090 M ethylene glycol concentration.

zero) instead of oxygen (300 kPa oxygen pressure), or by sufficiently reducing the oxygen pressure. The flow of the ethylene glycol solution was not interrupted during the reactivation. The system was run with nitrogen overnight; it was then switched back to oxygen the following morning. The deactivation curve following reactivation was much more rapid than the original deactivation. The catalyst activity was initially very much higher than the previous day; however, it deactivated rapidly to the previous day's activity within 24 hours. As shown in Figure 6.3, the catalyst was cycled between nitrogen and oxygen with reproducible results. The same effect was achieved by running with reduced oxygen pressure (63 kPa) for a longer time period. When the oxygen pressure was returned to previous levels, the same deactivation curve as that with the nitrogen reactivation was followed.

Both this experiment and Run 960909 eliminate several possible sources of the poison. The catalyst poison does not appear to be present in the feed or in the catalyst support. Reactivation would not have been possible with the liquid flowing if this were the case.

The effect of the ethylene glycol solution on the reactivation was checked by switching from oxygen feed to nitrogen and then turning off the liquid flow. In this experiment, Run 970527, shown in Figure 6.4, the catalyst deactivated for two days at an oxygen pressure of 300 kPa, with a total pressure of 347 kPa. The oxygen pressure was reduced on the following day and some reactivation occurred. The oxygen pressure was then returned to 300 kPa and the activity was measured. At this point the oxygen feed was switched to nitrogen and the liquid flow was stopped. Higher activity was observed when
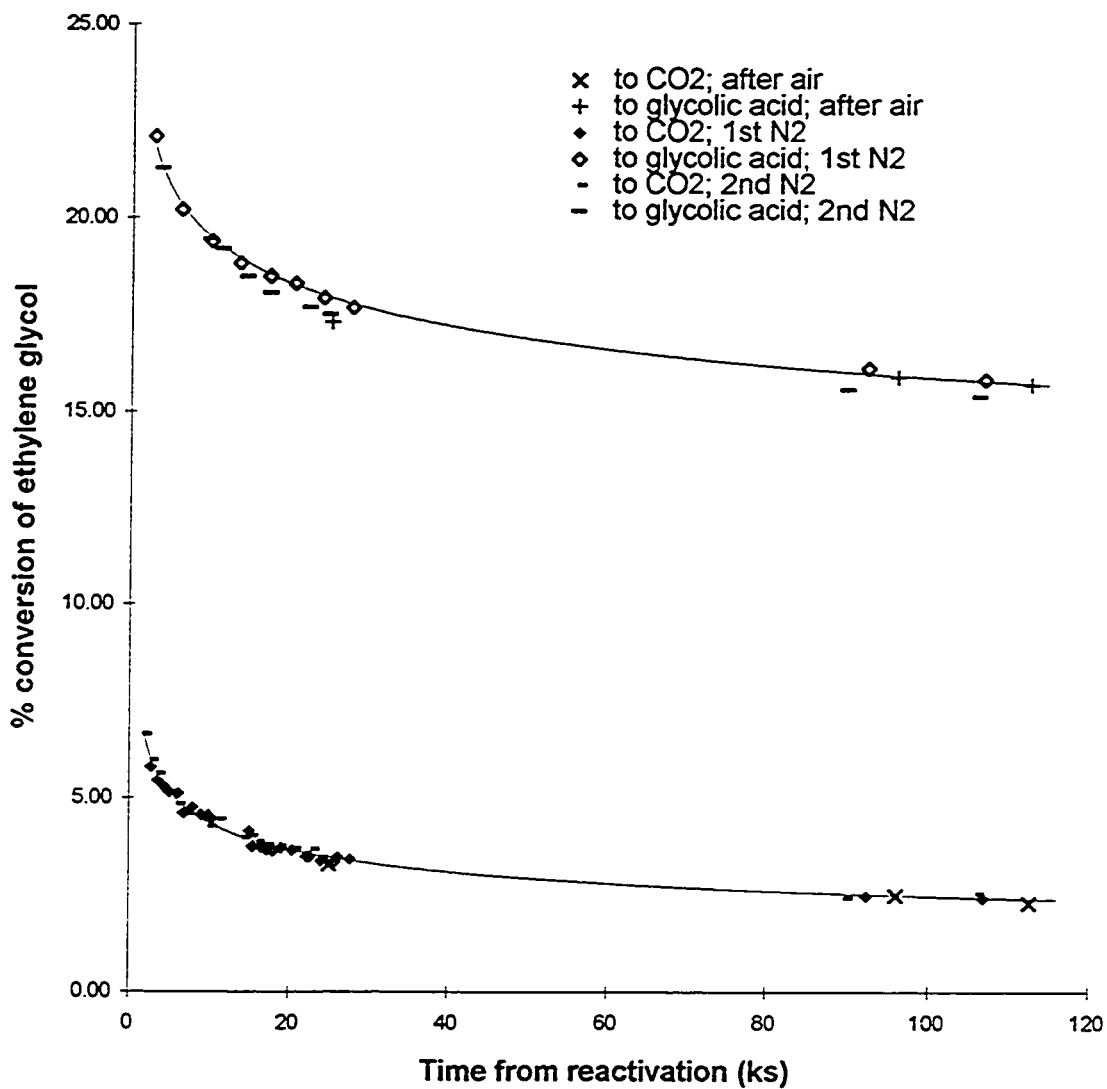
Figure 6.3: Deactivation following reactivation with either nitrogen or air.; Run 960524.

Operating conditions: 80°C; 300 kPa O_2 pressure; O_2 flow rate 450 mL/min; liquid flow rate 20 mL/min; 0.090 M ethylene glycol concentration.
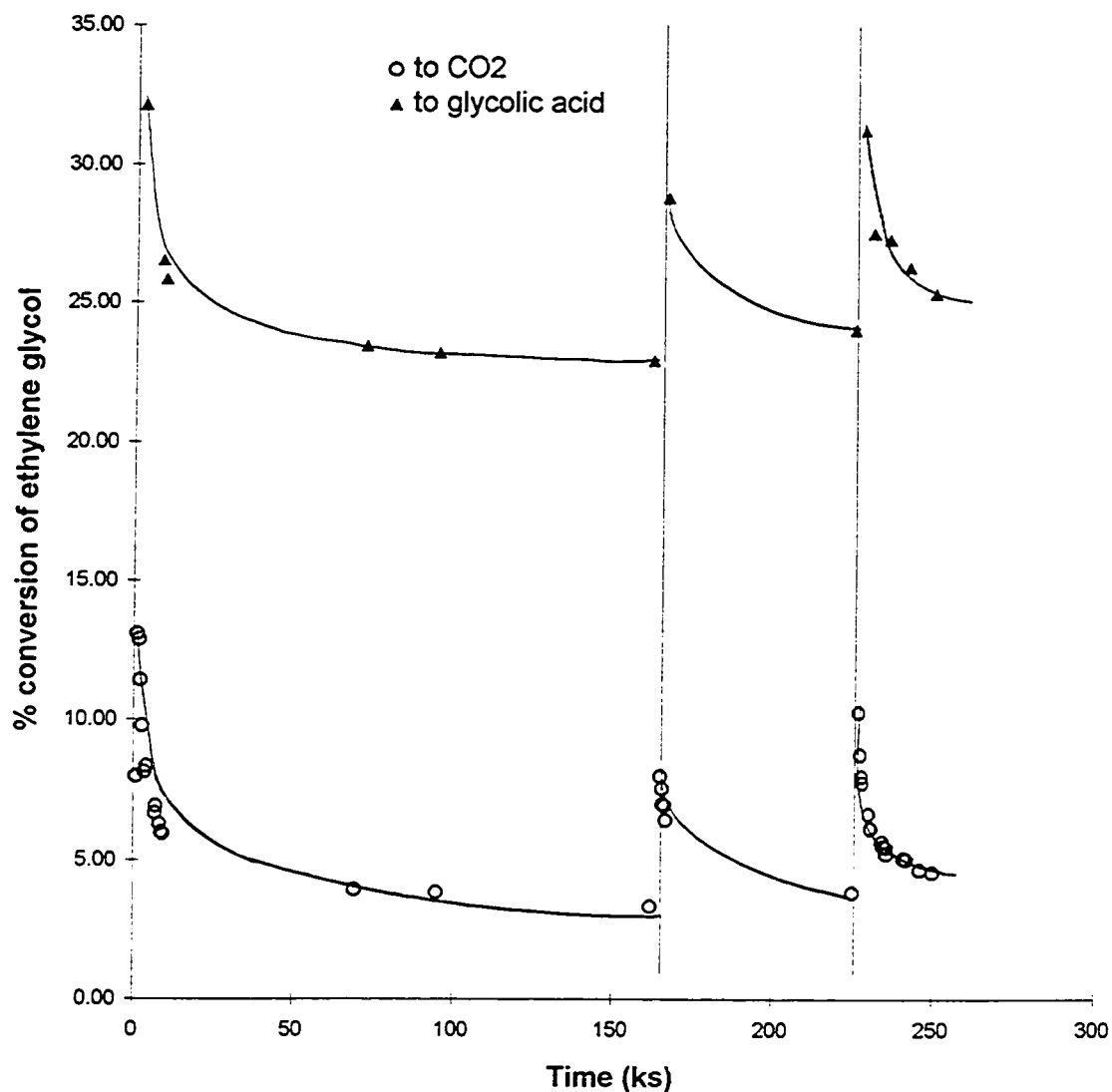
Figure 6.4: The effect of reducing the oxygen pressure with and without the liquid flowing.

The first vertical line marks the time at which the oxygen pressure was reduced for five hours and the liquid flow was left on. The second vertical line marks the time at which nitrogen completely replaced the oxygen for four hours and the liquid flow was switched off.

Operating conditions: 80°C; 300 kPa O_2 pressure; O_2 flow rate 450 mL/min; liquid flow rate 20 mL/min; 0.090 M ethylene glycol concentration.

the liquid flow was reintroduced and the gas flow was switched back to oxygen. This result indicates that the liquid flow does not effect reactivation.

A possible explanation for the reactivation is that the poison desorbs from the active sites relatively rapidly when no poison is being added to the system. The poison may be added either in one of the feed streams or be generated via reaction. However, the poison does not immediately leave the catalyst support, rather it diffuses slowly away. When significant reactivation was observed in Run 960909, approximately two weeks of reactivation improved the activity of the catalyst to a point that corresponded to the activity at approximately day eight of the original deactivation curve (see Figure 6.2); both the deactivation and the reactivation take similar lengths of time. The reactivation, and by analogy the deactivation, can be explained by diffusion and a concentration gradient of the poison. When the poison is no longer accumulating, the amount of poison on the catalyst sites decreases with its diffusion outwards to the support where the concentration of poison is lower.

6.4.2 Effect of Ethylene Glycol Concentration

As part of Run 960524, following two weeks of uninterrupted operation, the ethylene glycol concentration in the feed was increased from 0.090 mol/L to 0.180 mol/L. The amount of glycolic acid produced increased by 45 percent, from 19 to 27 mmol/L. The amount of carbon dioxide produced increased by only eight percent. Later in the same run, the ethylene glycol concentration in the feed was decreased from 0.180 mol/L to 0.090 mol/L, with comparable results: the glycolic acid concentration decreased by 33

percent from 24 to 16 mmol/L and the carbon dioxide produced decreased by 11 percent. Clearly at this temperature, the amount of carbon dioxide produced is largely independent of the ethylene glycol concentration, whereas the amount of glycolic acid produced is a strong function of this concentration.

If the observed deactivation was the result of insufficient ethylene glycol, then the amount of carbon dioxide produced would not be expected to change greatly with time. Rather, a similar trend in catalyst deactivation when changing the ethylene glycol concentration would be expected, with a greater drop in glycolic acid production than in carbon dioxide production. Looking at the data from Run 961202 (Appendix E, Table E.8), it is apparent that this is not the case. The glycolic acid concentrations dropped by 29 percent from 29 mmol/L to 20 mmol/L, and the carbon dioxide levels dropped by 56 percent from 0.56 mmol/L gas to 0.24 mmol/L gas. This is the reverse of the expected trend, if a dropping ethylene glycol concentration on the support were responsible for the observed decrease in reaction rate.

Further evidence that insufficient ethylene glycol was not the cause of the decrease in reaction conversion comes from Run 970307, where the catalyst was not presoaked (see Chapter 3, The Trickle-Bed Reactor), and deactivation was still observed.

6.4.3 Effect of Oxygen

The effect of oxygen pressure on deactivation was observed in several experiments. Following the deactivation at 300 kPa oxygen pressure, in Run 960909, the oxygen pressure was lowered stepwise. Reactivation was observed at oxygen pressures of

150 kPa and lower. One to two days were allowed for each oxygen pressure, and the conversion was measured several times for each pressure. The final values were near steady-state and are plotted in Figure 6.5. At 150 kPa, the conversion of ethylene glycol to carbon dioxide was near a minimum. The conversion to glycolic acid reached a minimum near 100 kPa (see Figure 6.5).

The rate of reactivation at low oxygen pressure was studied more closely at 40 and 50 kPa (Figure 6.6). Continuing on with the reactivation shown in Figure 6.5, catalyst reactivation was studied first at 50 kPa. The amount of glycolic acid increased quite rapidly and then more gradually. The carbon dioxide increased correspondingly. The oxygen pressure was lowered to 40 kPa; the reactivation continued. While reactivation did continue, it was more gradual. With the decrease in oxygen pressure, the amount of glycolic acid dropped somewhat. Interestingly, the carbon dioxide produced stayed on approximately the same curve as at 50 kPa.

Two experiments were required to determine at what oxygen pressure deactivation did not occur with a fresh catalyst. In the first experiment, Run 961209, deactivation was observed at an oxygen pressure of 50 kPa. When the oxygen pressure was lowered to 25 kPa, an increase in catalyst activity occurred (Figure 6.7). In the second experiment, Run 970317, the reverse conditions were used. Initially the oxygen pressure was set at 25 kPa; no deactivation was observed. The total pressure was still 347 kPa in this experiment; increasing the gas flow rate, increased the rate of reaction indicating that mass transfer limitations existed. When the oxygen pressure was increased to 50 kPa, deactivation was once more observed (Figure 6.8).
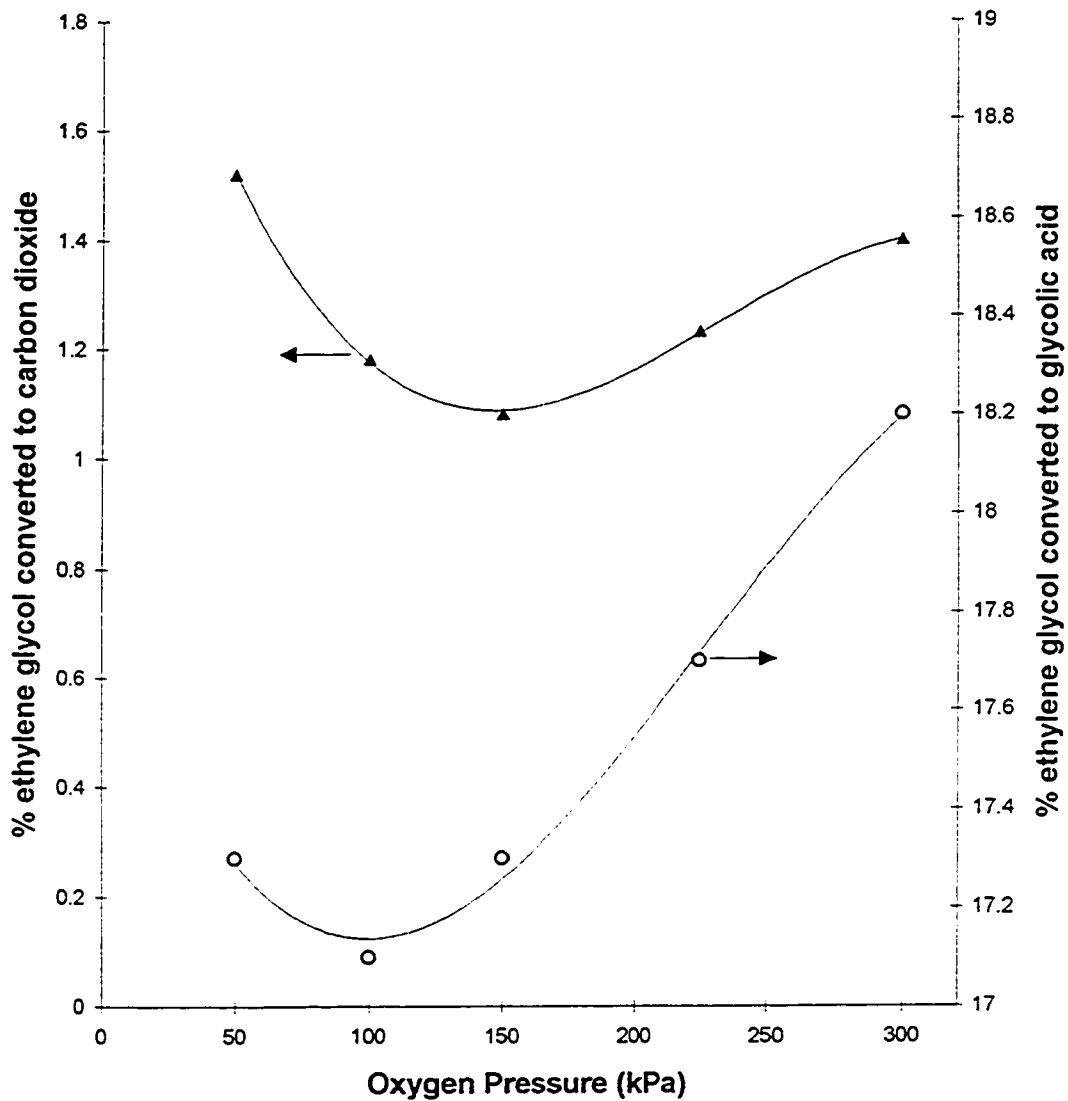
Figure 6.5: The effect of lowering oxygen pressure on reaction with a partially deactivated catalyst. Run 960909.

Operating conditions: 80°C; total gas flow rate 450 mL/min; liquid flow rate 20 mL/min; 0.090 M ethylene glycol concentration.
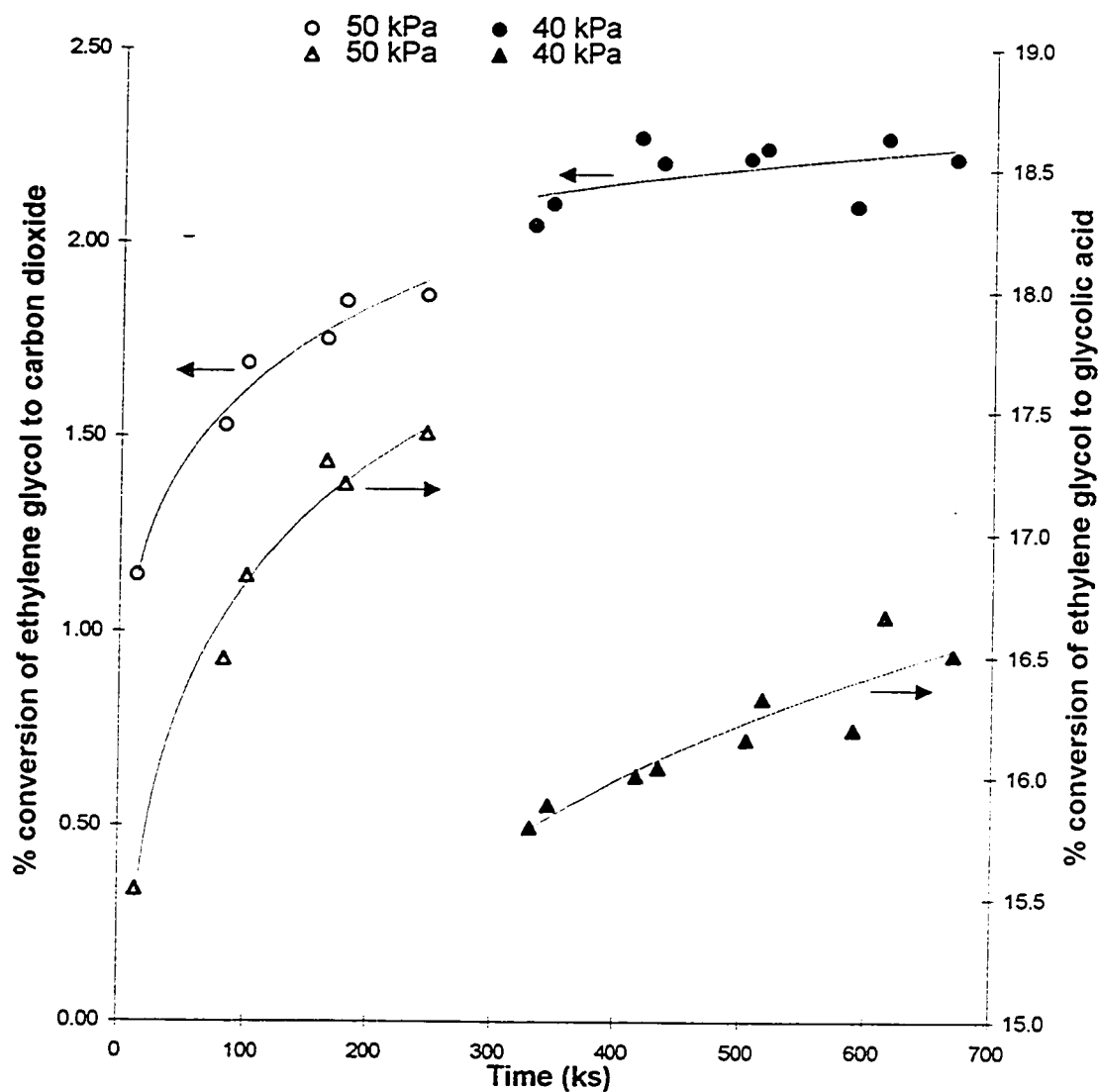
Figure 6.6: **Reactivation of catalyst with time at 50 kPa oxygen pressure and then at 40 kPa oxygen pressure; Run 960906, Table E.6 for the data.**

Operating conditions: 80°C; total gas flow rate 450 mL/min; liquid flow rate 20 mL/min; 0.090 M ethylene glycol concentration.
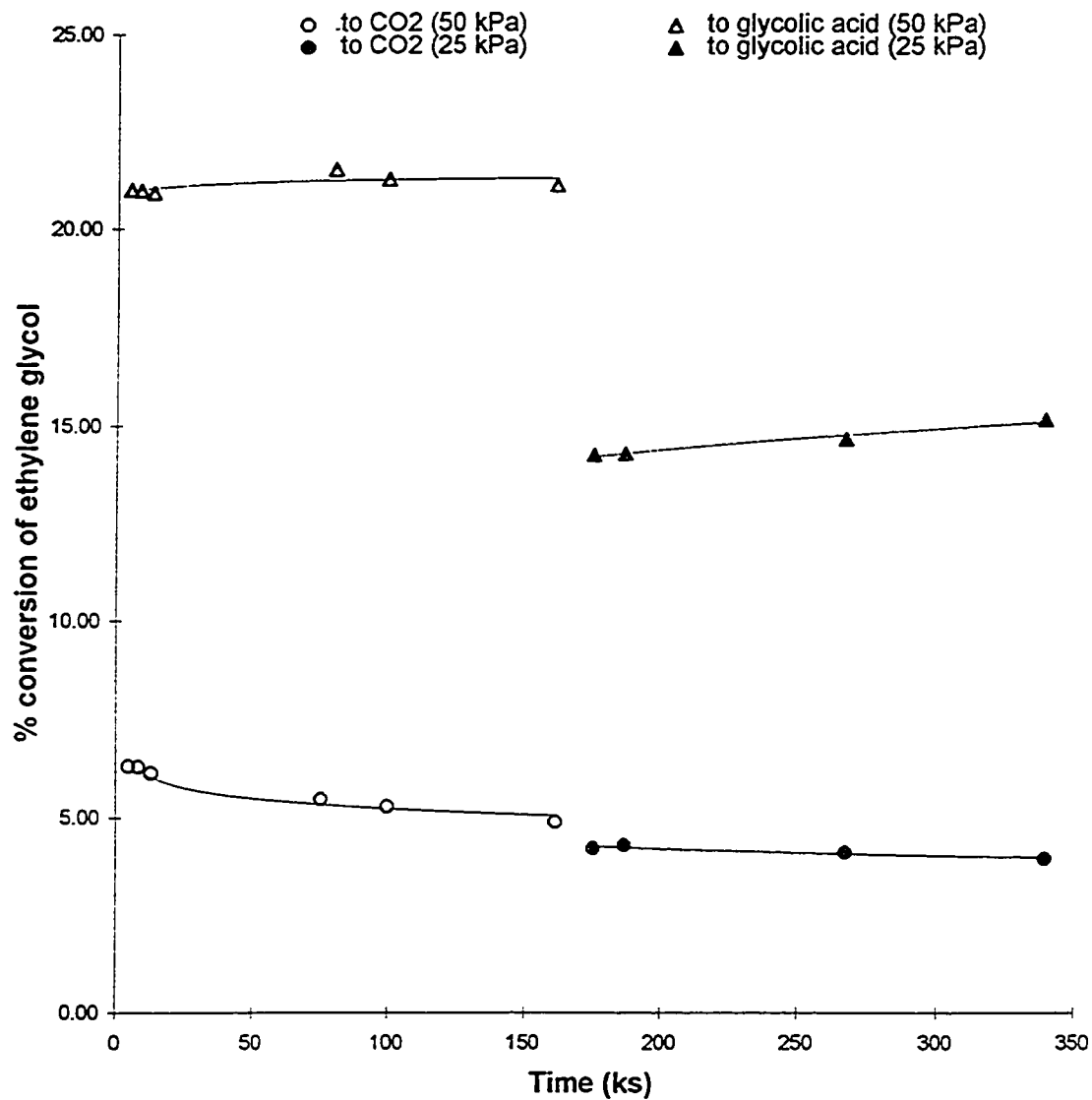
Figure 6.7: **Deactivation of fresh catalyst at 50 kPa oxygen pressure, followed by reactivation at 25 kPa oxygen pressure; Run 961209.**

Operating conditions: 80°C; total gas flow rate 450 mL/min; liquid flow rate 20 mL/min; 0.090 M ethylene glycol concentration.
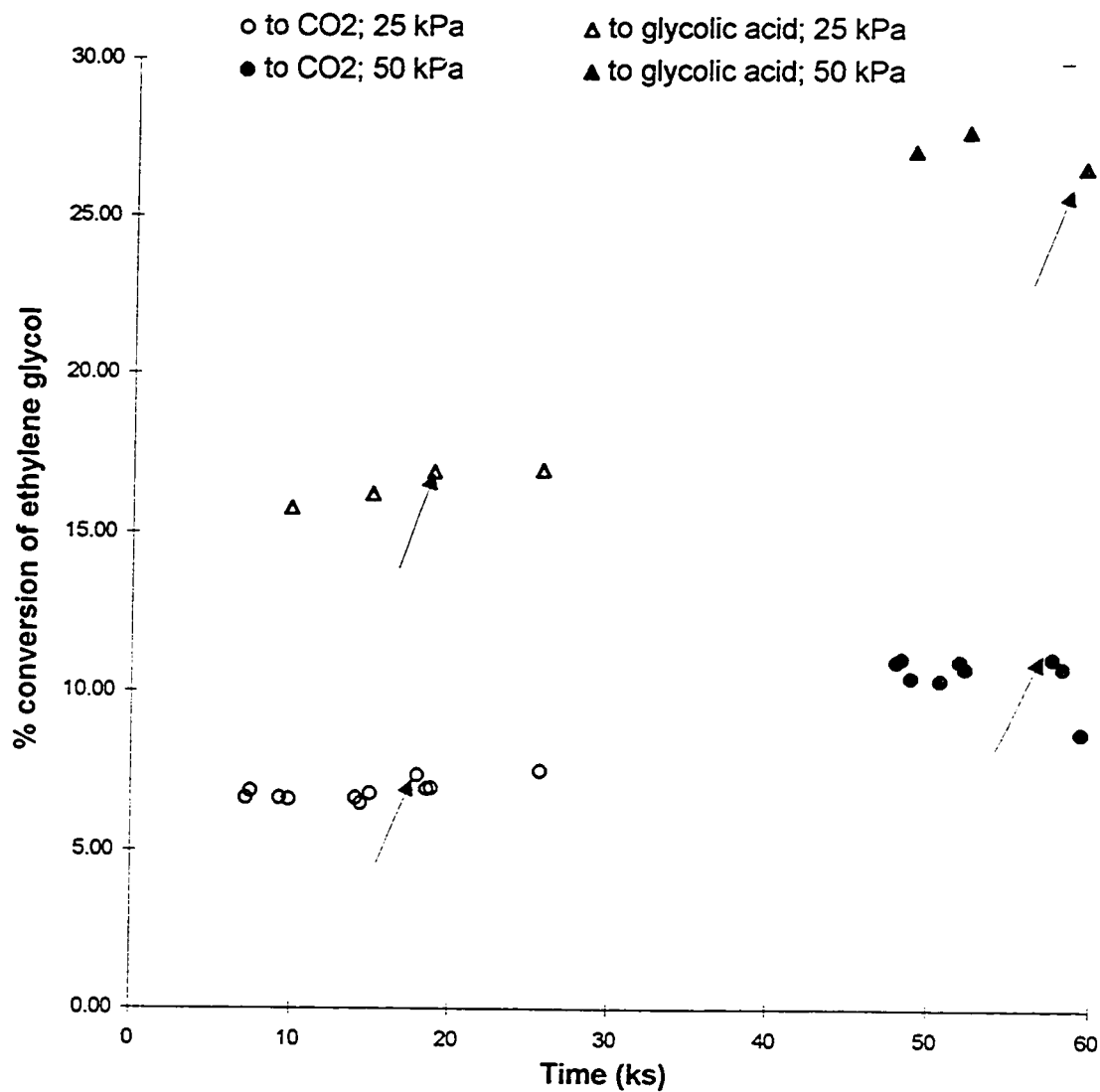
Figure 6.8: No catalyst deactivation observed at 25 kPa oxygen pressure; Run 970317.

At the start of each oxygen pressure, the gas flow rate was 450 mL/min. The two pairs of arrows indicate that the gas flow rate was increased to 600 mL/min for the remainder of the run at that oxygen pressure.

Operating conditions: 80°C; 300 kPa O_2 pressure; liquid flow rate 20 mL/min; 0.090 M ethylene glycol concentration.

Something accumulates on the catalyst surface when deactivation is observed. When the oxygen pressure is lowered, the poisoning decreases. A probable explanation is that a reaction product is responsible for the deactivation. At higher oxygen pressures, more reaction occurs and hence more products are formed, leading to more rapid deactivation. However, it is also possible that oxygen was directly responsible for the catalyst deactivation.

This hypothesis was favoured by a number of researchers in similar systems where deactivation was observed (see Table 6.2). Ali Khan et al. (1983ab) in the oxidation of ethylene glycol to glycolic acid ascribed the deactivation observed to the formation of some unknown oxidized species of platinum (not PtO_2) and/or catalyst poisoning. Dijkgraaf et al. (1988ab) believed that the oxygen atoms dissolved into the platinum lattice. The interaction of the platinum lattice and the oxygen atoms resulted in the platinum lattice being unable to catalyze the reaction. This hypothesis is inconsistent with fundamental research on platinum. Mallat et al. (1992) believed that the platinum was "over-oxidized". Schuurman et al. (1992) hypothesized that too much of the surface was covered by chemisorbed oxygen and hence not enough was covered by the organic to be oxidized.

Before the theory that oxygen is responsible for the deactivation can be discounted, it should be further explored. The first problem with this theory is that it does not adequately explain why deactivation is not observed in all similar systems (see Table 6.3). More specifically, between 170 and 700 K, oxygen is recognized to adsorb in an atomic state on platinum (Peng and Dawson, 1974; Gland et al., 1980, Boreskov; 1982; Légaré et al., 1984; Puglia et al., 1995). There is little evidence to support an additional

90

Table 6.2: Catalytic Oxidation over Platinum Deactivation Observed – a sampling of the literature

Reaction	Support	Temperature	Reactants	Deactivation	Reference
glucose → gluconic acid → glucaric acid	carbon	55°C	aqueous phase; 100% O_2 in gaseous phase	• rapid deactivation	Dirkx and van der Baan (1981)
ethylene glycol (EG) → glycolic acid	carbon	40°C	aqueous phase; 101 kPa; EG conc. 0.05 - 0.3 M; initial O_2 conc.: 0.96×10^{-3}M	• initial rapid deactivation, followed by more gradual decline	Ali Khan et al. (1983ab)
D-gluconate → D-glucarate	carbon	50-55°C	aqueous phase; oxygen pressure 20 to 100 kPa	• rapid deactivation initially, followed by more gradual decline • deactivation of catalyst during storage in air	Dijkgraaf et al. (1988ab)
1-methoxy-2-propanol → methoxy-acetone	carbon; alumina	30-60°C	aqueous phase; air as oxidant	• rapid deactivation at 30°C • minimal deactivation at 60°C	Mallat et al. (1992)
methyl α-D-glucoside	activated carbon; graphite	50°C	aqueous phase; oxygen pressure of 1, 10, 100 kPa	• rapid deactivation initially, followed by more gradual decline	Schuurman et al. (1992)
ethanol	carbon	50°C	aqueous phase; oxygen pressure 8 to 120 kPa; ethanol conc 100 to 2500 mol/m³	• three steady states observed depending on reactor start up; more active following reductive as opposed to oxidative start up	Jelemensky et al. (1995, 1997)

Table 6.3: Catalytic Oxidation over Platinum
No Deactivation Observed – a sampling of the literature

Reaction	Support	Temperature	Reactants	Deactivation	Reference
glyoxal → glyoxylic acid	carbon	33°C	aqueous phase; air as oxidant	• none	Gallezot et al. (1992)
formic/oxalic/ maleic acid → CO_2 + H_2O	carbon	20 -190°C	aqueous phase; 1 or 15 bar air pressure	• none	Gallezot et al. (1996)
methanol → CO_2 + H_2O	hydrophobic on hydrophilic	25-70°C	humid air; atmospheric pressure	• 30 hour run with no deactivation	Cheng and Chuang (1993)
benzene/toluene/xylene → CO_2 + H_2O	hydrophobic on hydrophilic	90-130°C	humid air; atmospheric pressure	• none	Chuang et al. (1992)
formaldehyde → CO_2+H_2O	hydrophobic on hydrophilic	60-150°C	humid air; atmospheric pressure	• same catalyst for several exp'ts and no deactivation	Chuang et al. (1994)
benzene/styrene → CO_2+H_2O	γ-alumina on monolith	100-350°C	gas phase; air, oxygen rich or poor as oxidant	• none observed	Barresi and Baldi (1992)
ethanol → CO_2+H_2O	γ-alumina on monolith	95-350°C	gas phase; air as oxidant	• none observed	Barresi and Baldi (1993)
dichloromethane/ chloroform → CO_2 + HCl + Cl_2	alumina	300-400°C	humid air; 101 kPa	• conversion decreased from 92 to 86% in 160 hours	Papenmeier and Rossin (1994)
ethanol → ethanal	carbon	30°C; 51°C	aqueous phase with 50 kPa oxygen pressure	• no significant deactivation observed	van den Tillaart et al. (1994)

92

adsorption mechanism for oxygen. Oxygen adsorbing in the platinum lattice is not consistent with fundamental research on platinum: Salmerón et al. (1981) extrapolated some data on oxygen diffusion in platinum. At temperatures of 1200°C, their estimates indicated rapid diffusion of oxygen through platinum. However, at temperatures below 300°C, the rate of oxygen diffusion would be essentially zero. Over-oxidation of the platinum surface would appear to be unlikely, and as will be shown by the following experiments, this was not the cause of catalyst deactivation in this research.

To understand the impact of oxygen on the catalyst activity better, a series of experiments was undertaken where the catalyst preparation was modified. In the first experiment, Run 961125, the catalyst was only reduced, and not calcined. In the second experiment, Run 961202, the catalyst was treated as usual, with both hydrogen reduction and calcination in air. In the final experiment, Run 970123, following the calcination in air, the catalyst was treated under a flow of oxygen for 22 hours at 80°C, the reaction temperature. For each run, 25.0 g of 0.34 (wt)% Pt catalyst was used in the reactor. The total pressure was 347 kPa, with an oxygen partial pressure of 300 kPa.

Unlike the results reported by Dijkgraaf et al. (1988ab) and Dirkx and van der Baan (1981ab), exposure to oxygen prior to the experiment did not have a negative impact on the catalyst performance (see Figure 6.9). Calcination increased the rate of conversion above that of the catalyst that had only been reduced. The performance of the non-calcined catalyst improved to almost the same level as that of the calcined catalyst after the same amount of time-on-stream. Similarly, the extra oxygen treatment improved the catalyst activity further. Both of these results indicate that increased oxidation of the
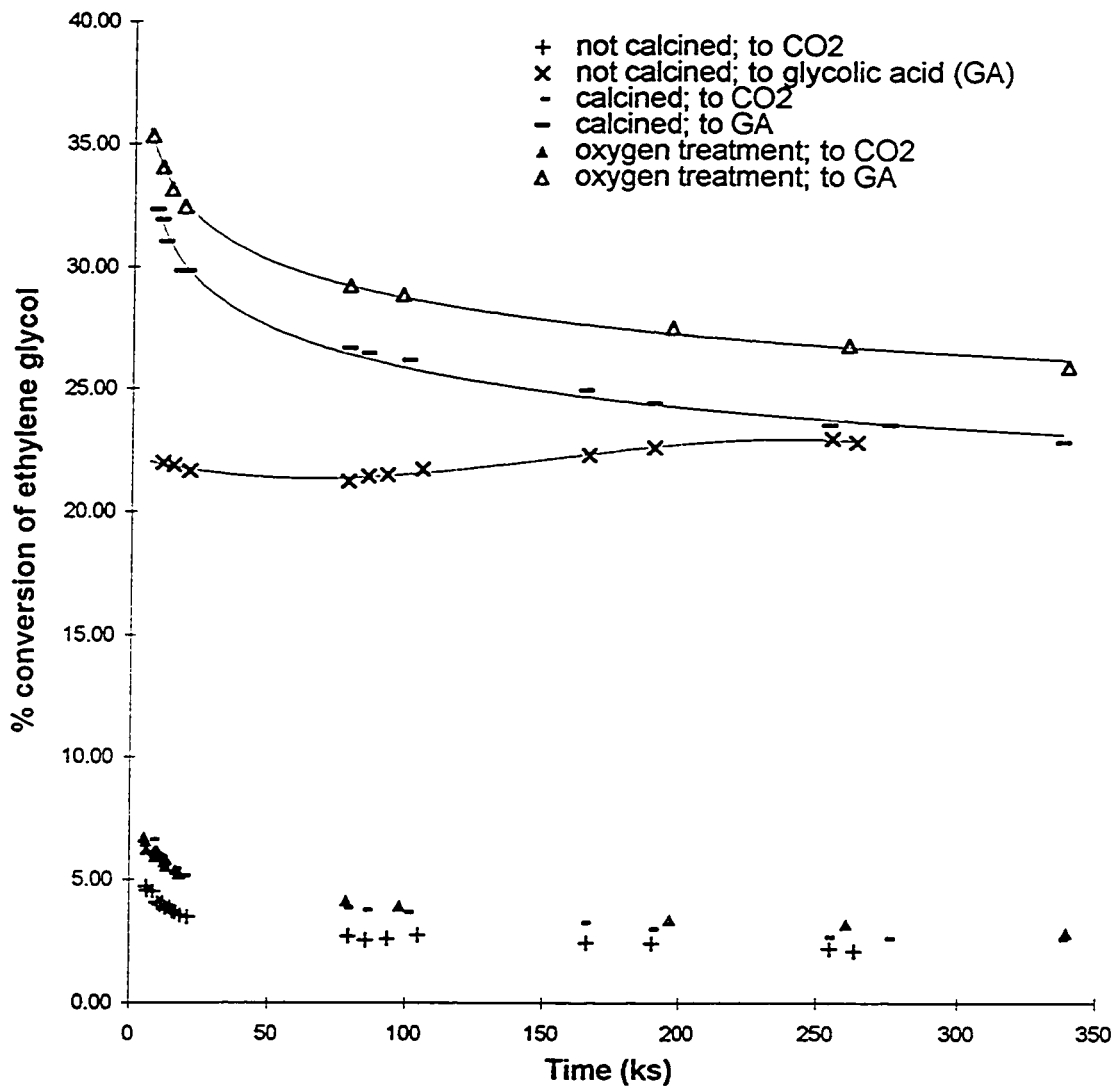
Figure 6.9: The effect of three different catalyst pre-treatments on catalyst deactivation; Runs 961125, 961202, and 970123.

Operating conditions: 80°C; 300 kPa O_2 pressure; O_2 flow rate 450 mL/min; liquid flow rate 20 mL/min; 0.090 M ethylene glycol concentration.

catalyst improves its performance. The rate of catalyst deactivation is slower with the catalyst that was only reduced. No noticeable difference was observed in the deactivation rate for the two calcined catalysts, despite the improved performance in overall conversion with the extra oxygen treatment. It is somewhat surprising that the results from the extra oxygen treatment do not converge with those of the reduced only and the calcined catalyst. This suggests that the extra oxygen treatment may improve the catalyst activity. However, with only one set of data and given the numerous difficulties encountered in achieving consistent results, it is quite possible that it is an anomalous result. Further experiments would be necessary to test this hypothesis.

These observations fit with fundamental research of oxygen adsorption on platinum. At these temperatures, it is widely believed that as an oxidation catalyst, platinum cycles between the oxidized state, Pt–O ($Pt^{(II)}$) and the reduced state, $Pt^{(0)}$ (Satterfield, 1980). It is the oxidized state of the platinum that reacts with the organic molecules:

$$Pt\text{–}O\ +\ EG\ \rightarrow\ EGO\ +\ Pt$$
$$2\,Pt\ +\ O_2\ \rightarrow\ 2\,Pt\text{–}O$$
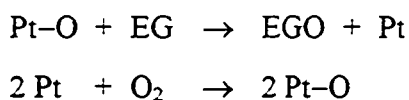
where EG represents ethylene glycol. The increase in the rate of reaction with both the calcination and the extra oxygen treatment suggests that the reoxidation of the platinum is rate limiting. The supply of oxygen is limited by the rate of its diffusion through the liquid film. Both the experimental results and Satterfield's widely accept theory are inconsistent with the hypothesis of either Mallat et al. or Schuurman et al. that too much oxygen causes a decrease in catalyst activity.

From these results, it can be concluded that oxygen on its own is not responsible for the catalyst deactivation. In the absence of a better explanation, it is conceivable that the presence of the organic compound has the same effect as high temperature and facilitates the conversion of oxygen into a more strongly adsorbed (and hence less reactive) form such as $Pt-O_2$ or lattice oxygen. It is difficult to explain how the presence of an organic molecule would allow some of the oxygen to adsorb on the platinum in the more active form, while increasingly cause oxygen to be adsorbed on the platinum in a less active form. As will be seen shortly, evidence of by-product formation was found, and this theory was discarded.

6.4.4 Effect of Catalyst Presoak

However, as already mentioned, it is probable that an oxidation product, either glycolic acid or another product, was responsible for the deactivation. To this end, a series of experiments looked at the effect of changing the ethylene glycol presoak to glycolic acid or to a mixture of ethylene glycol and glycolic acid. In each experiment the platinum catalyst was presoaked with 25 mL of solution, either 100 % ethylene glycol solution (Run 970728), 70% glycolic acid solution (balance water) from Aldrich Chemicals (Run 970324), or an equal mole percentage of ethylene glycol and glycolic acid (with a small amount of water present from the glycolic acid solution; Run 970805). No difference in the activity and rate of deactivation was observed between the ethylene glycol presoak and the equal molar ethylene glycol/glycolic acid presoak (see Figure 6.10). The glycolic acid presoak was done with a different batch of catalyst; however, it was clear that the activity
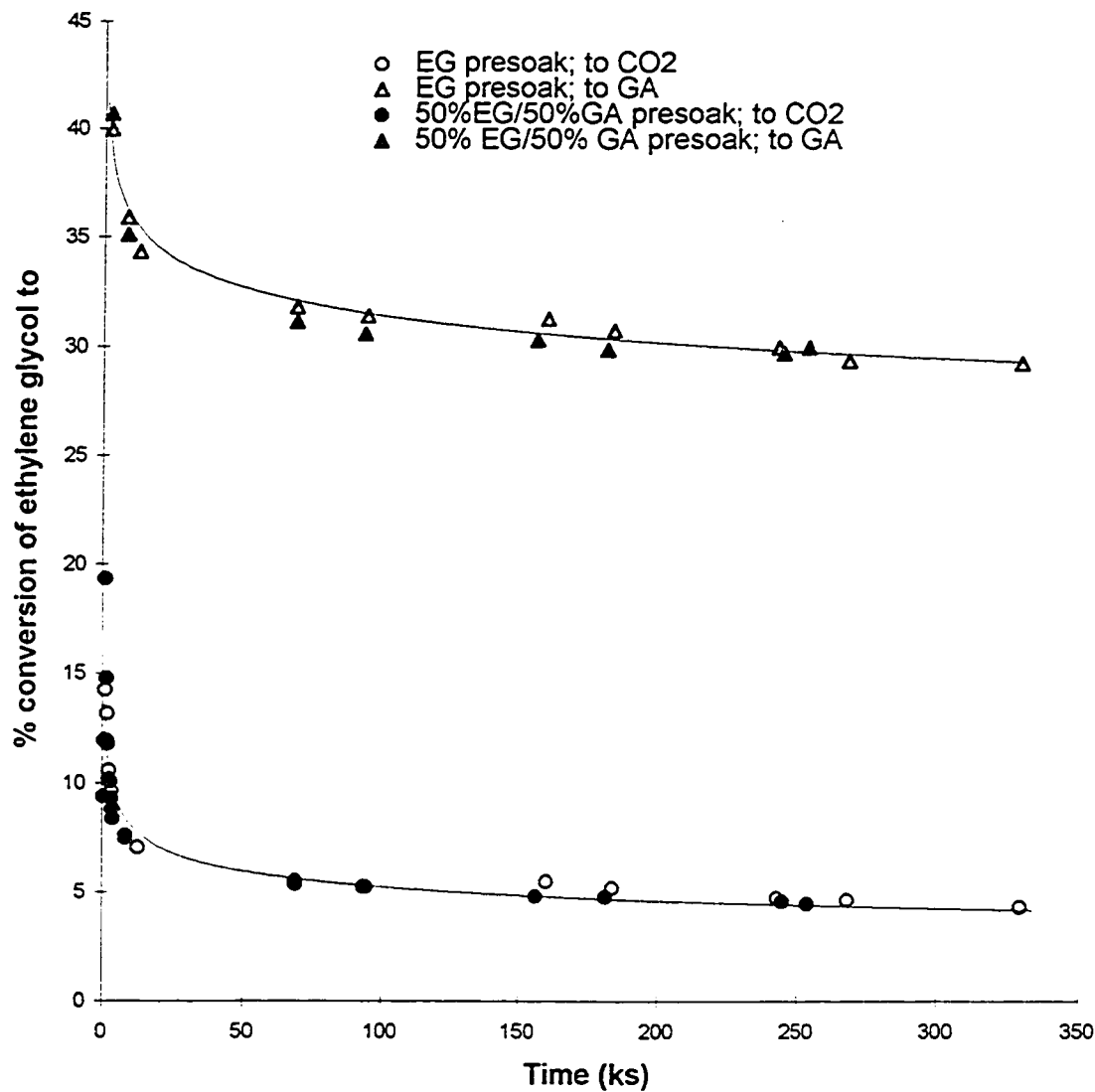
Figure 6.10: Comparison of catalyst activity following two different catalyst presoaks; Runs 970728 and 970805.

Operating conditions: 80°C; 300 kPa O_2 pressure; O_2 flow rate 450 mL/min; liquid flow rate 20 mL/min; 0.090 M ethylene glycol concentration.

of the catalyst was greatly depressed. When the reactor was heated to 120°C in the absence of oxygen (and therefore reaction), and then returned to the operating conditions, the rate of reaction improved to expected levels (Figure 6.11). Heating the reactor to 120°C caused much of the glycolic acid to vaporize.

To understand these results, it is instructive to look at the vapour pressure data of glycolic acid. In its pure form, glycolic acid is a crystal at room temperature and melts at 80°C. It has a vapour pressure of 30.3 kPa at 75°C and a normal boiling point of 100°C (Lide, 1996). From these data, it is evident that at 80°C, a small increase in temperature would significantly increase the vapour pressure of glycolic acid. When the catalyst is presoaked in a combination of glycolic acid and ethylene glycol, sufficient reaction occurs to cause a significant rise in temperature across the catalyst particles. This temperature rise is sufficient to significantly increase the vapour pressure of the glycolic acid such that the glycolic acid rapidly desorbs from the support and does not adversely affect the rate of reaction. When the catalyst presoak is with the 70% solution of glycolic acid, the glycolic acid strongly adsorbs to the catalyst sites and the support. Very little reaction occurs and as a result, insufficient heat is generated to volatilize the acid. The rate of reaction remains depressed, because the ethylene glycol is largely unable to reach the catalyst sites.
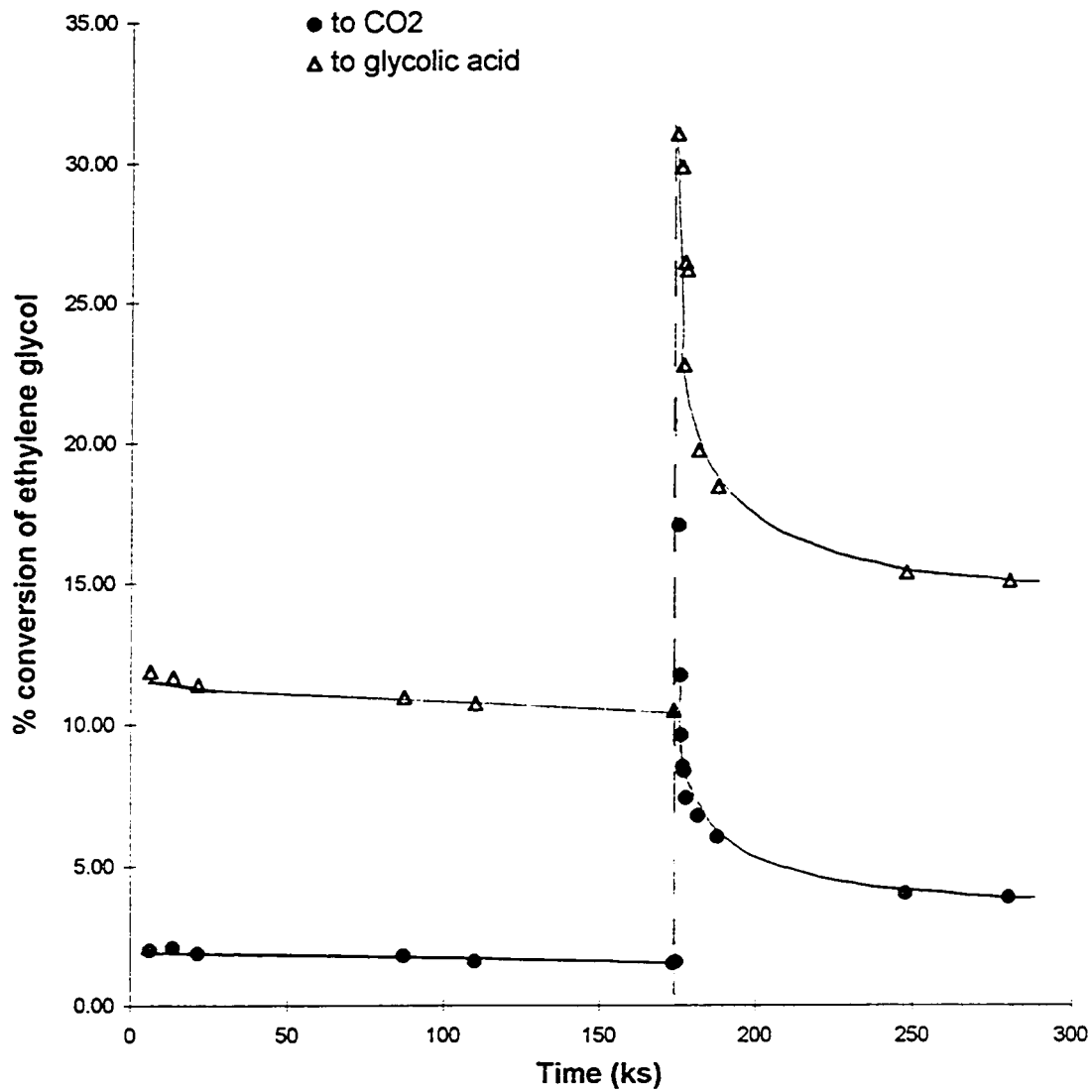
Figure 6.11:   Effect of glycolic acid presoak on catalyst activity;   Run 970324.

Operating conditions: 80°C; 300 kPa O_2 pressure; O_2 flow rate 450 mL/min; liquid flow rate 20 mL/min; 0.090 M ethylene glycol concentration.

6.4.5 Effect of Sodium Hydroxide

When sodium hydroxide was added to the feed solution, the rate of reaction was higher while the rate of deactivation did not change noticeably. In Run 970401, the 0.090 mol/L ethylene glycol feed was made basic by adding sodium hydroxide to the solution. The resulting concentration of sodium hydroxide was 0.0267 M. In Figure 6.12, the rate of deactivation with fresh catalyst is compared to a standard run (Run 961202) with no sodium hydroxide in the feed. Only a short time span is shown for this run, because a slight variation in concentration of sodium hydroxide has a big impact on the reaction rate.

It was thought that adding base to the liquid feed might have slowed the rate of deactivation, if the deactivation was caused by an acid by-product. It is suspected that many of the by-products are the result of acid catalyzed, condensation reactions (see Chapter 5, The Chemistry). The results were inconclusive, for although the rate of reaction increased, the rate of deactivation remained approximately the same. This result may simply indicate that the base remained largely on the surface of the catalyst spheres, where it increased the rate of oxidation by increasing the rate of glycolic acid desorption and suppressed deactivation at the surface. However, in the catalyst pores both the rate of reaction and deactivation may have remained unaffected by the sodium hydroxide.

The catalyst in Run 970401 was run intermittently with a sodium hydroxide feed for five days. Following this run, it was noticed that the percentage conversion of ethylene glycol had increased. A number of runs were carried out with different catalyst batches under various conditions. These runs had higher conversions than previously; in Figure 6.13, Run 961202, a standard run is compared to two other runs after the sodium
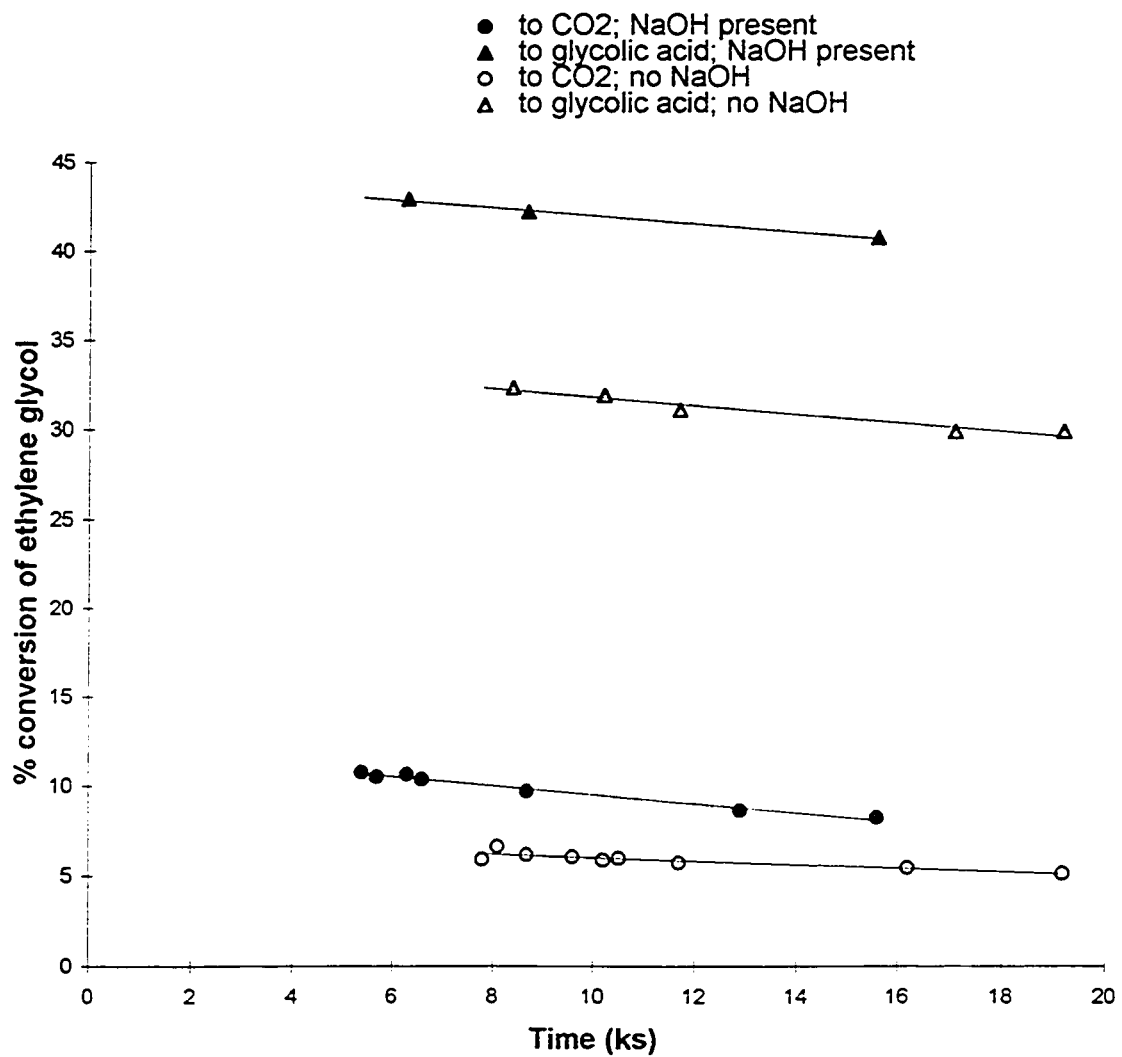
Figure 6.12: Effect of sodium hydroxide in the feed solution on the rate of catalyst deactivation; Run 970401.

Operating conditions: 80°C; 300 kPa O_2 pressure; O_2 flow rate 450 mL/min; liquid flow rate 20 mL/min; 0.090 M ethylene glycol concentration; 0.0267 N NaOH.
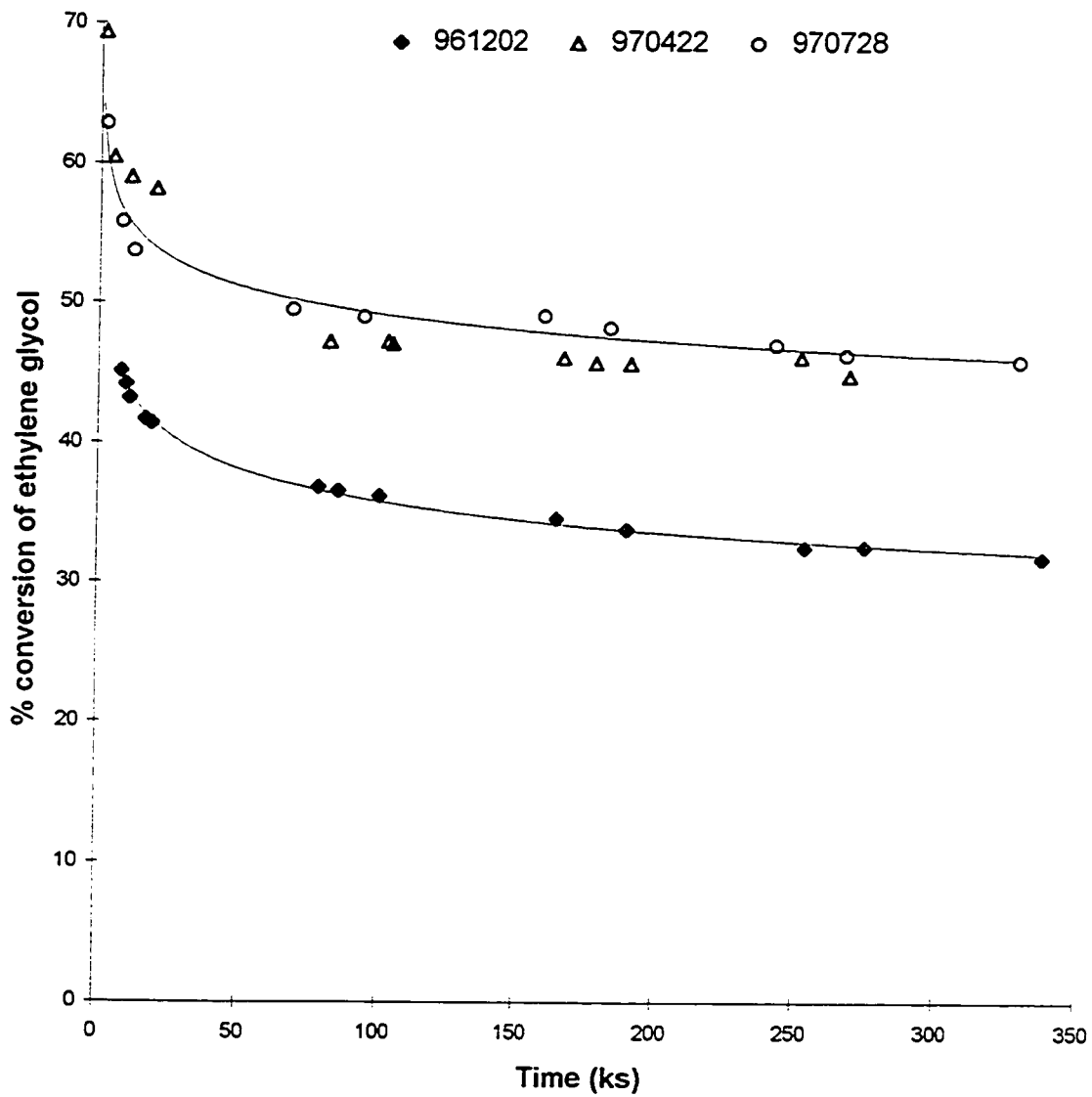
Figure 6.13: Difference in catalyst activity and deactivation rate before and after sodium hydroxide run, (Run 970401).

Operating conditions: 80°C; 300 kPa O_2 pressure; O_2 flow rate 450 mL/min; liquid flow rate 20 mL/min; 0.090 M ethylene glycol concentration.

hydroxide run. The catalyst loading and the operating conditions were the same for all three runs; the only differences between the runs was the catalyst batch and that the catalyst in Run 970422 was presoaked in an equal molar concentration of ethylene glycol and glycolic acid, instead of just ethylene glycol.

A possible explanation for this result, supported by the following analysis, is that the sodium hydroxide removed an impurity from the reactor system. Following the sodium hydroxide run, the reactor was opened and the catalyst bed removed. It was noticed that the ceramic rings at the top of the reactor were distinctly orange; this contrasted with the new rings, which are off-white, or the slight discoloration normally observed when the reactor was opened. Four of the rings removed from the reactor and four fresh rings were extracted with a dilute solution of hydrochloric acid (approximately 10 %) in water overnight at 80°C. The two liquid extracts were analyzed for metals using Inductively Coupled Plasma Spectroscopy. The results are shown in Table 6.4. For metals not listed, insignificant quantities were detected. The alumina and silica came directly from the ceramic rings. The various metals present in the liquid from the fresh ceramic rings were present likely in the water from the reverse osmosis process; some of the fittings are brass. The ceramic rings at the top of the reactor filtered out some of the trace impurities in the water, which led to elevated levels of these metals. This is somewhat concerning, since copper is a known poison of platinum (Marginean and Hodor, 1994). However, the quality of the water was beyond the control of this research. The elevated iron levels in the used ceramic ring extract came from the stainless steel of the systems. The source of the titanium remains elusive. Minimal discolouration of the crushed ceramic rings in the

reactor was observed. However, it is likely that a small amount of catalyst deactivation can be attributed to trace metal impurities.

Another possibility is that the difference in catalyst batches, made from different lots of styrene divinyl benzene copolymer, was responsible for the increase in activity. Certainly considerable variability exists in both pore size distribution and total surface area of the support as well as the platinum dispersion. Further experiments would be required to test this hypothesis.

Table 6.4: Results from Inductively Coupled Plasma analysis comparing the extract of unused ceramic rings to that of ceramic rings removed from top of the catalyst bed.

Metal	Unused Rings mg/L	Used Rings mg/L
Aluminum	9.3	15.4
Chromium	--	0.08
Copper	0.04	1.1
Iron	1.0	24.7
Nickel	0.04	1.1
Lead	--	0.2
Zinc	0.6	2.7
Calcium	6.5	12.5
Potassium	3.9	6.1
Magnesium	2.5	27.2
Titanium	--	19.2
Sodium	2.8	saturated
Phosphorus	--	1.5
Silicon	1.9	2.1

6.4.6 Mass Balance Results

In support of the hypothesis that the catalyst deactivation was the result of poisoning by a reaction byproduct is the reactor mass balance (see Chapter 3, The Trickle-Bed Reactor, Table 3.4). More carbon was missing in the mass balance initially, when the rate of deactivation was highest. At the first sampling time, 2.3 mg/min or 5.3% of the carbon was unaccounted for. After two days of running, only 0.6 mg/min, or 1.5% of the carbon remained unaccounted for and the rate of deactivation had greatly slowed down. It is estimated that for the first two days the average rate of carbon accumulating in the reactor was 1.0 mg/min. This is equivalent to a total of 2.9 g for the first two days. The rate of carbon accumulation, (the unaccounted carbon in the mass balance), after two days of operation was 0.6 mg/min, becoming increasingly more gradually. At steady state, when deactivation had ceased, approximately five grams of carbon are estimated to have accumulated. This carbon would be spread over the entire surface area of the catalyst and would not be readily detected when the catalyst was removed from the reactor.

6.5 Deactivation Model

All of these experiments, including the results from the uncalcined catalyst (Figure 6.9) can be explained by a fairly simple model. In this, both the rate of reaction and the rate of deactivation are functions of oxygen pressure. More specifically, the rate of deactivation is faster at higher activities, which corresponds to higher oxygen pressures, all things being equal. Whether deactivation or reactivation was observed at a given oxygen pressure depended on the amount of catalyst activity remaining. Deactivation is a result of

reaction, most likely the result of a byproduct that is strongly adsorbed onto catalyst sites. As the concentration of the poison accumulates on the active sites, the activity of the catalyst drops. However, the poison diffuses away from the active sites, on the catalyst support (Figure 6.14). When the rate of accumulation equals the rate of removal, deactivation stops, and steady state exists, until the balance is upset.

When the reactor was shutdown for several days and then restarted, no deactivation was observed for a time (Figure 6.15). The concentration of poison in the immediate vicinity of the catalyst sites was constant because of diffusion that had occurred when the reactor was off. Insignificant reactivation had occurred during shutdown because, at room temperature, any poison adsorbed onto a platinum site remained adsorbed. The poison is too strongly adsorbed at 20°C for significant desorption to happen. In this study at the reaction temperature, the adsorption of the poison was not as strong as at room temperature and some poison desorption would be possible. This conclusion is consistent with the finding of Mallat et al. (1992) that severe deactivation at 30°C is virtually eliminated at 60°C. In the case of the results of Mallat et al., the adsorption of the poison onto the catalyst active sites is significant at 30°C, but not at 60°C.

At both room temperature and the reaction temperature, diffusion on the support occurred. The diffusion at room temperature is significantly slower than that at 80°C, the operating temperature for the reactor. The diffusion at 80°C was estimated using the Wilke-Chang equation to be 3.4 times the rate of that at 20°C (see Appendix F).

When the oxygen pressure was either lowered or replaced entirely with nitrogen, a dramatic increase in catalyst activity was observed temporarily following the increase of
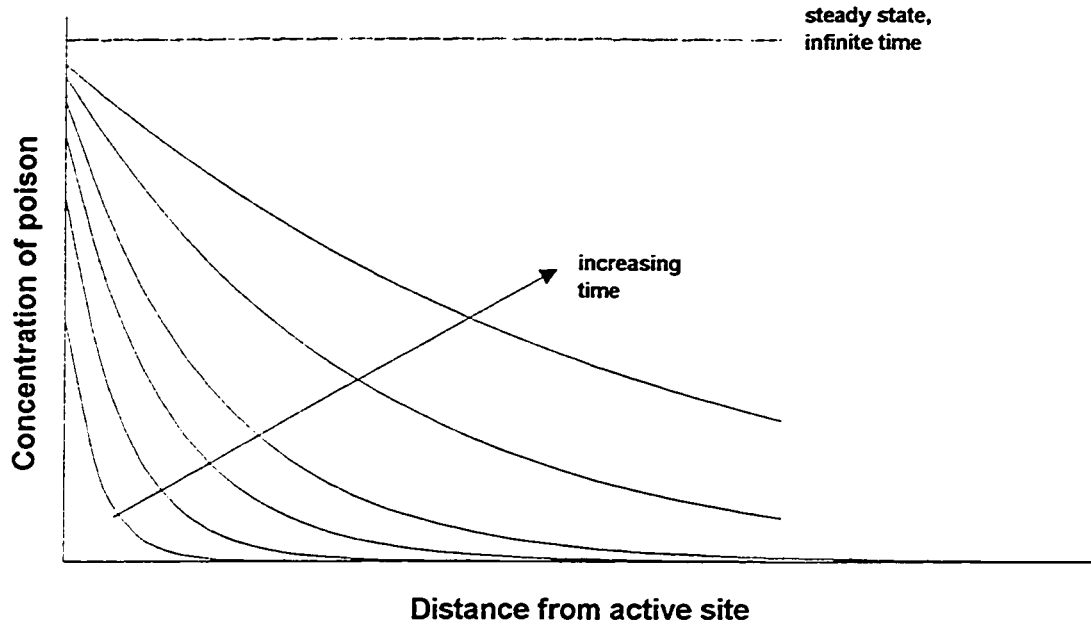
Figure 6.14: Concentration of poison versus the distance from the active site at constant operating conditions.
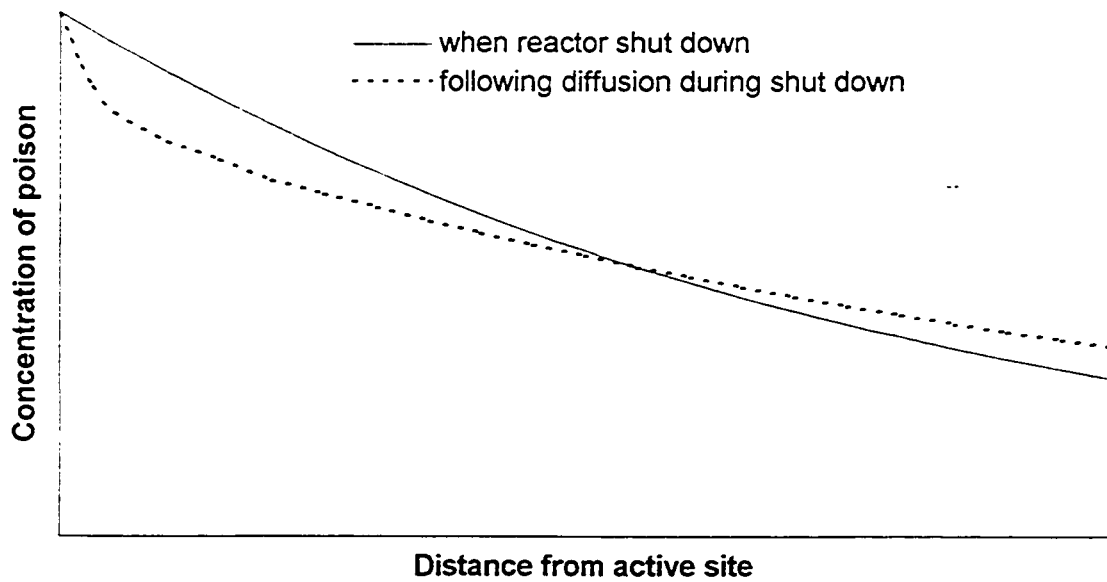
Figure 6.15: Concentration of poison as a function of distance from an active site when no change in catalyst activity is observed after the reactor is shut down and then restarted.

108

the oxygen pressure. This dramatic increase was followed by rapid deactivation. Whether the liquid was left on or switched off, similar results were observed. During the reduced rate of reaction, less of the byproduct(s) causing deactivation appears to have been produced. The net result was that some of the poison desorbed from the deactivated sites (Figure 6.16). However, the poison remains on the catalyst support, and diffusion of the poison away from the active sites is slow. The concentration profile of the poison moving away from an active site becomes flatter. When the oxygen pressure is increased to previous levels, the initial rate of reaction is much higher because much of the poison has desorbed from the active sites. Similarly the rate at which the poison is produced increased and the poison accumulates rapidly. Unlike the results with fresh catalyst, the poison diffusion away from the active sites is slower. This results from the concentration gradient being not as steep, because much of the poison remains adsorbed onto the catalyst support. Therefore, deactivation occurs rapidly following reactivation.
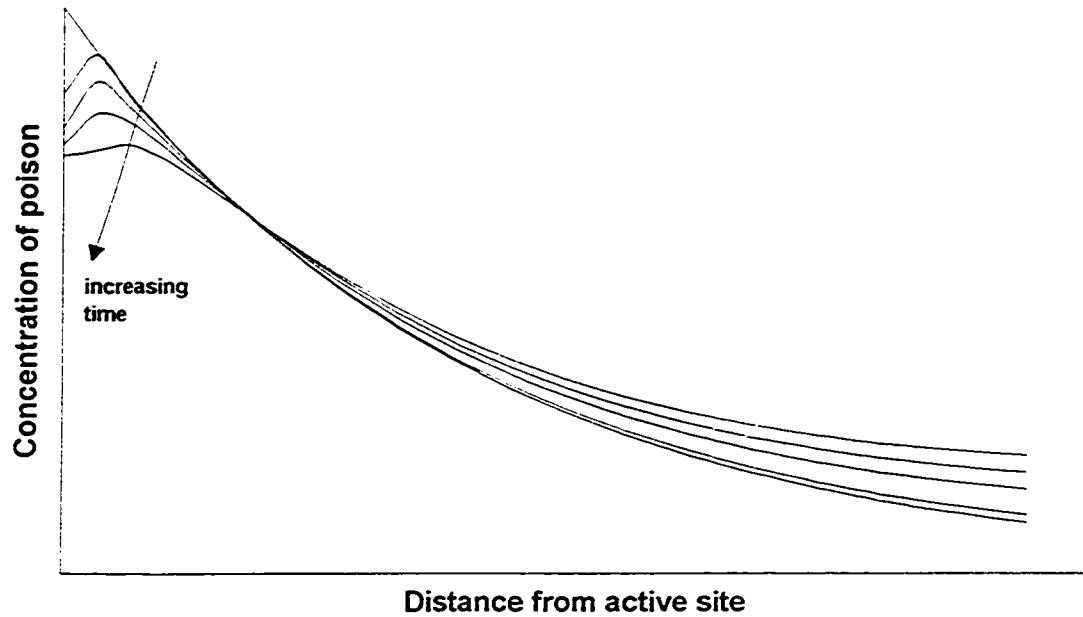
Figure 6.16: Concentration of catalyst poison versus distance from active site when catalyst reactivation is observed following a drop in oxygen pressure.

7. Reaction Kinetics

An integral part of reactor design is determining a rate equation and the reaction rate constant. Much of the work in the previous chapters has been leading up to this point. Before any attempt at kinetic modeling can be made, reproducible experimental data is essential. The nature of a trickle-bed reactor, such as was used in this study, will introduce some variability. As already discussed in the chapter on the trickle-bed reactor, various measures were taken to improve the reproducibility of the data. The catalyst support also introduced some problems with reproducibility. Some data were discarded, because of irreproducible results, thought to be connected to the catalyst batch. The final obstacle to obtaining reproducible data was the deactivation. Deactivation is generally divided into two categories: separable and non-separable. For separable deactivation, it is possible to clearly distinguish the kinetics from the deactivation in the modeling. With non-separable data, as was the case here, this is not possible.

The ability to get reproducible data was demonstrated. Three sets of data are plotted with three reactor bed loadings in Figure 7.1. While the data do not correspond perfectly, two different catalyst batches are represented, which would account for the discrepancy. Mass transfer limitations and temperature gradients were minimized as much as possible. The measurements of composition and temperature used to interpret the data are those of the bulk fluid, yet the rate of reaction is determined by the conditions existing at the active sites of the catalyst. In the absence of any diffusional effects, the bulk conditions are the same as the surface conditions and the intrinsic kinetics are observed. If

111
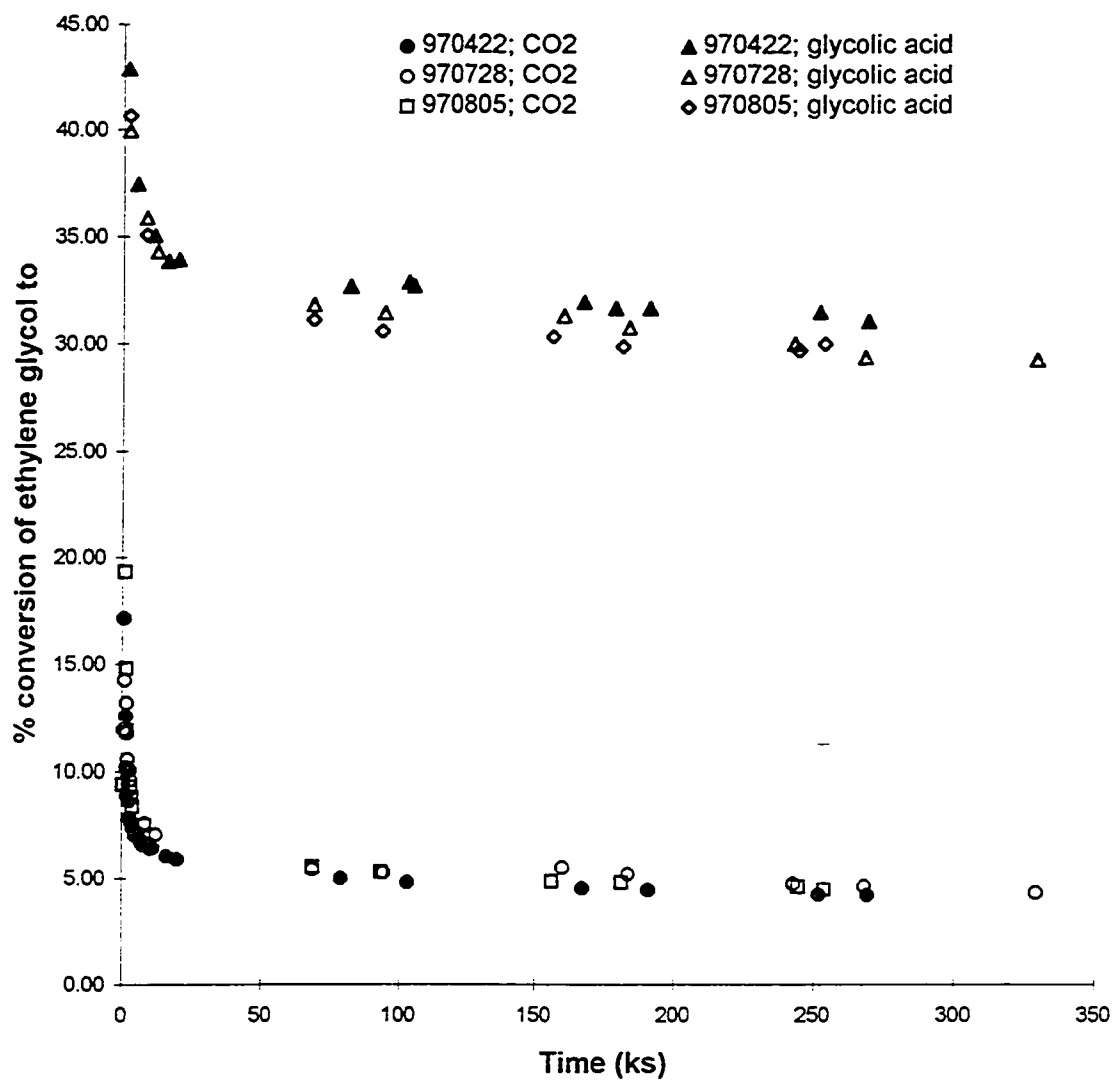
Figure 7.1: Reproducibility of experimental data with standard reaction conditions.

Operating conditions: 80°C; 300 kPa O_2 pressure; O_2 flow rate 450 mL/min; liquid flow rate 20 mL/min; 0.090 M ethylene glycol concentration.

112

concentration gradients caused by the limitations of diffusion are significant, the rate and selectivity of the reaction change with the bulk concentration and temperature in a different manner than they would in the absence of such gradients, and the kinetic behaviour observed is termed "apparent" or "effective" (Satterfield, 1970).

As was discussed in Chapter 3 on the trickle-bed reactor, mass transfer effects were not observed at 80°C with a liquid flow rate of 20 mL/min, a gas flow rate of 450 mL/min, oxygen pressure of 300 kPa, and catalyst spheres of 20-50 mesh and 1.0 (wt)% platinum loading. However, as mentioned in Chapter 6 on catalyst deactivation, when the oxygen pressure was 25 kPa, still with a total pressure of 347 kPa, the presence of external mass transfer limitations was confirmed. In Run 970317, the gas flow rate was increased from 450 mL/min to 600 mL/min and the conversion of ethylene glycol increased. The same experiment was attempted at 50 kPa oxygen pressure. However, the catalyst deactivation meant that the results were inconclusive. For this reason, the lowest oxygen pressure used in the kinetic experiments was 150 kPa. When the data were analyzed, the results at this pressure were checked to be sure that they were consistent with the rest of the data.

The approach taken here is first to discuss the reaction data qualitatively, and to develop a rate equation.

7.1 Qualitative Discussion

In the section on the chemistry, glycolic acid and carbon dioxide were successfully identified. Various other byproducts were observed, but not identified. However, these

byproducts are believed to be larger molecules than ethylene glycol and not intermediate products in the oxidation of ethylene glycol to either glycolic acid or carbon dioxide.

In the reaction kinetics, it is useful to determine whether the carbon dioxide is formed from the glycolic acid or from the ethylene glycol through a different pathway for which no reaction intermediates have been identified. With the exception of carbon dioxide, no single carbon molecules were detected. This is not surprising, since breaking the carbon carbon bond requires a large amount of energy. The reaction would proceed rapidly to completion following this step. It is beyond the scope of this study to determine what other intermediate steps occurred and a more detailed reaction pathway.

To determine whether the carbon dioxide was formed from glycolic acid, three situations were studied. In all three experiments, the operating conditions were the standard conditions described in Chapter 6 on catalyst deactivation: 80°C, 347 kPa total pressure, 300 kPa oxygen pressure, 450 mL/min oxygen flow rate, and 20 mL/min liquid flow rate. In the first scenario, Run 970429, 25.0 g of 0.34 (wt)% platinum catalyst was presoaked in 25 mL of an aqueous solution of 70 % glycolic acid. A fairly high concentration of glycolic acid, 0.0893 mol/L, was used in the feed solution. This concentration is approximately the same as one of the ethylene glycol concentrations used, and four times the effluent concentration of glycolic acid with an ethylene glycol feed of 0.090 mol/L. These results were compared with two different runs. The first of these was a standard run, Run 970505; in this run, the catalyst was presoaked in 25 mL of ethylene glycol and the feed solution was 0.090 mol/L of ethylene glycol. The glycolic acid presoak is believed to decrease the rate of reaction through its strong adsorption to the active sites

(see Chapter 6, Catalyst Deactivation). Because the glycolic acid presoak did reduce the rate of conversion of ethylene glycol (Run 970324), the results are also compared with this run.

The conversion to carbon dioxide for all three runs is compared in Figure 7.2. When compared with the quantities of carbon dioxide produced from the glycolic acid alone, ten times more carbon dioxide was produced from the ethylene glycol when the catalyst was presoaked in ethylene glycol and about three times more was produced from the ethylene glycol when the catalyst was presoaked in glycolic acid. From these results, it was concluded that the majority of the carbon dioxide was formed from the ethylene glycol, not via the intermediate of glycolic acid. A small portion of the carbon dioxide was produced from the glycolic acid. A series/ parallel reaction network exists:

$$\tag{7.1}$$
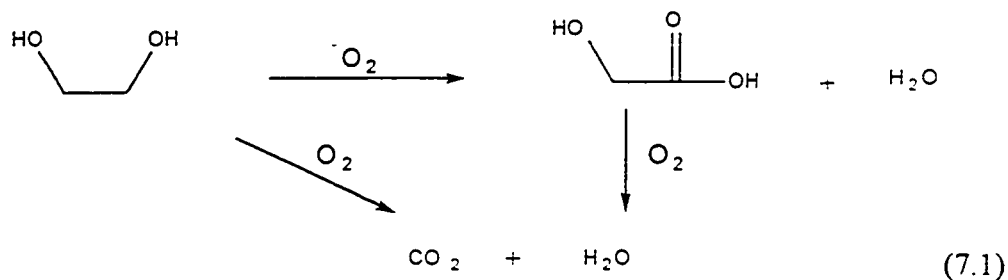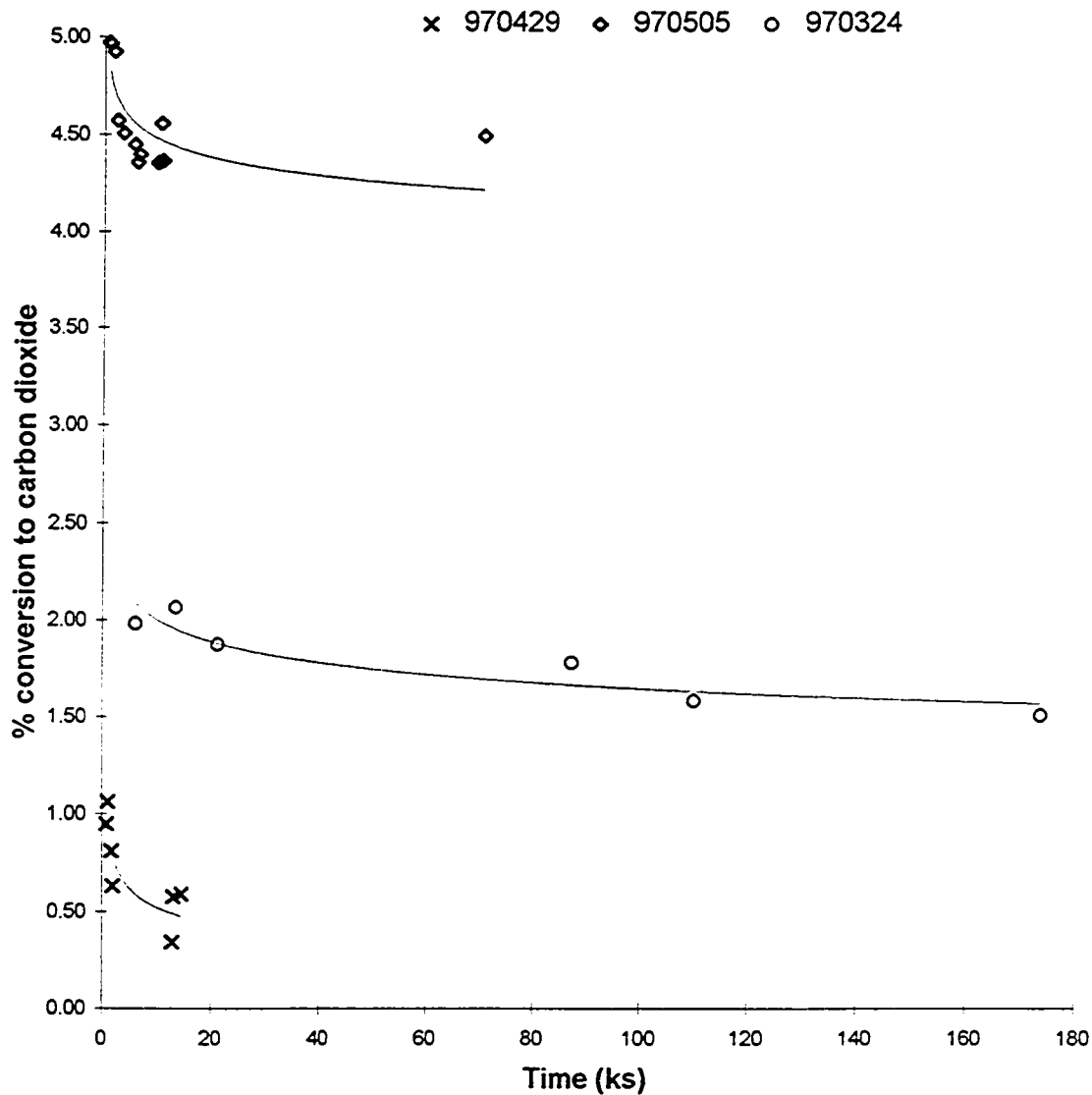
Figure 7.2: Conversion of glycolic acid to carbon dioxide (Run 970429), compared to that of ethylene glycol to carbon dioxide with different presoak treatments for the catalyst (Runs 970505 and 970324)

Operating conditions: 80°C; 300 kPa O_2 pressure; O_2 flow rate 450 mL/min; liquid flow rate 20 mL/min; 0.090 M ethylene glycol concentration.

7.2 Kinetic Modeling

A number of experiments were carried out to examine at the effects of oxygen pressure and ethylene glycol concentration on conversion and rate of reaction. Studying the effect of oxygen pressure was somewhat challenging: at low oxygen pressures, a sufficiently deactivated catalyst would start to regain activity. (This reactivation of catalyst is believed to result from reduced formation of the byproduct that is responsible for the poisoning.) Because the identity of this byproduct was not determined, and no method was available for accurately quantifying the byproduct, it was not possible to develop a kinetic model that would account for this phenomenon. Instead, the data were adjusted to remove the effects of the deactivation as much as possible. Data from a single experimental series were used to develop the kinetic model, because of the variations in results that were observed, particularly between catalyst batches. The other experimental data added qualitative insight into the reaction mechanism.

The trickle-bed reactor was modeled as a plug flow reactor in an integral manner, that is to say with relatively high conversions. The continuity equation for component A, in this case ethylene glycol, is

$$F_{AO} \, dx_A = -r_A \, dW \tag{7.2}$$

where F_{AO} = inlet flow rate of A, mol/h

x_A = conversion of A

$-r_A$ = rate of reaction, $\mathrm{mol \cdot h^{-1} \cdot g^{-1}}$ catalyst

W = weight of catalyst, g

and over the whole reactor,

$$\frac{W}{F_{AO}} = \int \frac{dx_A}{-r_A} \qquad (7.3)$$

To find a model to fit the experimental data, there are two options. The rate

equation can be assumed and then the right hand side of the equation integrated. This

requires an iterative approach until the data fits acceptably with the assumed rate equation.

The other option is to differentiate the data which is the approach that was used here. This

gives the rate of reaction, which then is plotted against the various values of C_A, the exit

concentration of A. The objective is to find a linear relationship between r_A and $f(C_A)$

(Levenspiel, 1962; Froment and Bischoff, 1990).

All of the data for the kinetic model were collected with the same catalyst bed.

This eliminated any variability that existed between catalyst batches and that occurred

when packing the reactor bed. These data were collected as a continuation of Run

970805. At this point in the experiment, the catalyst was no longer deactivating rapidly.

The ethylene glycol concentration was varied between 0.045 M and 0.72 M for

four different partial pressures of oxygen: 150 kPa, 225 kPa, 300 kPa, and 450 kPa.

During these measurements, when the feed concentration of ethylene glycol was changed,

at the higher concentrations, a lag occurred in the change in conversion. For example,

when the ethylene glycol concentration was decreased from 0.72 M to 0.090 M, initially

the conversion was unstable; it dropped quite rapidly from an inflated value to a value

consistent with the other measurements. The reverse trend was also observed, with an

increase in conversion occurring when the ethylene glycol feed concentration was

increased to a higher level. This hysteresis is separate from the deactivation discussed in

the previous chapter. It is the result of the lag in absorption and desorption of ethylene

glycol from the catalyst support. For this reason, some of the conversion data were

adjusted slightly to ensure that the lower conversions of ethylene glycol at lower oxygen

pressures were accurately reflected. This was achieved by using the data that were

collected consecutively at a given ethylene glycol concentration for several oxygen

pressures.

The conversion of ethylene glycol was determined directly via gas chromatography

for several liquid samples. For the samples from the liquid effluent of the 0.045, 0.090 and

0.18 M ethylene glycol feed concentration, the amount of ethylene glycol converted was

approximately 35 percent greater than the combined amount of glycolic acid and carbon

dioxide produced. This 35 % (or 25 % of the reacted ethylene glycol) represents the

portion of ethylene glycol that was converted to other oxidation products. In the case of

the liquid effluent samples where the ethylene glycol feed concentration was 0.36 and

0.72 M, the amount of ethylene glycol unaccounted for by conversion to glycolic acid and

carbon dioxide was significantly more than 35 percent of the reaction products (see

Table 7.1).

Table 7.1: Percentage of ethylene glycol converted to reaction products and the percentage that represents of the total conversion.

Ethylene glycol feed concentration (M)	0.045	0.090	0.18	0.36	0.72
% conversion of ethylene glycol (EG)	57.7	43.2	31.1	25.0	16.8
% conversion of EG to glycolic acid	34.9	28.0	20.4	14.5	9.8
% conversion of EG to carbon dioxide	8.92	4.20	2.14	1.45	1.10
% EG unaccounted for by glycolic acid and carbon dioxide	14.0	11.0	8.5	9.1	5.9
% that the unaccounted portion represents of total EG converted	24	25	27	36	35

For the liquid effluent sample for the 0.36 M feed, 9.3 % of the ethylene glycol was not accounted for by the glycolic acid and carbon dioxide. Similarly for the 0.72 M feed, 5.9 % was unaccounted for. If the other oxidation products were 25 % of the total reacted ethylene glycol, one would expect that 6.3 % and 4.2 % of the ethylene glycol would be unaccounted for in the case of the 0.36 M and 0.72 M ethylene glycol feeds, respectively. Three of the liquid effluent samples from the 0.72 M ethylene glycol feed were analyzed for total organic carbon. In all these samples, 4 % of the inlet carbon was unaccounted for in the effluent streams. This result is much larger than the 1 % that was observed in the mass balance calculations (Chapter 3, Trickle-Bed Reactor). However, it is consistent with the observation that the ethylene glycol conversion did not immediately reach its maximum value when the feed concentration was increased. Based on the discussion in Chapter 6, Catalyst Deactivation, it is expected that a portion of this carbon

was in a reacted form. However, some of the missing carbon is thought to have remained in the reactor as unreacted ethylene glycol. This would cause a rise in the surface concentration of ethylene glycol and would explain the observed hysteresis in the conversion when the ethylene glycol feed concentration was changed. This would also explain the discrepancy observed between the expected 25 % of the reacted ethylene glycol that was attributed to other reaction products, and the actual amount of ethylene glycol that was missing from the liquid effluent. Therefore, for all samples, the conversion of ethylene glycol was calculated by adding together the fraction of ethylene glycol converted to carbon dioxide and that converted to glycolic acid and multiplying by 1.35.

With these data, a rate equation was developed. For each oxygen pressure, the conversion was plotted against W/F_{EGO}, the weight of the catalyst divided by the initial flow rate of ethylene glycol, and a smooth curve was drawn by hand through the data. The slope of these curves gives the rate of reaction. This slope was determined by drawing a tangent to the curve at each data point. Figure 7.3 illustrates this method.

The equation shown in the figure:

$$-r_A = \frac{\Delta x}{\Delta \dfrac{F_{AO}}{W}}$$
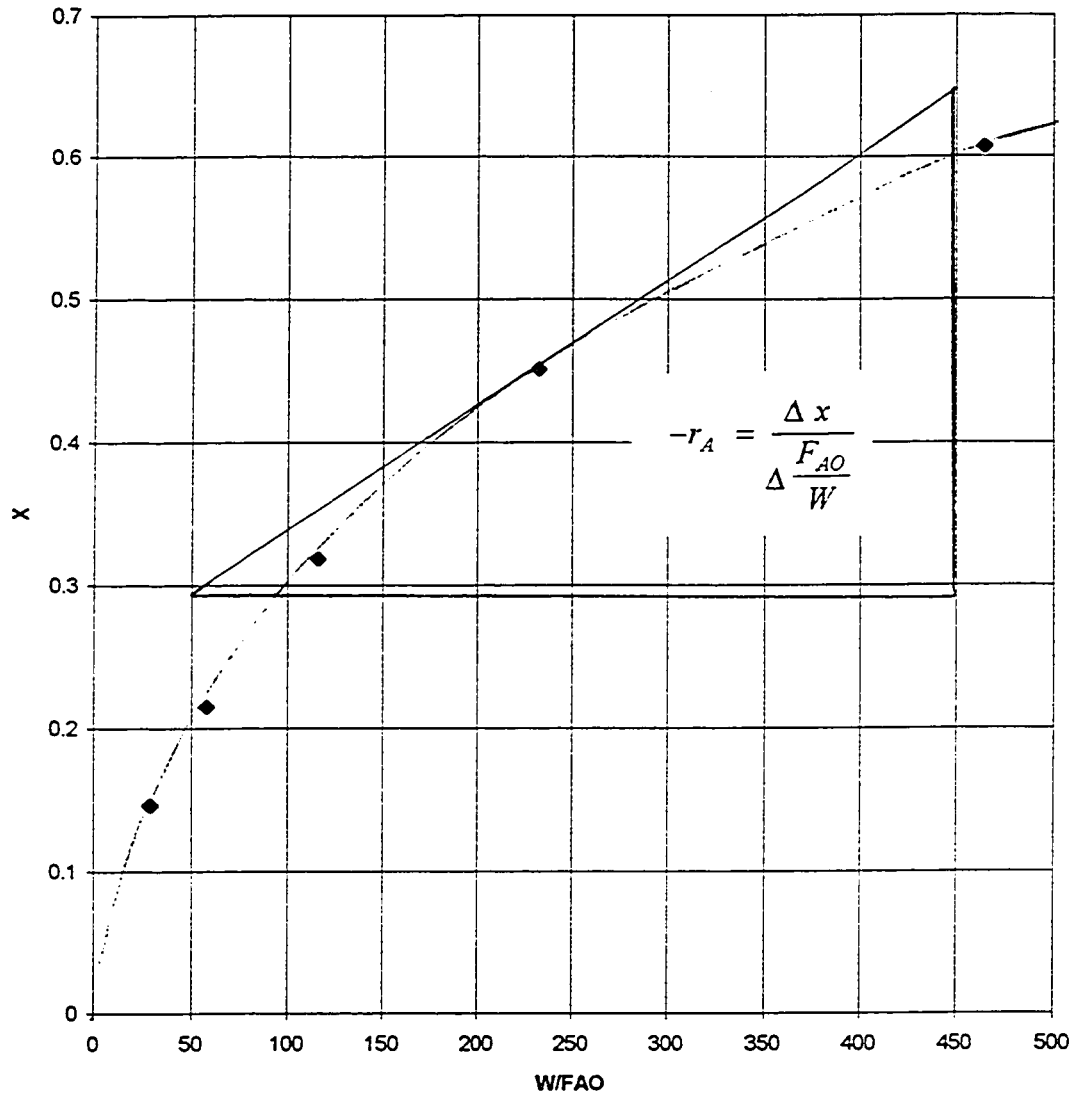
Figure 7.3: Calculating the rate of reaction for the oxygen pressure of 300 kPa.

The dependence of the rate of reaction on the ethylene glycol concentration was determined by first assuming a simple power law model:

$$-r_{EG} = k' C_{EG}^\alpha \tag{7.4}$$

where

$-r_{EG}$ = rate of reaction of ethylene glycol, $mol \cdot h^{-1} \cdot g^{-1}$ catalyst

k' = reaction rate constant, and includes any dependence on oxygen pressure and glycolic acid concentration

C_{EG} = final concentration of ethylene glycol, mol/L

α = order of the reaction in terms of ethylene glycol concentration

This equation was transformed by taking the logarithm of both sides:

$$\ln(-r_{EG}) = \ln k' + \alpha \ln C_{EG} \tag{7.5}$$

The order of the reaction in terms of ethylene glycol concentration was readily found by plotting $\ln(-r_{EG})$ versus $\ln C_{EG}$; α is the slope of the curve. Similarly, $\ln k'$ is the intercept of the curve. A value of α was found for each oxygen pressure. The results are compared in Table 7.2. Examination of the rate of reaction data does not reveal any effect of oxygen pressure on the rate of reaction. However, it was observed when the data were collected that the conversion tended to be higher at higher oxygen pressures. In the analysis, it was not possible to reflect this for two reasons: the method of analysis is subject to error, and various factors when the data were collected meant that the slight inaccuracies (as a result of deactivation and hysteresis) confounded the effect of oxygen pressure.

Table 7.2: The calculated values of ln k' and α for each oxygen pressure from the data of Run 970805 for the kinetic modeling (Table E.18).

Oxygen Pressure (kPa)	ln k'	α
150	−5.6797	0.456
225	−5.7119	0.415
300	−5.5164	0.514
450	−5.575	0.425
Average		0.45 ± 0.04

If the rate of reaction equation were limited to a power law model, the final step would be to plot all of the values of the rate of reaction versus $C_{EG}^{0.5}$. The reaction rate constant, k, is the slope of the line.

However, this model does not account for any effect that glycolic acid might have on the rate of reaction. If glycolic acid were to have an effect, it would be expected to be in the form of competitive adsorption with ethylene glycol. Evidence was found in the experiments that glycolic acid competed with ethylene glycol for reaction sites. Some of these results were discussed already in Chapter 6, Catalyst Deactivation, where the glycolic acid presoak greatly suppressed the rate of reaction. An additional test at the end of Run 960524 supports this conclusion. For the first set of measurements, no glycolic acid was added to the feed; the ethylene glycol concentration in the feed was 0.18 M. Two different concentrations of glycolic acid, 0.05 M and 0.09 M, were added to a 0.18 M ethylene glycol feed. This represents approximately two to four times the amount of

glycolic acid that would be produced during the reaction. The results from this experiment are shown in Table 7.3. The rate of reaction decreased greatly in the presence of 0.05 M of glycolic acid. However, the conversion of ethylene glycol when 0.09 M glycolic acid was added to the feed was quite high, but largely unaccounted for in the reaction products of carbon dioxide and glycolic acid. It is suspected that a previously small side reaction between ethylene glycol and glycolic acid may have dramatically increased. Additional experiments would be required to determine if this were in fact the case. Because of the difficulties encountered with the reactor system and the steps required to ensure consistent data, further experiments in this direction were not pursued.

Table 7.3: Effect of the addition of glycolic acid to the ethylene glycol feed; Run 960524.

Glycolic Acid in Feed	0.0 M	0.053 M	0.091 M
% conversion of ethylene glycol	22.7	6.6	20
% conversion to glycolic acid	15.2	4.3	1.5
% conversion to CO_2	4.6	1.0	0.4

At this point, it is instructive to look at rate equations developed using a Langmuir-Hinshelwood approach. The assumptions of the Langmuir adsorption isotherm are as follows:

- All species are attached to a specific site.

- Each site can only accommodate one adsorbed entity.

- The energy of adsorbed species is constant and independent of both the site and the fractional coverage.

For most solids, the sites for adsorption are not equivalent and interactions between adsorbed molecules may not be negligible (Gates, 1992). However, despite these limitations, this model often brings useful insight into the reaction mechanism.

The classic papers of Boudart (1956) and Weller (1956) argue for and against the use of the Langmuir-Hinshelwood approach. Central to Weller's argument is that because the underlying assumptions of the Langmuir isotherm are often not valid, the Langmuir-Hinshelwood approach brings unjustified complexity to the modeling. He argues in favour of a simpler method of analysis using the power law approach, where the concentration of the reactants and any products or foreign substances are raised to exponents with integral or half-integral values. This is the approach that has been used up to this point in this analysis.

Boudart argues that the added insight gained from using the Langmuir-Hinshelwood model justifies its use. The limitations of the approach, while they should be borne in mind, do not prevent useful understanding from being gained. Boudart goes as far as to recommend that when a mechanistic model is not available, an attempt can be made to derive a mechanism from the empirical rate equation.

No attempt was made at developing a mechanistic model for this system either before or after developing a rate equation. Numerous steps exist for each reaction shown. Intermediates in these reactions were not detected, although they may be present. In addition, no reactions are shown for the byproducts which were detected. The identities of

the byproducts were not conclusively determined making it difficult to postulate a reliable equation for the rate of reaction. Rather, it was useful to investigate the form of the equation and the values of the rate constants. From the equation some of the important parameters in determining the rate of reaction were identified and one can postulate as to some of the important steps in the reaction mechanism.

In a Langmuir-Hinshelwood rate equation, the rate controlling reaction is found in the numerator, similar to the power law expression that was derived here. The competitive adsorption of all species is found in the denominator of the equation in the form of a site balance where the various species compete for a fixed, total number of sites. This term also accounts for the number of sites required in the reaction. Without a mechanistic model, it is unreasonable to assume how many sites were required for the reaction to occur. It was not possible to distinguish how many sites were required by the fit of the data, since no improvement was found in the model by changing the number of sites. For this reason, the simplest case that fit the data was assumed; a one site mechanism was used. It is recognized that this almost certainly does not reflect the number of sites required for the reaction. As a result, while the relative magnitudes of the adsorption coefficients are correct, the calculated values are higher than they would be if a multisite mechanism were used.

All species were considered in the competitive adsorption for active sites. Based on the work of Abbas and Madix (1981), carbon dioxide was not expected to compete for adsorption sites. On Pt(111) surface, they reported that carbon dioxide did not adsorb. No

accurate concentrations were available for the by-products that were formed. Therefore, it was not possible to include them in the rate equation. This left ethylene glycol, oxygen and glycolic acid as competitors for the active sites. The approach taken was to fit several equations to the data and compare the results. The values of the rate of reaction calculated from the experimental data were plotted against those predicted by the model. Plotting the values has the added advantage of highlighting potential problems with the model and areas where the model does not fit the data (Figure 7.4).

The first equation shown in Table 7.4 is that developed for the power law model. This is the simplest model presented. For a Langmuir-Hinshelwood equation, it is not generally meaningful to have orders of reaction other than integral or half-integral values. Therefore, to compare the various models better, a power law model with the ethylene glycol to the half order is also presented. The next two models in Table 7.4 are of the Langmuir-Hinshelwood form. The sum of the squares of the residuals is used to compare the success of the various models. As can be seen from this value, there is not much to distinguish the various models. Perhaps the last model is to be preferred, because it is somewhat simpler than the previous model while still accounting for competitive adsorption suspected of occurring between the ethylene glycol and the glycolic acid. The calculated values of $-r_{EG}$ using this equation are plotted against the experimental data in Figure 7.4. A degree of scatter is apparent in the data. This is believed to be the effect of oxygen pressure that was not included in the data, because of the problems with collecting very accurate data. Further experimentation would be required to truly determine which model best represents the data and to account for the effect of oxygen pressure.

Table 7.4: Values for parameters of rate equations considered to describe the rate of reaction

Rate Equation	k	K_1	K_2	$\sum\left[-r_{\text{exp't}} - \left(-r_{calc}\right)\right]^2$
$k\ C_{EG}^{0.45}$	.00361	–	–	5.44×10^{-7}
$k\ C_{EG}^{0.5}$	.00377	–	–	7.64×10^{-7}
$\dfrac{k\ C_{EG}^{0.5}}{1 + K_1 C_{GA} + K_2 C_{EG}^{0.5}}$	.00439	2.0	0.10	6.12×10^{-7}
$\dfrac{k\ C_{EG}}{1 + K_1 C_{GA} + K_2 C_{EG}}$	.0356	17	9.8	7.69×10^{-7}
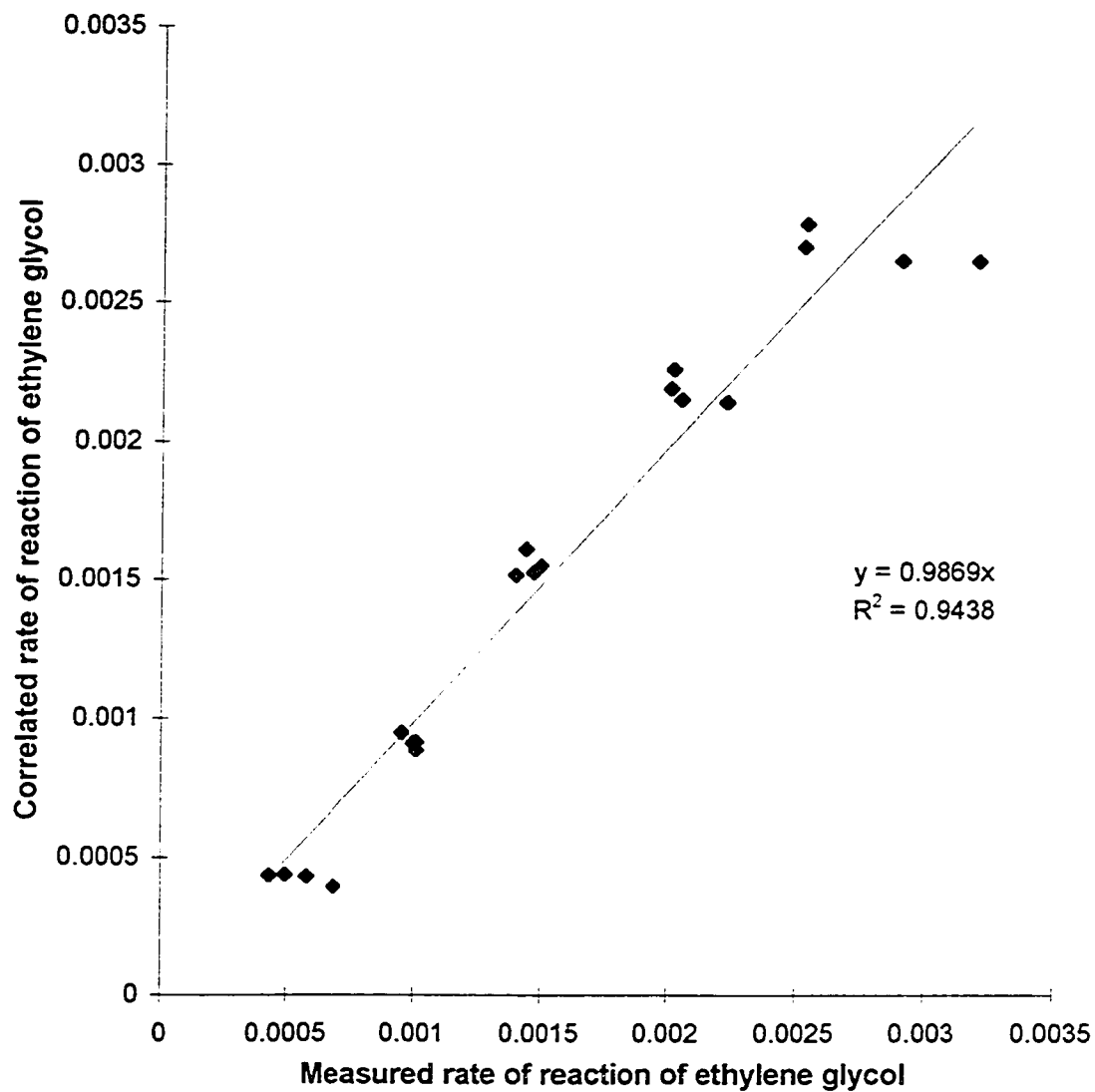
Figure 7.4: The second Langmuir Hinshelwood model shown in Table 7.4, including an adsorption term for both the glycolic acid and the ethylene glycol, is used to calculate the rate of reaction and plotted against the measured values.

7.3 Coda: Some Preliminary Experiments for Possible Future Work

The Effect on Conversion of the Addition of Base to the Feed

Considering the difficulties that had to be surmounted, the results to this point are very satisfactory. However, in an attempt to further elucidate the role of glycolic acid in the reaction, base was added to the feed. These results, like much of the preceding work, were not entirely clear. However, they do provide a possible direction for future work.

It is well documented that acids adsorb relatively strongly on metal surfaces (Gallezot et al., 1992, 1993). The strong adsorption of glycolic acid to the platinum sites is suspected of limiting the rate of reaction. The rate equation selected as best representing the data includes an adsorption term for the glycolic acid. By adsorbing to the catalyst, the glycolic acid molecules compete with the ethylene glycol molecules for the active sites. By adding a base to the feed solution, it was expected that the reaction rate would increase if this were the case. The weak base, ammonium hydroxide ($K_b = 1.76 \times 10^{-5}$) was added to the feed solution at the end of Run 970317 at a concentration of 0.0478 mol/L. The catalyst was only slightly deactivated when the base was added. This was an excess amount of base than that required to neutralize all of the acid that would have been produced in the absence of any base. Almost no acid was produced following the addition of the ammonium hydroxide; the conversion of ethylene glycol to glycolic acid was just 5 %, or 0.0045 mol/L of glycolic acid. No carbon dioxide was detected in the gas stream. This was to be expected since the effluent was still quite basic. The presence of the base had a detrimental effect on the conversion. From these experiments, it is not possible to

determine if this particular base interacted with the system in an unexpected manner, or rather that too much base was the cause of the low conversion.

The addition of sodium hydroxide to the feed solution was also studied. In Run 970401, running under standard conditions, 0.0267 mol/L of sodium hydroxide was added to the 0.090 M ethylene glycol feed solution. An increased rate of reaction was observed and as was discussed previously, deactivation still occurred. When the sodium hydroxide concentration was increased slightly to 0.0293 mol/L, this, combined with the loss in catalyst activity, resulted in lower levels of acidity in the effluent (Table 7.5); the conversion to carbon dioxide also dropped. In a neutral and slightly basic solution, some carbon dioxide remains dissolved in the liquid phase. This was investigated more thoroughly later in the experiment. The amount of glycolic acid was higher than would be expected in the absence of any base. The standard run, Run 961202, is shown in Figure 7.5 to better indicate this. The other point of interest in these data is the final point before the base was removed from the system. The acid production was considerably lower than the previous point, more than can reasonably be accounted for by deactivation. It may be that too much base slows the reaction rate.

The feed was then switched such that it contained no sodium hydroxide. It took some time for the base to wash out of the system (as indicated by the low acid conversions, which were calculated via titration results). At this point, the conversion levels were similar to those where no base had been added to the feed. The reactor was then run at 110°C for the next two days before it was shut down for four days. Following this shutdown, the study of the effect of sodium hydroxide on conversion was continued.

132

45.00

40.00

35.00

30.00

25.00

20.00

15.00

10.00

5.00

0.00

% conversion of ethylene glycol to

- 970401; CO2   ◇ 970401; GA
+ 961202; CO2   ▲ 961202; GA

0   50   100   150   200   250   300   350

Time (ks)
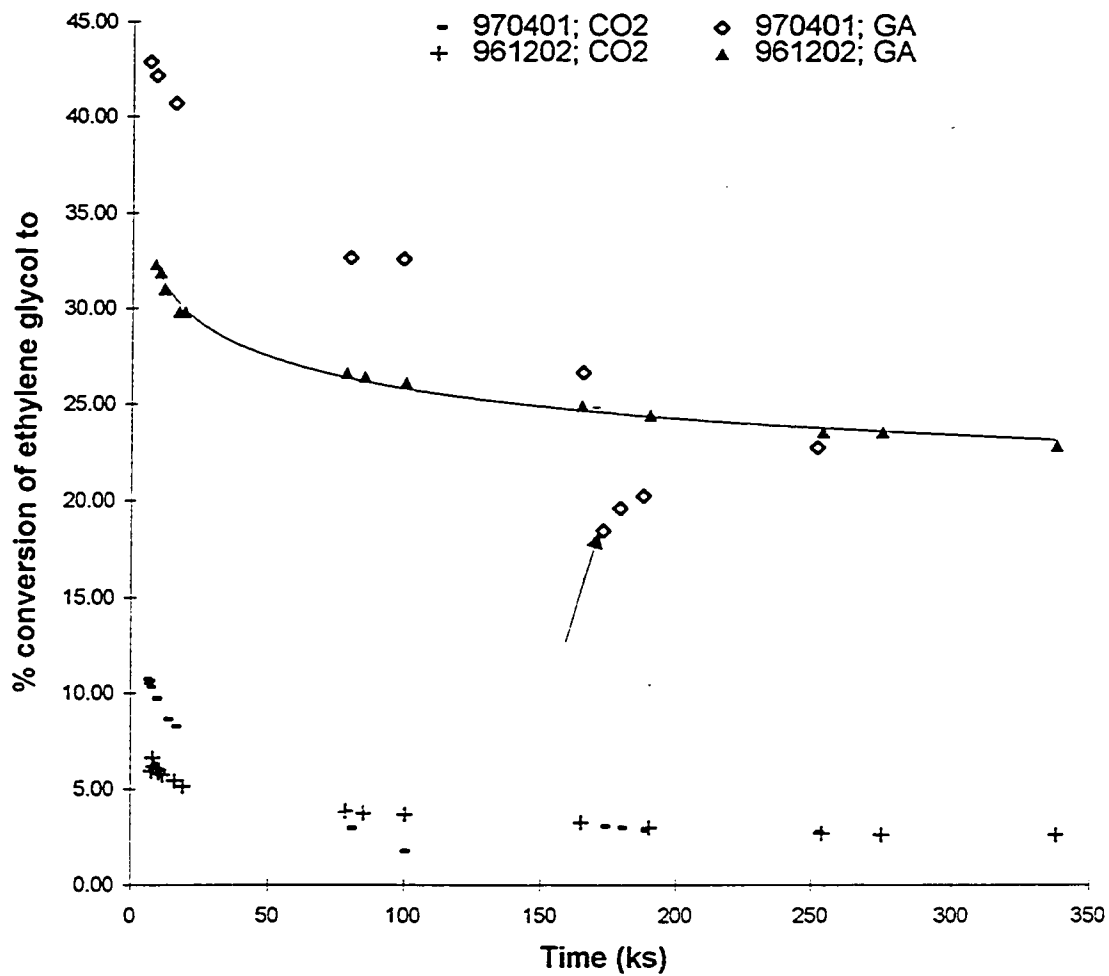
Figure 7.5: The effect of sodium hydroxide on the rate of deactivation (Run 970401) compared to a standard run (Run 961202).

The arrow indicates the point at which the sodium hydroxide was removed from the feed in Run 970401.

Table 7.5: Effect of NaOH on rate of deactivation; Run 970401

Time (ks)	Feed conc'n of NaOH (mol/L)	pH of effluent	← % conversion of ethylene glycol to → Carbon Dioxide	Glycolic Acid
5.4	.0267		10.76	
5.7	.0267		10.50	
6.3	.0267		10.64	42.9
6.6	.0267		10.35	
8.7	.0267		9.70	42.1
12.9	.0267		8.62	
15.6	.0267		8.24	40.7
80.1	.0293	5.3	2.94	32.6
99.6	.0293	7.3	1.71	32.6
165.6	.0239	8.9		26.6

NaOH removed from feed at 171.2 ks

Time (ks)	Feed conc'n of NaOH (mol/L)	pH of effluent	Carbon Dioxide	Glycolic Acid
173.1			3.02	18.4
179.1			2.95	19.6
187.8			2.84	20.2
252			2.74	22.7

Further testing with sodium hydroxide in the feed was then undertaken with the same catalyst bed. This time a more systematic approach was taken in the addition of sodium hydroxide. The concentration of sodium hydroxide was gradually increased, the conversion was measured, and the effluent pH was recorded (Table 7.6). The conversion of ethylene glycol to glycolic acid rose with increasing base concentration (see Figure 7.6).

Table 7.6: Effect of increasing concentration of sodium hydroxide on conversion; Run 970401.

Time (ks)	Feed concentration of NaOH (mol/L)	pH of feed	pH of effluent	% conversion of ethylene glycol to	
				Carbon Dioxide	Glycolic Acid
429.3	.0201	12.3	3.7	10.7	42.4
433.5	.0201	12.3		8.33	38.7
438.9	.0240	12.4	4.1	8.18	39.0
444.9	.0342	12.5	4.4	8.16	43.2
447.9	.0380	12.6		7.87	
461.4	.044	12.6	5.7	6.32	49.7
464.1	.0457	12.7	6.7	5.47	51.0
468.9	.049	12.7	7.7	3.33[*]	54.6
473.1	.0504	12.7	8.2	1.60[*]	56.1

[*] These values include both the carbon dioxide detected in the gas phase and the measurements for the dissolved inorganic carbon in the liquid.
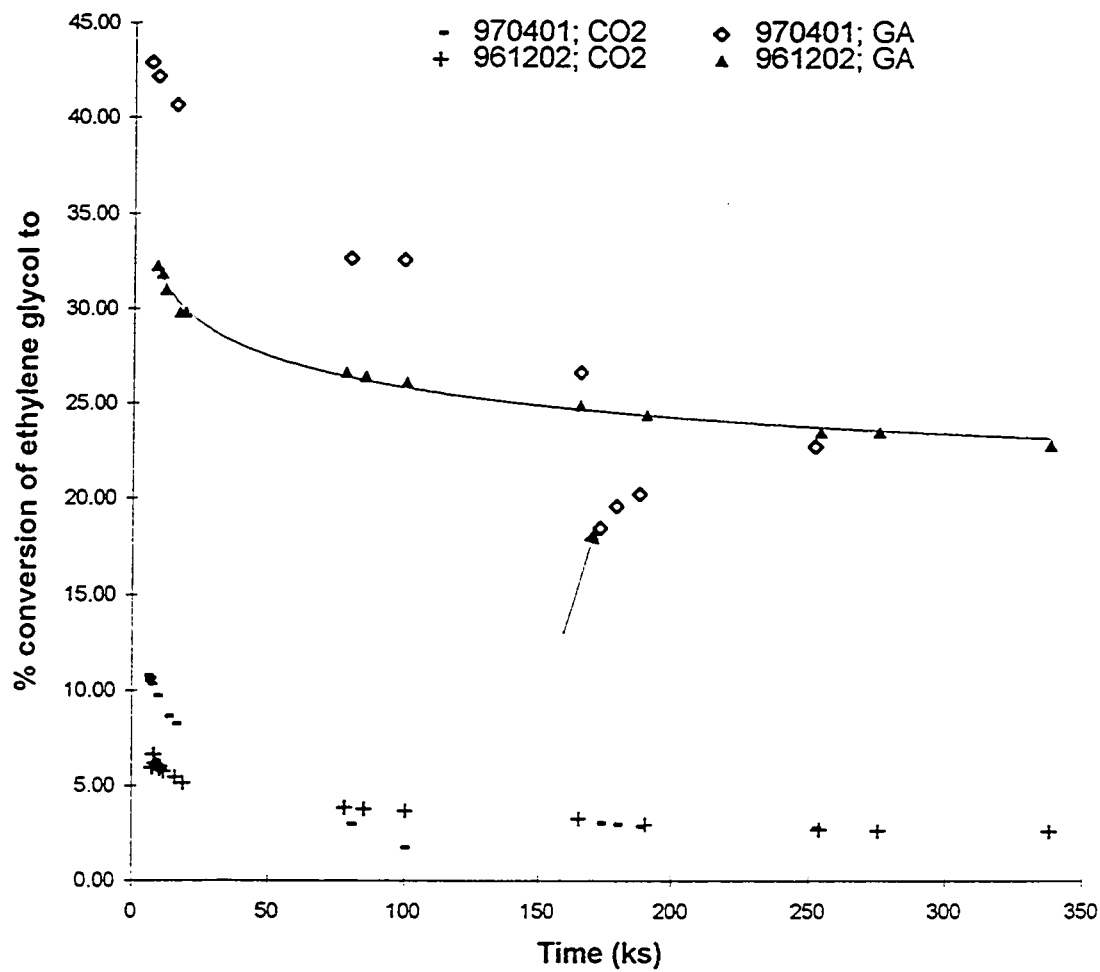
Figure 7.6: The conversion of ethylene glycol to glycolic acid and carbon dioxide as a function of sodium hydroxide concentration.

While the total conversion of ethylene glycol increased, the portion of the ethylene glycol converted to other byproducts remained approximately constant. Typically, about eight to eleven percent of the ethylene glycol was converted to products other than glycolic acid and carbon dioxide with a 0.090 M feed of ethylene glycol and no base was present in the system. In the absence of any base, the overall conversion of ethylene glycol was between 30 and 40 %. In the presence of the sodium hydroxide, with a total conversion of ethylene glycol of 61 %, 9 % of the ethylene glycol feed was converted to byproducts. This result is consistent with the hypothesis that some of the reaction byproducts are formed through acid catalyzed reactions.

The conversion to carbon dioxide remained elevated as long as the effluent remained reasonably acidic; (pH somewhat less acidic than 4.4). Some drop in carbon dioxide production was observed in this region, but it was attributed to catalyst deactivation. The conversion to carbon dioxide started to decrease when the effluent pH rose to near neutral values. At a pH of 7.7, the carbon dioxide levels in the gas phase had dropped considerably. By the time the pH had reached 8.2, almost no carbon dioxide was detected in the gas phase. Both of these liquid samples were analyzed for dissolved inorganic carbon. Some inorganic carbon was present in the liquid, but not enough to discount the large drop in the observed carbon dioxide production. It should be noted that Ali Khan et al. (1983b) also observed an increase in conversion of ethylene glycol to glycolic acid on a platinum catalyst in the presence of sodium hydroxide. No discussion of their results was presented.

This result can in part be explained by the shortened adsorption period of the glycolic acid on the catalyst sites. It is quite possible that the other pathway(s) to carbon dioxide are via short lived acid intermediates. In the presence of a sufficiently basic solution, some of the acid intermediates may desorb from the platinum sites before they have a chance to react. This would account for the large drop in the carbon dioxide levels that were observed.

The literature provides further insight into understanding these results. As already discussed in Chapter 5 on the chemistry, the presence of carbon monoxide in the effluent was not detected or expected. Carbon monoxide adsorbs strongly to platinum and in the presence of oxygen oxidizes to carbon dioxide. In the electrocatalytic oxidation of ethylene glycol, Leung and Weaver (1990) reported quite high carbon monoxide coverage on a platinum electrode in an aqueous acidic medium. The extent of formation of adsorbed carbon monoxide decreases with increasing pH (Mallat and Baiker, 1994). These observations may help to account for the effects of increasing the pH of the ethylene glycol solution. The drop in carbon dioxide production follows from the decreased levels of carbon monoxide. Carbon monoxide is a logical precursor for carbon dioxide. The increase in reaction rate would result because carbon monoxide no longer occupies as many active sites. However, this explanation does not explain all of the effects that were observed.

In Figure 7.6, at no point was a drop in conversion to glycolic acid observed with increasing pH. The final pH was 8.2. There are two possible explanations for this apparent inconsistency with the final point in the first part of the run when the feed was basic (Table

138

7.5). The first, and rather unsatisfactory explanation, is that something other than the pH was responsible for the drop in activity. The other possibility is that either an excessively basic feed solution or a rapid increase in pH adversely affects conversion. This explanation would also explain the difference in results between the two parts of the run. The base concentration must be increased gradually, to allow the conversion of acid to increase, and hence rapid reduction from the high pH values. If the base is added too quickly, the overly basic feed solution interferes with the reaction and the rate of reaction is greatly decreased.

This hypothesis agrees in part with the conclusions of Mallat et al. (1992) in the oxidation of methoxy-propanol over a palladium/bismuth catalyst. These researchers observed strong chemical deactivation when sodium hydroxide was added to their system and the pH was above 11.5. Dimeric or polymeric material was the suspected cause of the deactivation. Mallat and coworkers (1992) state that the favourable pH range is 8.5 to 11.5, although no clear correlation between pH and reaction rate was found in the oxidation of a range of alcohols.

The results of Mallat et al. (1992) do not provide a satisfactory explanation for the results with ammonium hydroxide in the feed solution. The initial pH was below the 11.5 that is recommended and below that when sodium hydroxide was added to the feed. It would appear that different bases interact with the system differently. It may be that the amount of base, as well as the pH plays a role in the reaction. The favourable pH range does help explain the observed results when sodium hydroxide was added to the feed.

The nature of a trickle-bed reactor is such that the pH will be highest at the entrance of the reactor before any acidic products are formed. The base will be neutralized along the length of the reactor with the reaction. A balance between the initial pH and the reaction rate at the entrance occurs. If too much base is added initially, rapid catalyst deactivation means that insufficient of the base is neutralized. The rate of reaction drops rapidly. However, if the concentration of base is slowly increased, there is time for neutralization of the acid byproducts. The increased reaction rate is able to neutralize increasing amounts of base such that the pH does not remain at overly high levels for long enough to cause significant deactivation.

More experiments would be required to confirm this mechanism. It would be worthwhile to try adding weak bases, other than ammonium hydroxide, to the system. In this manner the pH throughout the length of the reactor could be kept in the range 8.5 to 11.5. Currently with sodium hydroxide, there is a trade-off between having enough basicity to increase the reaction rate over as much of the reactor length as possible, without having so much that the reaction is essentially shut down.

8. Conclusions and Recommendations

8.1 The Catalyst and Its Support

Styrene divinyl benzene copolymer (SDB) can successfully concentrate organic compounds from an aqueous solution. A significant degree of variability was found between the different lots of the SDB received from the supplier. This was manifest in the BET isotherm measurements, where both the total surface area and the pore size distribution varied between different lots. This in turn led to different platinum dispersions for the catalyst made from different lots of SDB. If further work with SDB is to be continued, its preferred physical properties, such as pore size distribution, should be determined. A homogeneous and consistent supply of SDB having these properties should be secured. Before any testing in an agitated can be attempted, the integrity of the SDB also needs improvement.

The literature indicates that different polymers adsorb different organic materials to varying degrees (Stevens and Kerner, 1975). Although SDB did concentrate ethylene glycol successfully, because of the polar nature of ethylene glycol, a polar polymer would be expected to be even more effective at concentrating the compound, although a compromise is likely the preferred choice because of the polar nature of water. It is recommended that the feasibility of obtaining and using high surface area acrylic and acrylic esters polymers be investigated. Temperature stability would also be a requirement. Acrylic polymers strongly adsorb polar molecules. Acrylic esters with both a hydrophobic

141

and a hydrophilic end are better at adsorbing molecules of intermediate polarity or mixtures of organic compounds with a wide range of polarities.

In this research, no attempt was made to quantify the improvement in the performance of the catalyst because of the increased concentration of the ethylene glycol. A comparison between two different platinum catalysts, one supported on SDB and the other supported on alumina would provide useful information. Alumina is hydrophilic and would not be expected to concentrate organic compounds to the same degree. Care would be required to ensure that the platinum dispersion on the alumina and the SDB supported catalysts were as nearly the same as possible. Depending on the success of the experiments, it might also be valuable to try a range of catalyst supports.

8.2 The Chemistry

Ethylene glycol is oxidized over a platinum catalyst to glycolic acid and carbon dioxide at 80°C. With increasing temperature, the selectivity to carbon dioxide increases, such that at 110°C, ethylene glycol is almost entirely oxidized to carbon dioxide and water.

Tentative identification of some of the other reaction products was made. Esters and 1,3-dioxolanes are believed to present as the result of condensation reactions between carboxylic acid and alcohol groups in the presence of an acid. Confirmation of these reaction products should be pursued. Silylation of the reaction mixture (following evaporation of all of the water) should be attempted once more. This time most, if not all,

of the ethylene glycol should be reacted, since the ethylene glycol is suspected to interfere with the derivatization process.

Investigation into the oxidation of other organic compounds would have relevance in the broad ranging treatment of wastewater. The hydrophobic nature of the SDB, which is nonpolar, would be expected to be particularly successful at concentrating organic compounds with a similar, aromatic nature. This includes many of organic compounds that are recalcitrant to conventional biological treatment, such as phenols and chlorophenols.

8.3 Catalyst Deactivation

The cause of catalyst deactivation is attributed to trace metal poisoning by copper, and the strong adsorption of one or more reaction byproducts on the catalyst active sites. The deactivation increases at higher oxygen pressures when more of the reaction byproduct is produced. A steady state is achieved once the rate of formation of the byproduct is equal to the rate of desorption of the byproduct.

It is recommended that the deactivated catalyst be checked for the presence of copper. Once all of the reaction products are identified, it is recommended that the catalyst be extracted with solvent to see if any of the byproducts is in excess concentration. In this manner, it may be possible to positively identify the cause of the catalyst deactivation.

8.4 Reaction Kinetics

The kinetics of the oxidation of ethylene glycol was successfully modeled by the following equation:

$$-r_{EG} = \frac{0.0356\, C_{EG}}{1 + 17\, C_{GA} + 9.8\, C_{EG}} \qquad \frac{mol}{h \cdot g} \tag{8.1}$$

This equation indicates that the surface reaction has a first order dependence on the ethylene glycol concentration. It reflects the competitive adsorption occurring between the ethylene glycol and the glycolic acid.

This reaction equation should be tested over a wider range of operating conditions. A term to account for the slight effect of oxygen pressure should be added. It might be preferable to do this in a CSTR where mass transfer resistances are more easily eliminated and initial rates can be measured. Measuring initial rates would eliminate catalyst deactivation and problems with polymerization. If the reaction byproduct(s) causing the catalyst deactivation were identified, an attempt could be made to include a term in the competitive adsorption for catalyst sites in the denominator of the kinetic model.

Sodium hydroxide was found to dramatically increase the conversion of ethylene glycol to glycolic acid. In the presence of sufficient base, it almost totally suppressed the formation of carbon dioxide. It would be valuable to determine the effect of sodium hydroxide on the formation of the reaction byproducts. Preliminary results indicate that the presence of sodium hydroxide inhibits their formation, because even with the large increase in glycolic acid concentration no increase in byproduct formation was observed. This may be a viable method for the manufacture of glycolic acid.

The effect of sodium hydroxide on the rate of reaction is not clearly understood. Increasing its concentration too quickly depresses the rate of reaction. It is suspected that the reaction mechanism may change with the rapid addition of large amounts of base. When the concentration of sodium hydroxide was increased gradually, the rate of reaction

increased far more than if the base was just facilitating the desorption of the glycolic acid. These effects should be further explored.

It is likely that the pH as well as the amount of base present in the solution also plays a role in the rate of reaction. Although ammonium hydroxide rapidly led to deactivation of the catalyst, it is recommended that other weak bases be tested in the system. In this way it may be possible to separate the effect of pH and base concentration. Obviously using different bases introduced an extra variable which might confound the results. It is suggested that these experiments be carried out in a CSTR. This would allow the researcher to observe the effect of pH on conversion more easily.

9. References

Abbas, N.M., Madix, R.J. (1981). The Effects of Structured Overlayers of Sulfur on the Kinetics and Mechanism of Simple Reactions on Pt(111): I. Formaldehyde Decomposition. Applications of Surface Science, 7, 241-275.

Ali Khan, M.I., Miwa, Y., Morita, S., Okada, J. (1983a). Liquid-Phase Oxidation of Ethylene Glycol on a Pt/C Catalyst. I. Deactivation and Regeneration of the Catalyst. Chem. Pharm. Bull., 31, 1141-1150.

Ali Khan, M.I., Miwa, Y., Morita, S., Okada, J. (1983b). Liquid-Phase Oxidation of Ethylene Glycol on a Pt/C Catalyst. II. Kinetic Study. Chem. Pharm. Bull., 31, 1827-1832.

Barresi, A.A., Baldi, G. (1992). Deep Catalytic Oxidation Kinetics of Benzene-Ethenylbenzene Mixtures, Chem. Eng. Sci., 47, 1943-1953.

Barresi, A.A., Baldi, G. (1993). Reaction Meahnisms of Ethanol Deep Oxidation over Platinum Catalyst, Chem. Eng. Comm., 123, 17-29.

Battino, R.(ed.) (1981). Solubility Data Series, 7, Oxygen and Ozone, Pergamon Press, Oxford.

Blau, K., King, G.S. (1978). Handbook of Derivatives for Chromatography, Heyden & Son Ltd., London.

Boreskov, G.K. (1982). Catalytic Activation of Dioxygen. Catalysis, 3, ed. J.R. Anderson; M. Boudart, Springer-Verlag, Berlin, 39-137.

Boudart, M. (1956). Kinetics on Ideal and Real Surfaces, AIChE. J., 2, 62-64

Butt, J.B., Petersen, E.E. (1988). Activation, Deactivation, and Poisoning of Catalysts, Academic Press, Inc., San Diego.

Charpentier, J.C., Favier, M. (1975). Some Liquid Holdup Experimental Data in Trickle-Bed Reactors for Foaming and Nonfoaming Hydrocarbons. AIChE. J., 21, 1213-1218.

Cheng, S., Chuang, K.T. (1992). Simultaneous Methanol Removal and Destruction from Wastewater in a Trickle-Bed Reactor. Can. J. Chem. Eng., 70, 727-737.

146

Christensen, G., McGovern, S.J., Sundaresan, S. (1986). Cocurrent Downflow of Air and Water in a Two-Dimensional Packed Column. AIChE. J., 32, 1677-1689.

Chuang, K.T., Cheng, S., Tong, S. (1992). Removal and Destruction of Bezene, Toluene, and Xylene from Wastewater by Air Stripping and Catalytic Oxidation. Ind. Eng. Chem. Res., 31, 2466-2472.

Chuang, K.T., Zhou, B., Tong, S. (1994). Kinetics and Mechanixm of Catalytic Oxidation of Formaldehyde over Hydrophobic Catalysts. Ind. Eng. Chem. Res., 33, 1680-1686.

Comninellis, C. (1992). Electrochemical Treatment of Waste Water containing Phenol. ICHEME Symposium Series, 127, 189-201.

Cullity, B.D. (1956). Elements of X-ray Diffraction, Addison-Wesley Publishing Company, Inc., Reading, 96-102.

Dijkgraaf, P.J.M., Rijk, M.J.M., Meuldijk, J., van der Wiele, K. (1988a). Deactivation of Platinum Catalysts by Oxygen. 1. Kinetics of the Catalyst Deactivation. J. Catal., 112, 329-336.

Dijkgraaf, P.J.M., Rijk, M.J.M., Meuldijk, J., van der Wiele, K. (1988b). Deactivation of Platinum Catalysts by Oxygen. 2. Nature of the Catalyst Deactivation. J. Catal., 112, 337-344.

Dirkx, J.M.H., van der Baan, H.S. (1981a). The Oxidation of Glucose with Platinum on Carbon as Catalyst. J. Catal., 67, 1-13.

Dirkx, J.M.H., van der Baan, H.S. (1981b). The Oxidation of Gluconic Acid with Platinum on Carbon Catalyst. J. Catal., 67, 14-20.

Enright, J.T., Chuang, T.T. (1978). Deuterium Exchange Between Hydrogen and Water in a Trickle-Bed Reactor. Can. J. Chem. Eng., 56, 246-250.

Froment, G.F., Bischoff, K.B., (1990). Chemical Reactor Analysis and Design, 2nd ed., John Wiley & Sons, New York.

Gallezot, P., de Mesanstourne, R., Christidis, Y., Mattioda, G., Schouteeten, A. (1992). Catalytic Oxidation of Glyoxal to Glyoxylic Acid on Platinum Metals. J. of Catal., 133, 479-485.

Gallezot, P., Fache, F., de Mesanstourne, R., Christidis, Y., Mattioda, G., Schouteeten, A. (1993). Liquid phase oxidation of glyoxal to glyoxylic acid by air on platinum catalysts. Stud. Surf. Sci. Catal, 75, 195-202.

Gallezot, P., Laurain, N., Isnard, P. (1996). Catalytic wet-air oxidation of carboxylic acids on carbon-supported platinum catalysts. Appl. Catal. B., **9**, L11-L17.

Gates, B.C. (1992). Catalytic Chemistry, John Wiley & Sons, Inc., New York.

Gland, J.L., Sexton, B.A., Fisher, G.B. (1980). Oxygen interactions with the Pt(111) surface. Surf. Sci., **95**, 587-602.

Golodets, G.I. (1983). Heterogeneous Catalytic Reactions involving Molecular Oxygen., English Translation and editing by J.R.H. Ross, Elsevier Science Publishing Company Inc., Amsterdam.

Gottstein, H.D., Zooj, M.N., Kuc, J.A. (1989). Detection and Quantification of Oxalic Acid by Capillary Gas Chromatography. J. Chromatogr., **481**, 55-61.

Gustafson, R.L., Albright, R.L., Heisler, J., Lirio, J.A., Reid, O.T.Jr. (1968). Adsorption of organic species by high surface area styrene-divinylbenzene copolymers. Ind. Eng. Chem. Prod. Res. Devel., **7**, 107-115.

Hegedus, L.L., McCabe, R.W. (1984). Catalyst Poisoning, Marcel Dekker, Inc., New York.

Herskowitz, M., Smith, J.M. (1978). Liquid Distribution in Trickle-Bed Reactors. AIChE J., **24**, 439-450.

Herskowitz, M., Smith, J.M. (1983). Trickle-Bed Reactors: A Review. AIChE J., **29**, 1-18.

Imamura, S., Fukuda, I., Ishida, S. (1988). Wet Oxidation Catalyzed by Ruthenium Supported on Cerium(IV) Oxides. Ind. Eng. Chem. Res., **27**, 718-721.

Ito, M.M., Akita, K., Inoue, H. (1989). Wet Oxidation of Oxygen- and Nitrogen-Containing Organic Compouns Catalyzed by Cobalt(III) Oxide. Ind. Eng. Chem. Res., **28**, 894-899.

Jank, B.E., Guo, H.M., Cairns, V.W. (1974). Activated Sludge Treatment of Airport Wastewater containing Aircraft De-Icing Fluids. Water Res., **8**, 875-880.

Janna, W.S. (1986). Engineering Heat Transfer, PWS Publishers, Boston, A.23.

Jelemensky, L., Kuster, B.F.M., Marin, G.B. (1995). Multiple steady-states for the oxidation of aqueous ethanol with oxygen on a carbon supported platinum catalyst. Catal. Lett., **30**, 269-277.

Jelemensky, L., Kuster, B.F.M., Marin, G.B. (1997). Relaxation Processes during the Selective Oxidation of Aqueous Ethanol with Oxygen on a Platinum Catalyst. Ind. Eng. Chem. Res., **36**, 3065-3074.

Kan, K.M., Greenfield, P.F. (1978). Multiple Hydrodynamic States in Cocurrent Two-Phase Downflow through Packed Beds. Ind. Eng. Chem. Process Des. Dev., **17**, 482-485.

Kan, K.M., Greenfield, P.F. (1979). Pressure Drop and Holdup in Two-Phase Cocurrent Trickle Flows through Beds of Small Packings. Ind. Eng. Chem. Process. Des. Dev., **18**, 740-745.

Kawakami, K., Isobe, M., Horiki, K., Kusunoki, K. (1988). Kinetic Study of Isotopic Exchange Reaction Between Hydrogen and Water Vapor Over a Pt/SDBC Hydrophobic Catalyst Sheet. Can. J. Chem. Eng., **66**, 338-342.

Kilroy, A.C., Gray, N.F. (1992). Pilot Plant Investigations of the Treatability of Ethylene Glycol by Activated Sludge. Environmental Technology, **13**, 293-300.

Klecka, G.M., Carpenter, C.L., Landenberger, B.D. (1993). Biodegradation of Aircraft Deicing Fluids in Soil at Low Temperatures. Ecotoxicology and Environmental Safety, **25**, 280-295.

Klug, H.P., Alexander, L.E. (1954). X-ray Diffraction Procedures, John Wiley & Sons, Inc. New York, 491-494.

Koros, R.M. (1986). Engineering Aspects of Trickle-Bed Reactors. Chemical Reactor Design and Technology., ed. H.I. deLasa, Martinus Nijhoff Publishers, Dordrecht, 579-630.

Légaré, P., Hilaire, L., Maire, G. (1984). Interaction of Polycrystalline Platinum and a Platinum-Silicon Alloy with Oxygen: An XPS Study. Surf. Sci., **141**, 604-616.

Leung, L.W.H., Weaver, M.J. (1990). Influence of Adsorbed Carbon Monoxide on the Electrocatalystic Oxidation of Simple Organic Molecules at Platinum and Palladium Electrodes in Acidic Solution: A Survey Using Real-Time FTIR Spectroscopy. Langmuir, **6**, 323-333.

Levenspiel, O. (1962). Chemical Reaction Engineering, John Wiley & Sons, Inc., New York.

Li, X., Fitzgerald, P., Bowen, L. (1992). Sensitized Photo-Degradation of Chlorophenols in a Continuous Flow Reactor System. Wat. Sci. Tech., **26**, 367-376.

Liang, W., Chuang, K.T., Zhou, B. (1997). Partial Oxidation of Propylene Over Hydrophobic Catalysts in a Slurry Reactor. Dev. Chem. Eng. Min. Proc., in press.

Lide, D.R. editor in chief. (1996). CRC Handbook of Chemistry and Physics, 78th ed., CRC Press, Boca Raton.

Mallat, T., Baiker, A., Botz, L. (1992). Liquid-phase oxidation of 1-methoxy-2-propanol with air. III. Chemical deactivation and oxygen poisoning of platinum catalysts. Appl. Cat. A.: Gen., 86, 147-163.

Mallat, T., Baiker, A. (1994). Oxidation of Alcohols with Molecular Oxygen on Platinum Metal Catalysts in Aqueous Solutions. Catat. Today, 19, 247-284.

Marginean, P., Hodor, I. (1994). Hydrophobic Bimetallic Catalysts for H/D Exchange Reaction between Hydrogen and Water. Isotopenpraxia Environ. Health Stud., 30, 23-28.

Mishra, V.S., Mahajani, V.V., Joshi, J.B. (1995). Wet Air Oxidation. Ind. Eng. Chem. Res., 34, 2-48.

PACE report 85-6 (December, 1985). Evaluation of the Variability of Trace Organic Substances in Petroleum Refinery Effluents. Prepared for Petroleum Association for Conservation of the Canadian Environment and Environment Canada. By Can Test Ltd. and IEC International Environmental Consultants Ltd., p. 8.

Papenmeier, D.M., Rossin, J.A. (1994). Catalytic Oxidation of Dichloromethane, Chloroform, and their Binary Mixtures over a Platinum Alumina Catalyst. Ind. Eng. Chem. Res., 33, 3094-3103

Peng, Y.K., Dawson, P.T. (1974). The Adsorption, Desorption, and Exchange Reactions of Oxygen, Hydrogen, and Water on Platinum Surfaces. I. Oxygen Interactions. Can. J. Chem., 52, 3507-3517.

Perry, R.H., Green, D.W. (1984). Perry's Chemical Engineers' Handbook, 6th ed., McGraw-Hill Inc., New York.

Pintar, A., Levec, J. (1992a). Catalytic Oxidation of Organics in Aqueous Solutions. J. of Catal., 135, 345-357.

Pintar, A., Levec, J. (1992b). Catalytic Liquid-Phase Oxidation of Refractory Organics in Waste Water. Chem. Eng. Sci., 47, 2395-2400.

Puglia, C., Nilsson, A., Hernnäs, B., Karis, O., Bennich, P., Mårtensson, N. (1995). Physisorbed, chemisorbed and dissociated O_2 on Pt(qqq) studied by different core level spectroscopy methods. Surf. Sci., 342, 119-133.

150

Rebsdat, S., Mayer, D. (1987). Ethylene Glycol. Ullmann's Encyclopedia of Industrial Chemistry, 5th edition, A10, Weinheim, 101-115.

Reid, R.C., Prausnitz, J.M., Sherwood, T.K. (1977). The Properties of Gases and Liquids, 3rd edition, McGraw-Hill Book Co., New York.

Sabeh, Y., Narasiah, K.S. (1992). Degradation Rate of Aircraft Deicining Fluid in a Sequential Biological Reactor. Wat. Sci. Tech., 26, 2061-2064.

Sadana, A., Katzer, J.R. (1974). Catalytic Oxidation of Phenol in Aqueous Solution over Copper Oxide. Ind. Eng. Chem. Fundam., 13, 127-134.

Salmerón, M., Brewer, L., Somorjai, G.A. (1981). The Structure and Stability of Surface Platinum Oxide and of Oxides of Other Noble Metals. Surf. Sci., 112, 207-228.

Sanger, A.R., Lee, T.T.K., Chuang, K.T. (1992). Catalytic Wet Air Oxidation in the presence of Hydrogen Peroxide. Prog. in Catal., 197-201.

Satterfield, C.N. (1970). Mass Transfer in Heterogeneous Catalysis, Robert E. Krieger Publishing Co., Malabar.

Satterfield, C.N. (1975). Trickle-Bed Reactors, AIChE J., 21, 209-228.

Satterfield, C.N. (1980). Heterogeneous Catalysis in Practice, McGraw-Hill Book Company, New York.

Sawyer, J.E., Abraham, M.A. (1994). Reaction Pathways during the Oxidation of Ethyl Acetate on a Platinum/Alumina Catalyst. Ind. Eng. Chem. Res., 33, 2084-2089.

Schuurman, Y., Kuster, B.F.M., van der Wiele, K., Marin, G.B. (1992). Selective oxidation of methyl α-D-glucoside on carbon supported platinum. Appl. Cat. A: Gen., 89, 47-68.

Seymour, R.B., Carraher, C.E. Jr. (1988). Polymer Chemistry. 2nd ed., Marcel Dekker, Inc., New York.

Spivey, J.J. (1987). Complete Catalytic Oxidation of Volatile Organics. Ind. Eng. Chem. Res., 26, 2165-2180.

Stevens, B.W., Kerner, J.W. (1975). Recovering Organic Materials from Wastewater. Chem. Eng., 84-87.

TRC Thermodynamic Tables, Non-Hydrocarbons. Thermodynamic Reserach Center, The Texas A & M University System, College Station, Texas.

Treybal, R.E. (1980). Mass-Transfer Operations, 3rd edition, McGraw-Hill Book Co., New York.

van den Tillaart, J.A.A., Kuster, B.F.M., Marin, G.B. (1994). Oxidative dehydrogenation of aqueous ethanol on a carbon supported platinum catalyst. Appl. Catal. A., 120, 127-145.

Washburn, E.W. (ed.), (1929). International Critical Tables of Numerical Data, Physics, Chemistry and Technology, 5, McGraw-Hill Book Company, Inc., New York.

Weller, S. (1956). Analysis of Kinetic Data for Heterogenous Reactions, AIChE J., 2, 59-62.

Yue, P.L., (1993). Modelling of Kinetics and Reactor for Water Purifaction by Photo-Oxidation. Chem. Eng. Sci., 48, 1-11.

Appendices

A.   Energy Balance Calculation on Reactor

<u>Conditions and Results for Run 96.02.12:</u>

1.0 (wt)% Pt with no catalyst bed dilution;

Nominal operating temperature	80°C;
Thermocouple readings	80, 87, 89 and 79°C;
Flow rate of the aqueous solution	20.0 mL/min;
Glycolic acid produced	1.01×10^{-3} mol/min;
Carbon dioxide produced	4.71×10^{-4} mol/min.
Heat of reaction: ethylene glycol to glycolic acid	-492 kJ/mol
Heat of reaction: ethylene glycol to CO_2	-1189 kJ/mol

Calculations on a one minute basis:

$$\Delta H_r = \left(4.71 \times 10^{-4}\ mol\right)\left(-1189\ \frac{kJ}{mol}\right) + \left(1.01 \times 10^{-3}\ mol\right)\left(-492\ \frac{kJ}{mol}\right)$$

$$= -1.057\ kJ$$

If all of the heat of reaction were adsorbed by the water, the temperature rise of the water would be calculated as follows:

$$\Delta T = \frac{1057\ J}{(20.0\ g)(4.196\ J/g \cdot K)} = 12.6\ K$$

In actual fact the observed ΔT was 10 K.

B. Checking for Mass Transfer Limitations

<u>B.1 Theoretical Calculations of external mass transfer</u>

The following are theoretical calculations based on the work of Satterfield (1970, 1975) to determine if external mass transfer limitations could be expected of the oxygen through the liquid phase.

For significant mass transfer limitations, the following expression would hold:

$$\frac{10\, r\pi\, d_p}{3c^*} > k_{ls}$$

The rate of oxygen consumption, r, was estimated from experimental results; based on Run 970527, 162 ks, $r = 3.3 \times 10^{-8}\ \dfrac{mol}{s \cdot cm^3}$ at 80°C and 300kPa oxygen pressure. At 90°C and 300 kPa oxygen pressure, $r = 8.0 \times 10^{-8}\ \dfrac{mol}{s \cdot cm^3}$ calculated from run 960317.

The catalyst diameter, d_p, ranged between 0.03 cm and 0.085 cm. The value of 0.03 cm was used in calculating the left hand side of the equation, since this is the most demanding condition.

The saturation concentration of oxygen in water, c^*, was estimated from the <u>Solubility Data Series</u>, for oxygen and ozone (Battino, 1981). The approach taken was to estimate the Henry's law constant, h, and then calculate the mole fraction of oxygen in solution, x, and convert this to c^*.

$$\ln h = 3.71814 + \frac{5.59617 \times 10^3}{T} - \frac{1.049668 \times 10^6}{T^2} \qquad \text{where } T \text{ is in Kelvin}$$

and

$$f = h\, x \qquad \text{where } f \text{ is in bar.}$$

For 300 kPa oxygen pressure at 80°C,

$$h = 69428; \qquad x = 4.32 \times 10^{-5}\ \frac{mol\ O_2}{mol\ solution}; \qquad c^* = 2.4 \times 10^{-6}\ \frac{mol\ O_2}{cm^3\ solution}$$

Similarly at 90°C, $c^* = 2.3 \times 10^{-6}$ mol O_2/cm^3 solution.

The left hand side of the equation was calculated:

$$L.\,H.\,S. = 4.5 \times 10^{-3} \frac{cm}{s} \text{ at } 80°C$$

and $\quad L.\,H.\,S. = 1.1 \times 10^{-2} \frac{cm}{s}$ at 90°C.

The overall liquid mass transfer coefficient, k_{ls}, was then calculated from

$$k_{ls} = \frac{D_{AB}\, a}{H_o}$$

where D_{AB} is the diffusivity of oxygen in water, a is the ratio of the outside area of the catalyst pellets to the reactor volume, and H_o is the liquid holdup.

The diffusivity was estimated using the Wilke-Chang Estimation Method (Reid et al., 1977; Treybal, 1980).

$$D_{AB} = \frac{117.3 \times 10^{-18} \left(\phi \, M_B\right)^{0.5} T}{\mu \, v_A^{0.6}} \quad , \frac{m}{s}$$

where A and B are oxygen and water respectively;

$\phi \quad$ = solvent association factor; 2.26 for water

$M_B \quad$ = molecular weight of water; 18.02

$T \quad$ = temperature, K

$\mu \quad$ = solution viscosity, kg/m·s

$v \quad$ = solute molal volume at normal boiling point, m^3/kmol; 25.6×10^{-3} for oxygen (Treybal, 1980).

The viscosity of water (neglecting the effect of ethylene glycol) was found in the International Critical Tables, volume 5 (Washburn, 1929):

$$\mu = 3.57 \times 10^{-4} \frac{kg}{m \cdot s} \text{ at } 80°C; \quad 3.16 \times 10^{-4} \frac{kg}{m \cdot s} \text{ at } 90°C$$

The diffusivity was then calculated:

$$D_{AB} = 6.7 \times 10^{-5} \frac{cm^2}{s} \quad \text{at } 80°C$$

and

$$D_{AB} = 7.8 \times 10^{-5} \frac{cm^2}{s} \quad \text{at } 90^\circ C$$

The ratio of the external catalyst surface area required an estimate of the void volume of the bed, ε. A reasonable estimate for this value is 0.36. The area was then calculated as follows:

$$a = \frac{6(1 - \varepsilon)}{d_p} \frac{cm^2 \ catalyst \ surface}{cm^3 \ reactor \ volume}$$

In this calculation, an arithmetic average of the particle diameter was used; d_p = 0.058 cm, and therefore, a = 66 cm^{-1}.

The liquid holdup was estimated from three runs giving a value of 0.215.

The overall liquid mass transfer coefficient was then calculated and the results were as follows:

$$k_{ls} = 2.1 \times 10^{-2} \frac{cm}{s} \quad \text{at } 80^\circ C;$$

$$k_{ls} = 2.4 \times 10^{-2} \frac{cm}{s} \quad \text{at } 90^\circ C.$$

Since in both cases the right hand side is larger than the left hand side, external mass transfer resistances through the liquid were not rate limiting.

Table B.1: Data for external mass transfer study at 80°C. The effect of varying the liquid and gas flow rates with a constant contact time.

Catalyst Volume	Liquid Flow	L/V	Gas Flow	G/V	← % conversion of EG →		
V	L		G		to CO_2	to GA	overall
mL	mL/min		mL/min				
15	10	0.67	347	23	2.11	11.9	20.1
23	15	0.65	497	22	2.37	20.0	32.8
31	20	0.65	675	22	2.24	19.1	25.5
40	26	0.66	878	22	2.18	19.1	31.1
52	34	0.65	1107	21	2.24	19.9	30.0
23	15	0.65	339	15	2.36	18.3	29.9
31	20	0.65	450	15	2.29	19.1	31.9
40	26	0.66	604	15	2.16	19.1	32.8
52	34	0.65	779	15	2.39	20.0	29.3

Table B.2: Data for external mass transfer study at 90°C. The effect of varying the liquid and gas flow rates with a constant contact time.

Catalyst Volume	Liquid Flow	L/V	Gas Flow	G/V	← % conversion of EG →		
V	L		G		to CO_2	to GA	overall
mL	mL/min		mL/min				
23	15	0.65	485	21	5.57	27.8	42.4
40	26.3	0.66	824	21	5.11	28.2	47.1
52	33.8	0.65	1108	21	6.65	29.7	45.4
23	15	0.65	304	13	6.03	27.8	41.6
40	26.3	0.66	587	15	5.85	27.8	48.7
52	33.8	0.65	756	15	5.73	29.8	38.9

Table B.3: Data for internal mass transfer study at liquid flow rate of 15 mL/min. The effect on conversion of two different sizes of catalyst particles.

Size of Catalyst Spheres	Temperature °C	Gas Flow mL/min	← % conversion of EG →		
			to CO_2	to GA	overall
20-50 mesh	80	497	2.37	20.0	32.8
20-50 mesh	80	339	2.36	18.3	29.9
>50 mesh	80	502	2.30	20.0	32.9
>50 mesh	80	339	2.35	19.8	34.0
20-50 mesh	90	485	5.57	27.8	42.4
20-50 mesh	90	304	6.03	27.8	41.6
>50 mesh	90	489	5.38	29.5	45.8
>50 mesh	90	339	5.57	29.1	47.0

C. X-ray Diffraction Results

Data used to calculate the mean crystallite size is shown in Table C.1. The platinum dispersion, the fraction of metal exposed at the surface, is then readily calculated:

$$D = \frac{N_S}{N_T} = \frac{A_P/A_A}{V_P/V_A}$$

where
N_S = number of surface atoms
N_T = total number of atoms
A_P = surface area of platinum particle
A_A = surface area of platinum atom (8.4 $\mathring{A}^2$)
V_P = volume of platinum particle
V_A = volume of platinum atom (15.1 $\mathring{A}^3$)

Assuming that the platinum particles are hemispheres on the surface of the support, their area and volume are easily calculated:

$$A_P = 2\pi \left(\frac{t}{2}\right)^2 \quad and \quad V_P = \frac{2}{3}\pi \left(\frac{t}{2}\right)^3$$

Catalyst	θ_B	B (radians)
95.12.12	19.81	.03787
96.02.23/27	19.77	.03159
96.09.05	19.83	.05236
97.01.20	19.73	.05166
97.03.07	19.75	.05550
97.04.21	19.86	.03648
97.06.27	19.78	.04782

Table C.1: X-ray diffraction data derived from the original analysis.

D. Analytical Chemistry Results
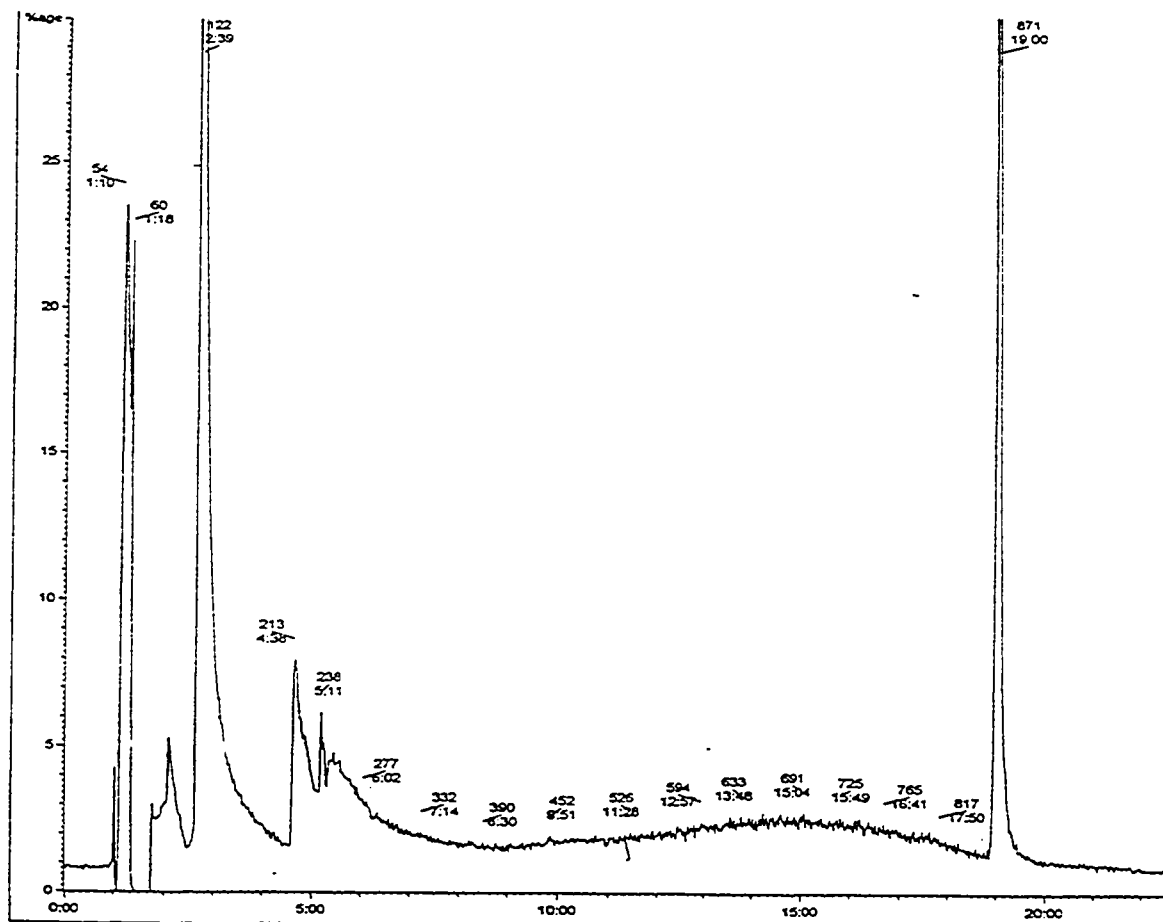
Figure D.1:   Gas chromatograph for sample 95.06.28 with scan numbers corresponding to the mass spectra. Sample analyzed by the mass spectrometry lab in the Chemistry Department at the University of Alberta.

a) Mass spectrum for scan 122

Library Scan 01. SI: 898. Formula: C2H6O2. MW: 62. Name: 1,2-Ethanediol.
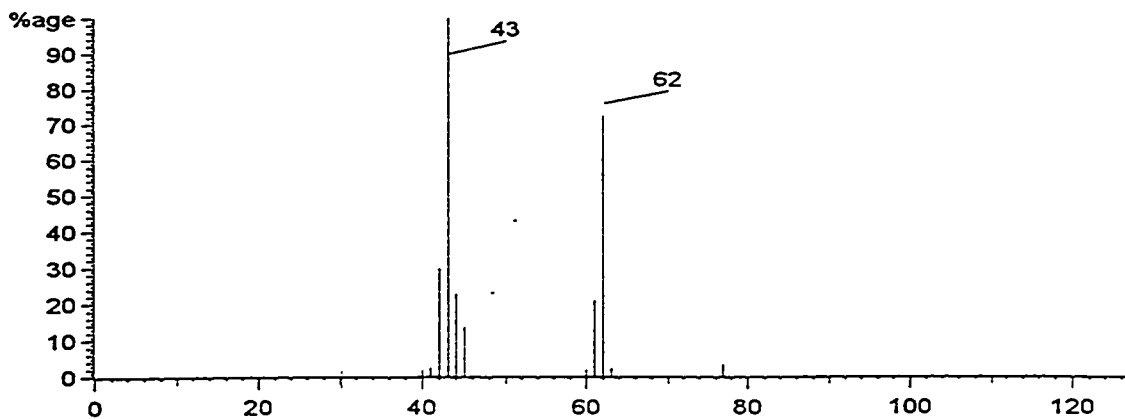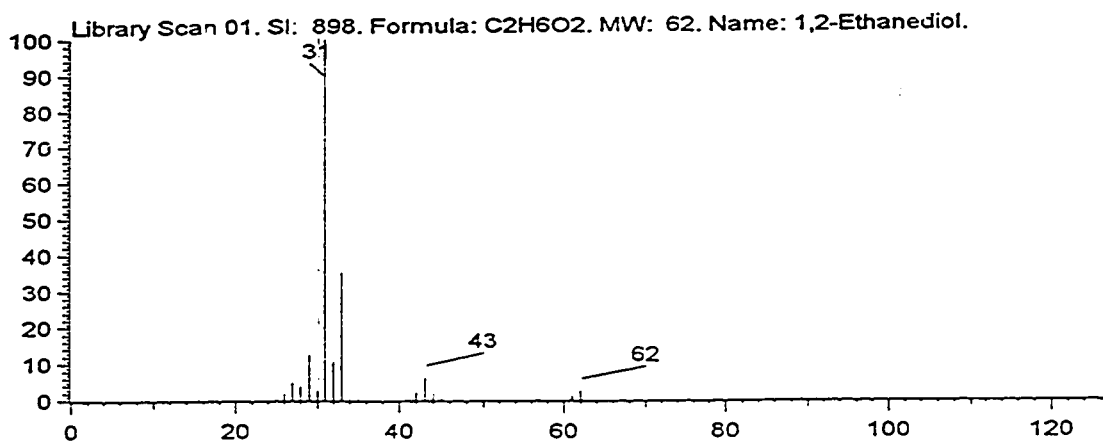
b) Mass spectrum for ethylene glycol

Figure D.2:   Mass spectrum corresponding to the gas chromatograph, scan 122 in
Figure D.1, and the spectrum of the library match, ethylene glycol.

162
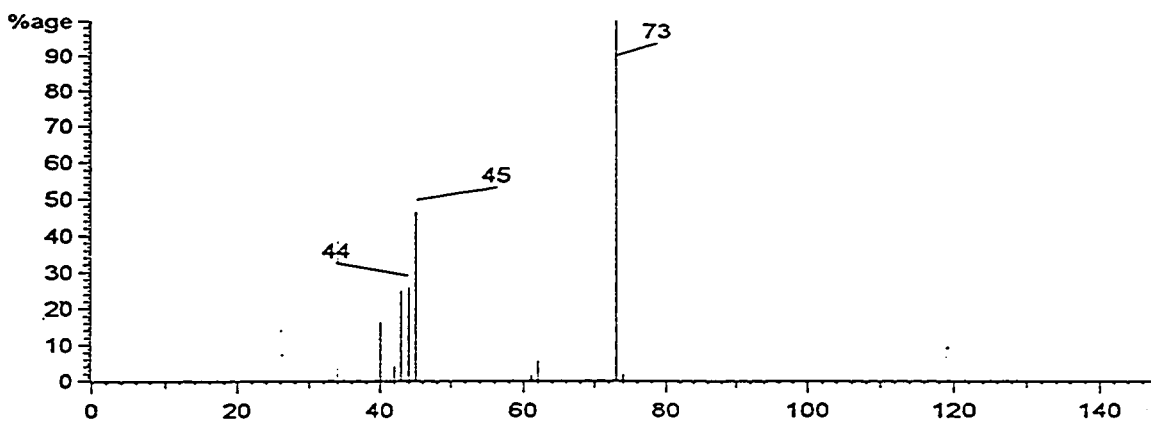
a) Mass spectrum for scan 213
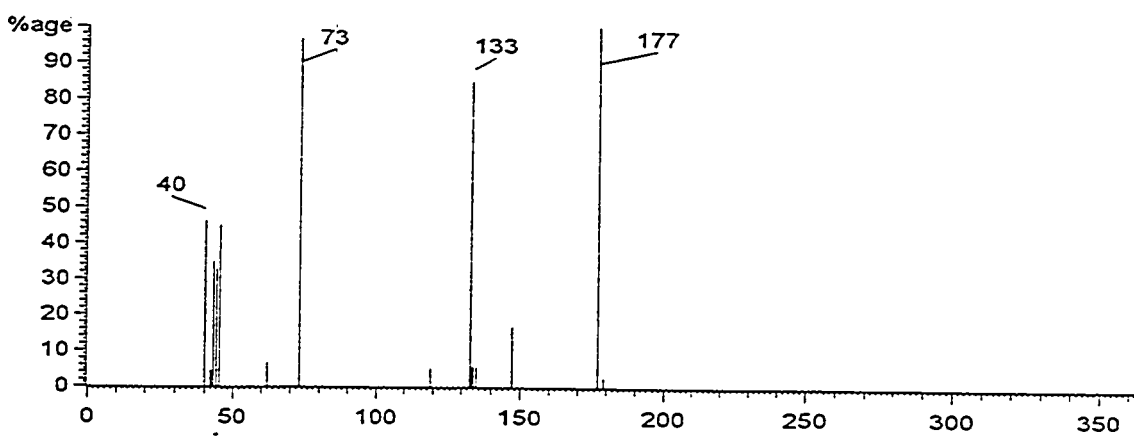
b) Mass spectrum for scan 238
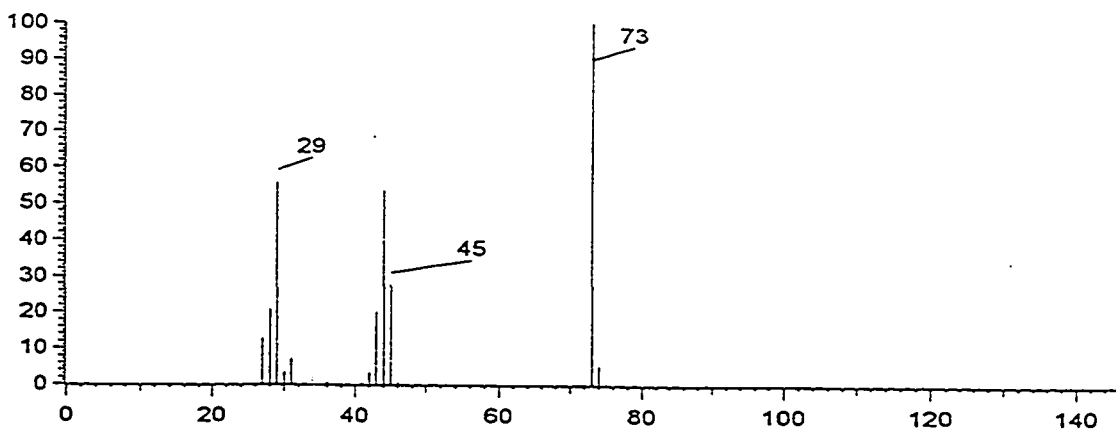
c) Mass spectrum of 1,3-dioxolane

Figure D.3:   Mass spectra corresponding to the gas chromatograph, scans 213 and 238 in Figure D.1, and the spectra of the library match in both cases, 1,3-dioxolane.

a) Derivatized glycolic acid

b) Derivatized sample

c) Derivatized sample spiked with derivatized glycolic acid
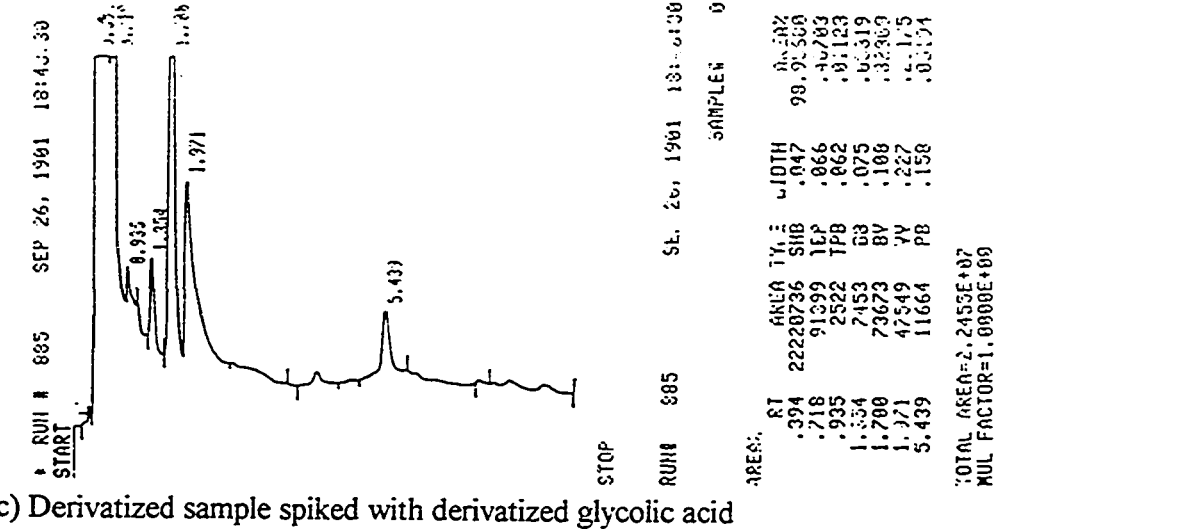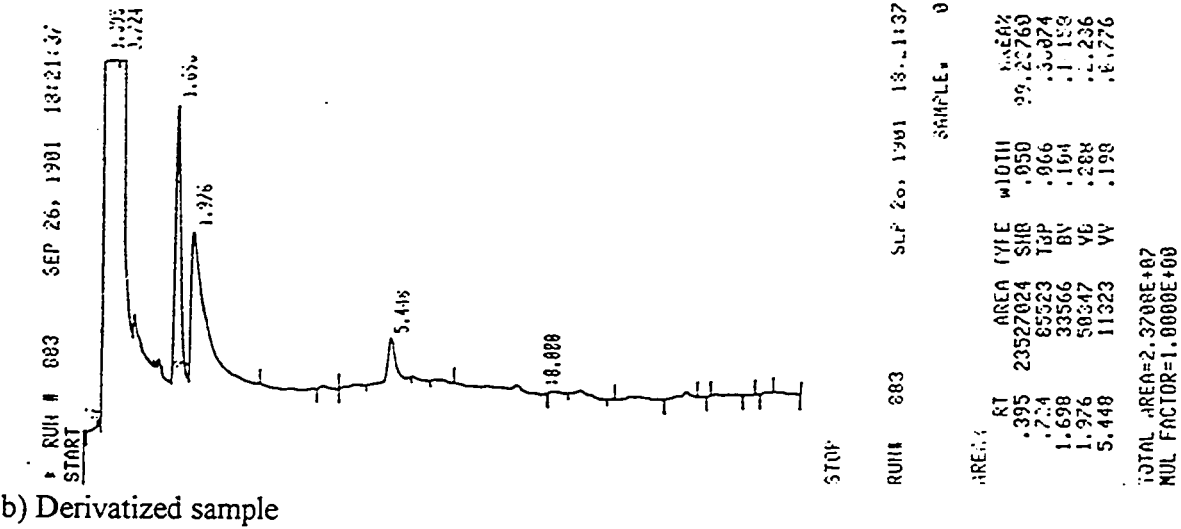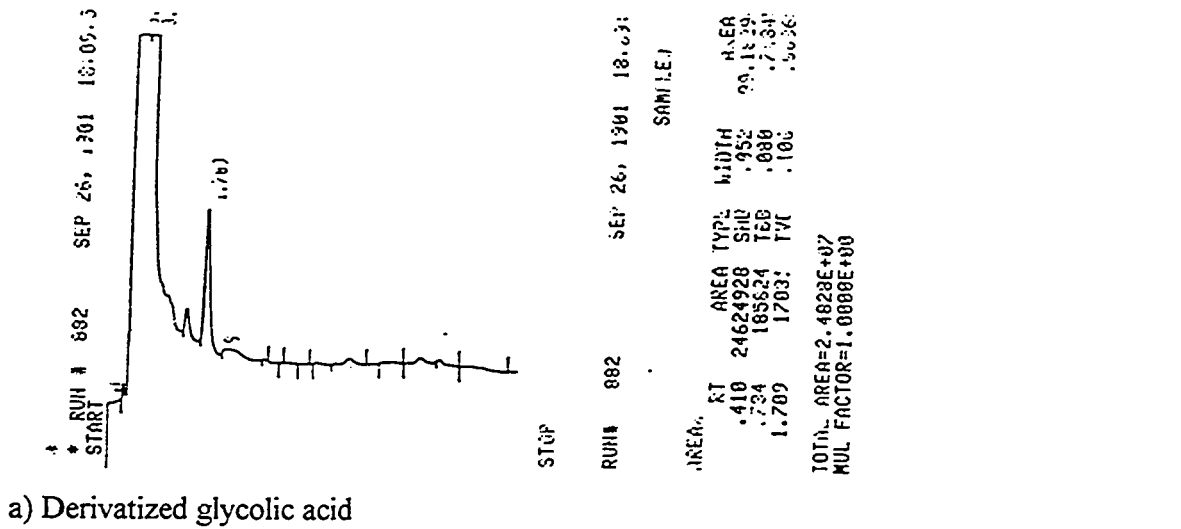
Figure D.4: Gas chromatographs of derivatized glycolic acid, derivatized sample
95-10-31, and the derivatized sample spiked with derivatized glycolic acid.

164

Table D.1: Results from ion chromatography, done by Norwest Labs, Edmonton, AB.

Sample	96-03-11; 80°C	96-03-24; 90°C
Chromatography		
Formate Anion (mg/L)	<0.20	<0.20
Acetate Anion (mg/L)	<0.50	<0.50
Glycolate Anion (mg/L)	2500	3825
Oxalate Anion (mg/L)	13	24

E. Experimental Results from Runs

All results are reported in order of the Run Number.

Table E.1: Data for run 950905, showing increasing overall conversion of ethylene glycol and specifically the increase in conversion to carbon dioxide with time.

Time (ks)	mol/min CO_2	% EG converted to CO_2	% ethylene glycol converted
14	1.68E-04	10.08	24
76	1.88E-04	11.25	
162	1.86E-04	11.18	
184	1.91E-04	11.43	
252	2.16E-04	12.93	36

Table E.2: Data for Figure 6.3. Catalyst reactivation with air or nitrogen; Run 960524. Actual data collected from 96.08.06 to 96.08.13.

| Time (ks) | ← % conversion to ethylene glycol → | |
	Carbon Dioxide	Glycolic Acid
Following one week of air		
25.2	3.29	17.3
96.1	2.50	15.9
113	2.30	15.7
Following overnight of nitrogen gas		
2.7	5.18	22.1
3.6	5.47	
4.3	5.32	
5.0	5.16	
6.1	5.11	20.2
6.8	4.61	
7.9	4.75	
9.0	4.57	
9.9	4.55	19.4
10.4	4.45	
13.5		18.8
15.1	4.14	
15.5	3.75	
16.6	3.73	
17.3	3.67	18.5
18.0	3.63	
19.1	3.72	
20.5	3.65	18.3
22.3	3.48	
22.7	3.48	
24.1	3.37	17.9
25.9	3.34	
26.3	3.47	
27.9	3.41	17.7
92.5	2.47	16.1
107	2.43	15.8
Following overnight of nitrogen gas		
1.8	6.65	
2.7	5.97	
3.6	5.63	21.3
4.7	5.15	
6.1	4.85	

166

	← % conversion to ethylene glycol →	
Time (ks)	Carbon Dioxide	Glycolic Acid
7.2	4.59	
9.7	4.42	19.4
10.1	4.27	
11.2	4.44	19.2
14.4	3.97	18.5
15.3	4.02	
16.2	3.86	
17.3	3.79	18.1
18.9	3.75	
20.7	3.68	
22.3	3.48	17.7
23.0	3.67	
24.1	3.45	
24.8	3.34	17.5
25.9	3.47	
90.0	2.43	15.6
106	2.54	15.4

Table E.3: Data for Run 960909, plotted in Figure 6.1. For this date, the actual operating dates were 96.09.09 to 96.10.11.

| Time (days) | ← %conversion of ethylene glycol to → | |
	Carbon Dioxide	Glycolic Acid
3	4.45	25.4
3	4.44	
4	4.09	
4	3.98	
7	2.89	23.0
7	3.21	
8	2.89	22.6
8	2.83	
9	2.54	22.1
9	2.70	
10	2.60	22.3
10	2.40	22.0
11	2.67	21.3
11	2.35	
12	2.26	20.9
12	2.22	
13	2.11	20.5
13	2.10	
14	2.04	20.2
14	2.23	
14	2.22	
15	2.01	19.8
15	2.10	
16	1.92	19.7
16	2.04	
17	2.13	
17	1.97	
18	1.61	19.9
18	1.33	
19	1.62	
20	1.67	19.8
20	1.51	
20	1.59	
20	1.52	19.7
20	1.62	
21	1.57	19.5
21	1.52	
21	1.76	
22	1.86	19.2
22	1.78	

Time (days)	← %conversion of ethylene glycol to →	
	Carbon Dioxide	Glycolic Acid
23	1.46	18.9
24	1.19	18.7
24	1.16	
24	1.28	
24	1.72	
25	1.26	18.6
25	1.28	
26	1.37	18.6
26	1.37	
26	1.23	
26	1.49	
27	1.34	18.2
27	1.67	
27	1.32	
28	1.40	18.3
28	1.17	
28	1.28	18.2
28	1.55	

Table E.4: Run 960909. Deactivation of catalyst following reactivation at lower oxygen pressure; plotted in Figure 6.2. For this data, the actual operating dates were 96.11.01 to 96.11.05.

Time (days)	Adjusted Time (days)	← %conversion of ethylene glycol to →	
		Carbon Dioxide	Glycolic Acid
0.10	6.60	5.36	
0.17	6.67	4.86	27.1
0.93	7.43	3.53	24.6
1.23	7.73	3.42	24.5
1.94	8.44	2.84	23.4
2.19	8.69	2.80	23.5
3.15	9.65	2.71	22.4
4.03	10.53	2.37	21.6

Table E.5: Run 960909; Data for Figure 6.5 showing the catalyst reactivation with reduced oxygen. For this data, the actual operating dates were 96.10.11 to 96.10.18.

O_2 Pressure (kPa)	Time (ks)	% conversion of ethylene glycol	% conversion of ethylene glycol to Carbon Dioxide	% conversion of ethylene glycol to Glycolic Acid
300	0	28.0	1.40	18.2
225	112	26.3	1.23	17.7
150	198	23.7	1.08	17.3
100	349	23.4	1.18	17.1
50	605	25.5	1.52	17.3

Table E.6: Run 960909. Catalyst reactivation at 40 and 50 kPa oxygen pressure. Data shown in Figure 6.6. For this data, the actual operating dates were 96.10.15 to 96.11.01.

Time (ks)	Adjusted Time (ks)	← % conversion of ethylene glycol to → Carbon Dioxide	← % conversion of ethylene glycol to → Glycolic Acid
Oxygen pressure reduced to 50 kPa			
14.4		1.14	15.5
82.8		1.53	16.5
101		1.69	16.8
166		1.75	17.3
180		1.85	17.2
245		1.86	17.4
Oxygen pressure reduced to 40 kPa			
86.4	331	2.04	15.8
101	346	2.10	15.9
173	418	2.27	16.0
191	436	2.20	16.0
260	505	2.21	16.2
274	518	2.24	16.3
346	590	2.09	16.2
370	614	2.27	16.7
425	670	2.21	16.5

Table E.7: Catalyst reduced only; no calcination; Run 961121

Time	← % conversion of ethylene glycol to →	
(ks)	Carbon Dioxide	Glycolic Acid
6.3	4.71	
6.6	4.56	
8.7	4.51	
10.2	4.07	
11.1	3.97	22.0
12.0	4.05	
12.9	3.85	
14.7	3.89	
15.0		21.9
15.6	3.73	
16.5	3.68	
18.3	3.54	
20.7		21.6
21.0	3.47	
78.6		21.2
79.5	2.69	
85.8	2.54	21.4
93.0		21.4
93.9	2.59	
105	2.73	
106		21.7
167	2.43	22.3
191	2.41	22.6
255	2.18	23.0
264	2.07	22.8

Table E.8: Standard run. Data from run 961202.

Time (ks)	mol/min CO2	mol/min GA	% EG converted to CO2	% EG converted to GA
7.8	2.11E-04		5.91	
8.1	2.36E-04		6.61	
8.4		5.76E-04		32.3
8.7	2.20E-04		6.16	
9.6	2.16E-04		6.04	
10	2.09E-04	5.69E-04	5.86	31.9
11	2.14E-04		5.98	
12	2.04E-04	5.54E-04	5.72	31.0
16	1.94E-04		5.42	
17		5.33E-04		29.8
19	1.83E-04	5.33E-04	5.13	29.8
79	1.36E-04	4.75E-04	3.82	26.6
86	1.34E-04	4.72E-04	3.74	26.4
101	1.31E-04	4.67E-04	3.66	26.1
165	1.15E-04	4.45E-04	3.23	24.9
190	1.06E-04	4.37E-04	2.96	24.4
254	9.50E-05	4.19E-04	2.66	23.5
275	9.34E-05	4.20E-04	2.61	23.5
338	9.26E-05	4.07E-04	2.59	22.8

Table E.9: Data for Figure 6.7; Deactivation of fresh catalyst at an oxygen pressure of 50 kPa. followed by reactivation at an oxygen pressure of 25 kPa; Run 961209.

Time (ks)	← % conversion of ethylene glycol to →	
	carbon dioxide	glycolic acid
Oxygen pressure 50 kPa		
4.8	6.31	21.0
8.4	6.29	21.0
12.9	6.13	20.9
75.3	5.47	
80.1		21.5
99.9	5.26	21.2
161.4	4.88	21.1
Oxygen pressure decreased to 25 kPa		
176	4.20	14.2
187	4.28	14.3
268	4.10	14.6
340	3.94	15.1

Table E.10:   Catalyst reduced and calcined with oxygen pretreatment; Run 970123

Time	← % conversion of ethylene glycol to →	
(ks)	Carbon Dioxide	Glycolic Acid
5.4	6.74	
6.0	6.59	
6.3	6.26	
6.6		35.3
9.0	6.19	
9.3	5.95	
9.9	6.21	
10.2		34.0
12.3	5.73	
12.6	5.76	
12.9	5.54	
13.5	5.82	33.1
16.5	5.42	
17.7	5.27	
18.0	5.25	32.4
78.6	4.14	29.2
98.1	3.93	28.8
197	3.38	27.5
261	3.19	26.8
340	2.86	25.9

Table E.11: Data from run 970307; effect of no presoaking of catalyst.

Time (ks)	mol/min CO2	mol/min GA	% EG converted to CO2	% EG converted to GA
2.4	5.30E-05		1.48	
5.4	4.39E-05		1.23	
7.5	5.18E-05	1.07E-05	1.45	0.60
11	4.22E-05		1.18	
12		1.15E-05		0.64
74	3.97E-05	1.36E-05	1.11	0.76
100	3.23E-05	1.32E-05	0.90	0.74

Table E.12: Data for Run 970317; total pressure 347 kPa.

| Time | ← % conversion of ethylene glycol to→ | |
(ks)	Carbon Dioxide	Glycolic Acid
Oxygen pressure 25 kPa; gas flow rate of 450 mL/min		
7.2	6.64	
7.5	6.84	
9.3	6.63	
9.9	6.59	15.8
14.1	6.63	
14.4	6.48	
15.0	6.77	16.2
Increased gas flow rate to 600 mL/min		
18.0	7.34	
18.6	6.93	
18.9	6.94	16.9
Overnight switched gas flow to nitrogen		
25.8	7.50	17.0
Oxygen pressure increased to 50 kPa; gas flow 450 mL/min		
48.0	10.96	
48.3	11.05	
48.9	10.45	27.1
Gas flow switched to nitrogen overnight		
50.7	10.38	
51.9	10.97	
52.2	10.76	27.8
Gas flow increased to 600 mL/min		
57.6	11.07	
58.2	10.77	
59.4	8.72	26.6

Table E.13: Catalyst presoaked in glycolic acid; Run 970324.

| Time (ks) | ← % conversion of ethylene glycol to → | | % conversion of Ethylene Glycol |
	Carbon Dioxide	Glycolic Acid	
6.3	1.98	11.9	13.8
13.5	2.06	11.7	
21.3	1.87	11.4	
87.3	1.77	10.9	19.9
110	1.58	10.7	
174	1.50	10.5	14.2
Following operation at 120°C			
174.6	1.56	31.0	
175.2	17.0		
175.8	11.7	29.8	
176.1	9.60	29.8	
176.7	8.49	22.7	
177.0	8.33	26.4	
177.6	7.38	26.1	
181.5	6.76	19.7	
188	6.02	18.4	
248	4.02	15.3	
280	3.88	15.0	20.6

Table E.14: Run 970422; catalyst presoaked with equimolar amounts of ethylene glycol and glycolic acid. Standard operating conditions.

Time (ks)	← % conversion of ethylene glycol to →		% conversion of Ethylene Glycol
	Carbon Dioxide	Glycolic Acid	
0.9	17.1		
1.5	12.6		
1.8	10.2	42.9	69.3
2.1	8.9		
2.7	8.6		
3.0	7.9		
3.6	7.6		
4.2	7.4		
5.1	7.0	37.4	
6.9	6.9		
7.2	6.7		
7.8	6.6		
10.2	6.6		
10.5	6.4		
11.4	6.4	35.0	59.0
16.5	6.0	33.8	
20.1	5.9	33.9	58.1
79.2	5.0		
82.2		32.6	
103	4.8	32.6	
105		32.6	
167	4.5	31.9	
179		31.6	
191	4.4	31.6	
252	4.2	31.4	46.1
269	4.2	31.0	

Table E.15: Run 970505; standard run.

Time (ks)	← % conversion of ethylene glycol to →	
	Carbon Dioxide	Glycolic Acid
0.9	4.97	
1.2	4.97	
1.8	4.92	
2.4	4.57	
3.0		25.2
3.6	4.51	
5.7	4.45	
6.3	4.36	
6.6	4.40	24.9
9.9	4.35	
10.5	4.56	
10.8	4.37	25.3
70.8	4.48	27.5
84.0	4.56	
96.0	4.53	28.3
159	4.55	29.4
183	4.64	29.5
244	4.47	29.6

Table E.16:   The effect of nitrogen flow in place of oxygen in the absence of liquid flow; Run 970527.

Time (ks)	← % conversion of ethylene glycol to →	
	Carbon Dioxide	Glycolic Acid
0.9	7.98	
1.2	13.08	
1.8	12.89	
2.4		32.2
2.7	9.77	
3.6	8.13	
4.2	6.66	
7.2	6.92	
8.4	6.29	26.5
9.0	5.98	
9.3	5.95	25.8
69.7	3.93	
72.6		23.4
95.1	3.83	23.1
162.3	3.34	22.9

Reduced oxygen pressure for five hours

Time (ks)	Carbon Dioxide	Glycolic Acid
165.3	7.97	
165.9	7.55	
166.2	6.99	
166.8	6.95	28.8
167.1	6.43	
225.2	3.85	24.0

Oxygen replaced with nitrogen for four hours; no liquid flow

Time (ks)	Carbon Dioxide	Glycolic Acid
227.0	10.26	
227.6	8.76	
228.2	7.97	
228.5	7.74	31.3
230.6	6.64	
231.2	6.16	
231.5	6.12	27.5

Reactor switched off for three days

Time (ks)	Carbon Dioxide	Glycolic Acid
235.1	5.64	
235.4	5.51	
236.0	5.45	
236.3	5.22	27.3
241.4	5.06	
242.3	5.01	26.3

| Time | ← % conversion of ethylene glycol to → | |
(ks)	Carbon Dioxide	Glycolic Acid
246.5	4.67	
250.1	4.58	25.3

Table E.17: Runs 970728 and 970805; Data for Figure 6.10.

| Time | ← % conversion of ethylene glycol to → | |
(ks)	Carbon Dioxide	Glycolic Acid
Run 970728; 100% ethylene glycol presoak		
0.9	12.0	
1.2	14.3	
1.8	13.2	
2.1	11.8	
2.4	10.6	
3.0	10.1	
3.3	9.61	
8.4	7.59	35.9
12.6	7.05	34.3
69.0	5.36	31.8
94.5	5.24	31.4
160	5.48	31.2
184	5.17	30.7
243	4.82	29.9
268	4.61	29.3
329	4.29	29.2
Run 970805; 50% ethylene glycol, 50% glycolic acid presoak		
0.6	9.39	
1.2	19.3	
1.5	14.8	
1.8	11.9	
2.4	10.2	40.7
3.3	9.29	
3.6	8.82	
3.9	8.37	
8.4	7.48	35.1
69.0	5.49	31.1
93.6	5.25	30.5
156	4.81	30.3
182	4.78	29.8
245	4.57	29.7
254	4.45	29.9

Table E.18: Experimental data from Run 970805 used for kinetic modeling; data collected from 97.08.26 to 97.09.05.

Time (ks)	C_{EG} Feed (mol/L)	P_{O2} (kPa)	W/F_{AO} (g·h·mol^{-1})	% conversion of EG to GA	% conversion of EG to CO$_2$	x_{EG}
32	0.18	300	116	21.7	2.65	0.329
85	0.18	300	116	21.1	2.45	0.318
92	0.36	300	58	14.5	1.45	0.215
98	0.72	300	29	9.8	1.10	0.147
172	0.090	300	232	28.0	4.77	0.442
180	0.045	300	465	34.3	9.76	0.595
187	0.18	300	116	20.7	2.34	0.311
194	0.18	450	116	21.7	2.56	0.328
260	0.090	450	232	28.0	4.20	0.435
268	0.045	450	465	34.9	8.92	0.592
275	0.18	450	116	20.4	2.14	0.304
282	0.36	450	58	14.3	1.17	0.209
287	0.72	450	29	9.7	0.74	0.141
294	0.72	450	29	10.1	0.89	0.148
301	0.72	450	29	10.2	0.91	0.150
306	0.72	300	29	9.5	0.99	0.142
311	0.72	225	29	8.7	1.00	0.131
372	0.18	225	116	20.9	3.05	0.323
381	0.36	225	58	13.9	1.79	0.212
388	0.090	225	232	30.3	6.12	0.492
396	0.045	225	465	37.1	10.66	0.645
460	0.18	225	116	20.2	2.67	0.309
467	0.18	300	116	21.4	2.74	0.326
480	0.18	150	116	18.9	2.33	0.287
487	0.090	150	232	27.7	4.64	0.437
544	0.090	150	232	26.9	4.57	0.425
552	0.045	150	465	35.5	9.00	0.601
559	0.36	150	58	12.0	1.54	0.183
567	0.72	150	29	7.2	1.28	0.114

Table E.19: Calculated values for kinetic modeling from experimental data of Run 970805.

C_{EG} Feed (mol/L)	P_{O2} (kPa)	adjusted x_{EG}	C_{EG} (mol/L)	C_{GA} (mol/L)	$-r_{EG}$ (mol·h^{-1}·g^{-1})
0.18	300	0.318	0.122	3.78×10^{-2}	0.00147
0.36	300	0.215	0.282	5.20	0.00205
0.72	300	0.147	0.612	7.03	0.00291
0.090	300	0.451	0.049	2.51	0.00101
0.045	300	0.607	0.018	1.54	0.000436
0.090	450	0.472	0.047	2.51	0.00101
0.045	450	0.648	0.016	1.56	0.000686
0.18	450	0.333	0.120	3.66	0.00140
0.36	450	0.229	0.277	5.13	0.00223
0.72	450	0.155	0.606	6.96	0.00321
0.72	225	0.140	0.617	6.24	0.00253
0.18	225	0.300	0.126	3.75	0.00150
0.36	225	0.197	0.288	4.98	0.00201
0.090	225	0.439	0.050	2.72	0.000998
0.045	225	0.604	0.018	1.66	0.00058
0.18	150	0.280	0.129	3.39	0.00144
0.090	150	0.425	0.052	2.48	0.000952
0.045	150	0.602	0.018	1.59	0.000496
0.36	150	0.183	0.293	4.30	0.00202
0.72	150	0.114	0.635	5.16	0.00254

F. Relative Rates of Diffusion of Ethylene Glycol

Compare the rate of diffusion of ethylene glycol in water at 20°C to that at 80°C using the Wilke-Chang estimation method (Reid et al., 1977; Treybal, 1980).

$$D_{AB} = \frac{117.3 \times 10^{-18} (\phi \ M_B)^{0.5} T}{\mu v_A^{0.6}}$$

For the same system, that is to say the diffusion of ethylene glycol in water, only the viscosity, μ and T, the temperature, are affected by a change in temperature. Therefore,

$$(D_{AB}) \quad \alpha \quad \frac{T}{\mu}$$

and

$$(D_{AB})_{80C} = \kappa \ (D_{AB})_{20C} \quad \text{where } \kappa \text{ is a constant.}$$

The viscosity of water (neglecting the effect of ethylene glycol) was found in Janna (1986):

$$\mu = 3.545 \times 10^{-4} \ \frac{kg}{m \cdot s} \text{ at } 80°C; \qquad \mu = 1.006 \times 10^{-3} \ \frac{kg}{m \cdot s} \text{ at } 20°C.$$

$$(D_{AB})_{80C} = 3.4 \ (D_{AB})_{20C}$$